Promotion of antitumor activity of CIK cells by targeting the NKG2D axis

Doctoral thesis

to obtain a doctorate (PhD)

from the Faculty of Medicine

of the University of Bonn

Xiaolong Wu

from Sichuan, China

2021

Written with authorization of

the Faculty of Medicine of the University of Bonn

First reviewer: Prof. Dr. Ingo G.H. Schmidt-Wolf

Second reviewer: Prof. Dr. Hans Weiher

Day of oral examination: 23.11.2021

For the Department of Integrated Oncology, CIO Bonn, University Hospital Bonn

Director: Prof. Dr. Ingo G.H. Schmidt-Wolf

Table of Contents

List of Abbreviations

A

Abs	antibodies
ACT	adoptive cellular therapy
ADAM	a disintegrin and metalloproteinase
ADCC	antibody-dependent cellular cytotoxicity
AICD	activation-induced cell death
ANOVA	analysis of variance
APC	Allophycocyanin
ATCC	American Type Culture Collection
ATM	ataxia telangiectasia, mutated
ATMP	advanced therapy medicinal product
ATR	ataxia telangiectasia and Rad3 related

B

BD	Becton, Dickinson
BV421	Brilliant Violet 421
BSA	bovine serum albumin

C

CAR	chimeric antigen receptor
CB	cord blood
CD	cluster of differentiation
CIK	cytokine-induced killer
CTLA-4	cytotoxic T-lymphocyte-associated protein 4
CCR	chemokine receptor
CCL5	C-C Motif Chemokine Ligand 5
CFSE	carboxyfluorescein succinimidyl ester
CR	complete remission
CRA	Chromium-51 release assay
CRS	cytokine release syndrome

D

DAP10	DNAX-activating protein of 10 kDa

DCs	dendritic cells
DLI	donor-derived lymphocyte infusion
DMSZ	Deutsche Sammlung von Mikroorganismen und Zellkulturen
DNAM-1	DNAX accessory molecule-1
E	
EDTA	ethylenediaminetetraacetic acid
e.g.	for example
ELISA	enzyme-linked immunosorbent assay
ERp5	endoplasmic reticulum protein 5
E/T	effector/target
F	
FACS	fluorescence-activated cell sorting
FBS	fetal bovine serum
FDA	US Food and Drug Administration
FITC	fluorescein isothiocyanate
FSC	forward scatter
G	
GVHD	graft versus host disease
H	
H	hours
H60	histocompatibility 60
HLA	human leukocyte antigen
HSCTs	haematopoietic stem cell transplants
I	
ICAM-1	intracellular cell adhesion molecule 1
ICI	immune checkpoint inhibitor
IFN-γ	interferon γ
IL	interleukin
IgG	Immunoglobulin G
iNKT	invariant natural killer T
IR	Ionizing radiation

IRCC	international registry on CIK cells
ITAM	immunoreceptor tyrosine-based activation motif
K	
KIRs	killer immunoglobulin-like receptors
L	
LAG-3	lymphocyte-activation gene 3
LAK	lymphokine-activated killer
LC-AA	ligand complex-based adhesion assay
LDH	lactate dehydrogenase
LFA-1	lymphocyte function associated antigen 1
M	
mAb	monoclonal antibody
MdFI	median fluorescence intensity
MHC	major histocompatibility complex
MIC	MHC I Chain-related molecule
MICA	MHC I Chain-related molecule A
MICB	MHC I Chain-related molecule B
Min	minutes
MMPs	matrix metalloproteinases
N	
NK	natural killer
NKG2A	natural killer group 2A
NKG2D	natural killer group 2D
NKp30	natural cytotoxicity triggering receptor 30
NKT	natural killer T
P	
PB	peripheral blood
PBLs	peripheral blood lymphocytes
PBMCs	peripheral blood mononuclear cells
PBS	phosphate-buffered saline
PD-1	programmed cell death protein 1
PD-1L	programmed death-ligand 1

PE	phycoerythrin
PerCP	peridinin-chlorophyll-protein
PMA	phorbol-12-myristat-13-acetat
PP1	protein phosphatase-1
RPM	revolutions per minute
RT	room temperature
S	
Sec	seconds
T	
TCR	T cell receptor
TGF-β	transforming growth factor beta
TILs	tumor infiltrating lymphocytes
TIM-3	T-cell immunoglobulin and mucin-domain containing-3
TNFα	tumour necrosis factor α
TMZ	temozolomide
TRAIL	Tumor necrosis factor-related apoptosis-inducing ligand
U	
UKB	Universitätsklinikum Bonn
ULBP	UL16 binding protein
R	
Rae1	retinoic acid early transcript 1
S	
SSC	side scatter
7AAD	7-aminoactinomycin D

1. Introduction

Immunotherapy has emerged as a promising approach for treatment of cancer patients, which includes immune checkpoint blockade, adoptive cellular therapy (ACT) and cancer vaccinology. A successful example is seen in immune checkpoint blockade, which has revolutionized the field of tumor therapy and become now first-line therapies for some solid and blood tumors. Although immune checkpoint inhibitor (ICI) therapies have improved patient outcomes across numerous tumor types, only a minority of patients respond to this treatment and some of the responders eventually develop therapeutic resistance with tumor relapse and progression. Therefore, other innovative immunotherapeutics are needed in this long-run fight against cancerous diseases.

As another type of immunotherapy, ACT has gained increasing interest of research since the viability of this therapy was first shown by Southam et al. (1966) in 1966, and subsequently the first clinical improvement was observed in allogenic haematopoietic stem cell transplants (HSCTs) for leukaemia (Weiden et al., 1979). In the early 1980s, lymphokine-activated killer (LAK) cells were the first ex vivo generated natural killer (NK) cell-enriched products utilized for adoptive immunotherapy by Rosenberg's group (Grimm et al., 1982; Rosenberg et al., 1985). The same group later pioneered the work using IL-2 expanded tumor infiltrating lymphocytes (TILs) for treatment of patients with metastatic melanoma (Rosenberg et al., 1988), showing complete tumour regression in 20 (22%) patients, 19 of whom were still in complete remission 3 years after treatment (Rosenberg et al., 2011). However, the modest efficacy and IL-2-related toxicity in LAK-based ACT and difficulties in expansion and isolation of TILs limited their clinical applications and led to the emergence of other alternatives, including ex vivo purified NK cells, NK cell line (NK92), cytokine-induced killer (CIK) cells and natural killer T (NKT) cells.

1.1 CIK cells

Cytokine-induced killer (CIK) cells were first described and generated in 1991 by Schmidt-Wolf IGH and colleagues, which are an ex vivo product typically generated from peripheral blood lymphocytes (PBLs) in the presence of a cocktail of stimuli (IFN-γ, anti-CD3 monoclonal antibody, IL-1β and IL-2) in a sequential process (Schmidt-Wolf et al., 1991). After 14-21 days of expansion, CIK cells become a heterogeneous population of lymphocytes consisting of a majority of CD3+CD56- T cells, CD3+CD56+ cells and a minor fraction of CD3-CD56+ NK cells (Schmidt-Wolf et al., 1993). The hallmark of CIK cells is the enrichment of CD3+CD56+ subset which is rare (around 3%) in peripheral blood of healthy individuals (Guo et al., 2013). The CD3+CD56+ subset of CIK cells under this culture condition is derived from CD3+CD56- T cells but not CD3-CD56+ NK and the primary CD3+CD56+ cells (Lu et al., 1994). As compared with the traditional LAK cells, CIK cells exhibit a higher proliferation rate and possess superior in vivo antitumor activity (Lu et al., 1994).

1.1.1 Ex vivo generation of CIK cells

The original protocol for production of CIK cells includes the addition of IFN-γ on day 0 to the freshly isolated and monocyte-removed PBLs, followed by adding anti-CD3, IL-1β and IL-2 on day 1 and subculture of cells in fresh complete medium supplemented with IL-2 every 3 days until 2-3 weeks (Schmidt-Wolf et al., 1991). In this pioneering work, it demonstrated that addition of IFN-γ resulted in an increase in cytotoxic activity only if added 24 h before the addition of IL-2, probably due to the induction of IL-2 receptors on the effector cells, resulting in a more efficient activation or recruitment of additional cell populations that are not activated by IL-2 alone (Teichmann et al., 1989; Itoh K et al., 1985). IL-1β also increased the activity when combined with IFN-γ and anti-CD3. CIK cells can be generated from both peripheral blood (PB) and cord blood (CB) (Schmidt-Wolf et al., 1991; Introna et al., 2006). As the major source of CIK cells, PB can be derived either from patients or healthy donors, producing the autologous and allogeneic CIK cells, respectively. Of note, Durrieu et al. (2014) observed that both the source of CIK and the type of tumor targets have an impact on the intensity of the cytolytic activity and on the

pathway used, suggesting that optimizing therapeutic efficacy may be dependent on the source of the CIK cells and on the target tumor cells.

Since its first introduction, many attempts have been made to improve the generation or antitumor activity of CIK cells. Cytokines are essential and important for the proliferation and function of CIK cells. Prior study showed that expansion of CIK cells with each of the exogenous IL-2, IL-7 or IL12 led to no difference in in vitro cytotoxic activity but exhibited significant differences in cell proliferation rates, antigen expression and percentage of necrotic cells (Zoll et al., 1998). Furthermore, transfection with IL-7 or IL-2 genes also was shown to increase the in vitro proliferation rate and antitumor cytotoxicity of CIK cells compared to non-transfected cells (Finke et al., 1998; Nagaraj et al., 2004). Another well-documented and commonly used cytokine for CIK generation is IL-15. Based on the original protocol, Rettinger et al. (2012) showed that addition of IL-15 instead of IL-2 in the subculture of CIK cells on day 4 significantly increased the in vitro anti-leukemic potential and this modification can shorten ex vivo expansion time of CIK cells to 10-12 days. The in vivo study performed by Rettinger et al (2013) showed homing of IL-15 activated CIK cells to leukemia sites, leukemia control, and complete disease clearance when repeatedly given. Moreover, this group proposed that IL-15 stimulation may change the outcome of CIK cell generation from terminally differentiated and potentially exhausted day 21 CIK cells to day 10 CIK cells with a more naïve phenotype and potent proliferative capacity (Rettinger et al., 2012).

In addition, early studies from our group demonstrated that the coculture of CIK cells with autologous tumor specific antigen-pulsed dentritic cells (DCs) can enhance the antitumor activity with a shift to much lower effector to target ratios, likely due to the increased IL-12 secretion from DC cells (Ziske et al., 2001; Märten A et al., 2001). This modified protocol has led to increasing DC-CIK cell-based clinical trials, among which some have shown encouraging results (Ren et al., 2016; Sun et al., 2017; Jiang et al., 2017).

Owing to the advances in biotechnology, synthetic chimeric antigen receptor (CAR) has been developed to specifically target tumors in a non-major histocompatibility complex (MHC)-restricted manner and the clinical success in CD19-CAR T cell therapy has been seen in treatment of B cell malignancies (Maude

et al., 2014; Mullard, 2017). Genetically engineered with CAR, CIK cells also showed antigen-redirected specificity and enhanced antitumor efficiency (Schlimper et al., 2012; Hombach et al., 2013; Oelsner et al., 2016).

1.1.2 Mechanisms involved in the recognition and lysis of tumor targets by CIK cells

Among the heterogeneous populations in bulk CIK culture, CD3+CD56+ subset is known to possess potent cytotoxicity, but have low proliferative capacity due to its terminal differentiation (Schmidt-Wolf et al., 1993; Linn YC et al., 2009; Franceschetti et al., 2009). In contrast, the CD3+CD56- counterpart, which represents early effector T cells, exhibits a higher proliferative capacity but inferior cytotoxicity. The granzyme content was also shown to be higher in the CD3+CD56+ subset, consistent with the report that late effector T cells possess more potent cytotoxicity than early effector T cells (Linn et al., 2009). The mechanisms underlying the cytotoxicity of CIK cells have not yet been completely understood, however some key molecules and pathways have been identified. Early studies (Schmidt-Wolf et al., 1993; Schmidt-Wolf et al., 1994) showed that the cytotoxicity of CD3+CD56+ CIK cells is MHC-unrestricted, as blocking antibodies against TCR (T cell receptor) αβ, and MHC class I and II molecules failed to inhibit the cytotoxic activity. Whereas cytolysis was inhibited by blocking lymphocyte function associated antigen 1 (LFA-1) and intracellular cell adhesion molecule 1 (ICAM-1), suggesting CIK cell-mediated cytotoxicity is dependent on cell-to-cell contact. Mehta et al. (1995) proposed two pathways by which CIK cells kill target cells, one is through stimulation by CIK recognition structure in concert with LFA-1, another is by stimulation of CD3 or CD3-like surface receptors on CIK cell. Both pathways involve exocytosis of cytoplasmic granule contents, which was later demonstrated in a perforin-dependent way (Verneris et al., 2001).

The above mentioned CIK recognition structures were subsequently and partially unveiled as the activating NK receptors were well clarified, including natural killer group 2D (NKG2D), DNAX accessory molecule-1 (DNAM-1), NKp30, CD16 (Verneris et al., 2004; Pievani et al., 2011; Cappuzzello et al., 2016). In CIK cells, both NKG2D and DNAM-1 are highly expressed while NKp30 is present at low

density and CD16 expression is donor-dependent. Engagement of these receptors can trigger and activate CIK cells, exerting the killing in a MHC unrestricted fashion. Apart from the direct granule-dependent cytolysis mechanism (Verneris et al., 2001), program cell death system Fas-FasL and tumor necrosis factor-related apoptosis-inducing ligand (TRAIL) signalings are also found to mediate the cytotoxic activity of CIK cells (Durrieu et al., 2014; Cappel et al., 2016). All these features are more analogous to NK cells, killing target cells in a MHC-unrestricted manner without prior priming. Unlike NK cells, the major inhibitory receptors (e.g., (KIRs) killer immunoglobulin-like receptors, CD94/NKG2A) are normally absent or express at low level on CIK cells with no significantly biological functionality (Linn et al., 2009; Franceschetti et al., 2009; Rettinger et al., 2012). However, other checkpoint molecules (e.g. PD-1 (programmed cell death protein 1), CTLA-4 (cytotoxic T-lymphocyte-associated protein 4), PD-L1 (programmed death-ligand 1), LAG-3 (lymphocyte-activation gene 3), TIM-3 (T-cell immunoglobulin and mucin-domain containing-3)) have been detected on CIK cells to varied extents and may have inhibitory implications as occurred in conventional CD8+ T cells (Poh and Linn, 2016; Zhang et al., 2016). Another difference from NK cells is that CIK cells exhibit a polyclonal TCR repertoire (Linn et al., 2009) and remain the ability to eradicate target cells in an MHC-dependent way. This has been implicated in the DC-CIK studies and was further confirmed by Pievani et al. (2011) showing that CIK cells can mediate both specific MHC restricted recognition and TCR-independent NK-like cytolytic activity. Therefore, sharing the phenotypic and functional properties of both NK and T cells confers CIK cells a great potential to recognize and eradicate a broad range of tumor targets, making it attractive in the realm of immunotherapy.

1.1.3 Preclinical and clinical studies

CIK cells were initially and mostly tested in hematologic cancer mouse models, including lymphoma, leukemia and multiple myeloma showing strong effectiveness (Schmidt-Wolf et al., 1991; Lu et al., 1994; Hoyle et al., 1998). The similar potency of CIK cells was also observed in mice with solid tumors, such as cervical carcinoma (Kim et al., 2009), cholangiocarcinoma (Wongkajornsilp et al., 2009), sarcomas (Sangiolo et al., 2014), sarcoma cancer stem cells (Mesiano et al., 2018),

hepatocellular carcinoma (Kim et al., 2007), non-small-cell lung cancer NSCLC (Kim et al., 2007), ovarian cancer (Chan et al., 2006) and melanoma (Gammaitoni et al., 2013) and so on. Interestingly, Edinger M and colleagues showed that CIK cells have the potential to directly home to the tumor sites (Edinger et al., 2003). However, the underlying mechanism is unclear since the chemokine receptors (CCR4, CCR5, CCR7, CXCR3 and CXCR4) were found dramatically down regulated during the ex vivo expansion (Zou et al., 2014). Due to this favorable property, CIK cells were used as vectors of vaccinia virus and obtained an increased intratumoral homing of CIK cells, demonstrating synergistic antitumor effects of immune cell-viral biotherapy (Thorne et al., 2006) and this effect was further improved through CCL5 (C-C Motif Chemokine Ligand 5) expression from the virus (Sampath et al., 2013).

Although IL-2 is essential for in vitro CIK cell growth, the exogenous administration of IL-2 was reported to have no impact on the in vivo proliferation index of CIK cells and mice survival (Nishimura et al., 2008). Moreover, this study also showed that the in vivo division rate of CIK cells was much less than naive splenocytes. This may be due to the majority of CIK cells were terminal differentiated effector cells with low capacity of proliferation at the time when injected into mice. Similar results were reported by Helms et al. (2010), showing that administration of IL-12 only increased the proliferation of CIK cells from short term cultures (6 days) but not from full term of enrichment (14 days). Of note, however, this study suggests that short-term cultured CIK cells can be ‘‘educated’’ in vivo by administration of IL-12, producing fully expanded CIK cells with anti-tumor efficacy (Helms et al., 2010). Another major advantage of CIK cell treatment is that these cells can be safely and tolerably injected into allogeneic mice with minimal graft versus host disease (GVHD) (Verneris et al., 2001). The low incidence of GVHD seems attributed to the limited expansion and/or survival of CIK cells in vivo. IFN-γ may also play a role as cells expanded from IFN-γ knock-out animals caused acute lethal GVHD, whereas cells expanded from animals defective in fas ligand, fas, IL-2, and perforin did not (Baker et al., 2001). Nevertheless, this feature has encouraged the initial clinical trials from the autologous setting to the allogeneic one, which allows CIK cells as an off-the-shelf product.

Since the first-in-human study showed the safety and feasibility of CIK cell therapy in treatment of lymphoma in 1999 (Schmidt-Wolf et al., 1999), the number of clinical trials using CIK cell therapy for treatment of patients with both blood and solid cancers has significantly increased. In order to collect and access the CIK cell-related clinical data globally and standardize the evaluation of clinical trials, our group established the international registry on CIK cells (IRCC) in 2010. The report of IRCC has been updated for three times (Hontscha et al., 2011; Schmeel et al., 2015; Zhang and Schmidt-Wolf, 2020) based on the registry database. In the latest report reviewed by colleague Zhang Y (Zhang and Schmidt-Wolf, 2020), a total of 106 clinical trials including 10,225 patients were enrolled in IRCC, of which 4,889 patients in over 30 distinct tumor entities were treated with CIK cells alone or in combination with conventional or novel therapies. Significant improvements in median progression free survival and overall survival were shown in 27 trials, and 9 trials reported a significantly increased 5 year survival rate. The adverse effects in all these studies were universally mild and manageable. Although the outcomes of these growing data seem impressive, it is still difficult to draw definitive conclusions as heterogeneity exists among most studies regarding the study design, clinical setting and response assessment. Whereas, in the limited and well-documented trials for hematological cancers (Introna et al., 2007; Laport et al., 2011; Linn et al., 2012; Introna et al., 2017; Rettinger et al., 2016; Narayan et al., 2019), CIK cell therapy appears to have potent antitumor activity with a high safety and tolerability profile. In a recent study, Merker et al. (2019) reported that CIK cell therapy induced a higher complete remission (CR) rate in patients with relapsing hematological malignancies after allogeneic HSCTs than donor-derived lymphocyte infusion (DLI) (53% and 29%, respectively), while relapse occurred in 47% and 71%. More importantly, no concurrent salvage therapies were used in this study, which could probably better interpret the efficacy of CIK cell therapy. In addition, in a phase I/II trial using donor-derived CD19-CAR CIK cells to treat B cell acute lymphoblastic leukemia patients relapsed after allogeneic HSCTs, one infusion of high doses of CAR CIK cells resulted in CR in 6 out of 7 patients, with only grade 1 or grade 2 CRS (cytokine release syndrome), but no GVHD and neurotoxicity (Magnani et al., 2020).

The encouraging results from hematological malignancies have led to the authorization of CIK cell as an advanced therapy medicinal product (ATMP) for patients with hematological malignancies at risk for relapse after allogeneic transplantation in Germany since 2014 (national authorization § 4b Abs. 3 AMG; “Hospital Exemption”). CIK cell therapy is safe and well-tolerated even in complete HLA (human leukocyte antigen)-mismatched settings and therefore can be used as an off-the-shelf product. The efficacy of CIK cell therapy in both hematological and solid cancers would be better known from future larger randomized phase III clinical trials with clear study designs and critical assessments. In the meantime, improvements in CIK cell culture, antitumor activity, or understanding of molecular mechanisms may also accelerate the “bench to bedside“ process.

1.2 NKG2D receptor

Among other NK activating receptors, NKG2D is considered the main contributor to the MHC-unrestricted cytolysis of CIK cells (Verneris et al., 2004; Lu et al., 2012; Yin et al., 2017). NKG2D is a C-type lectin encoded by a gene in the “NK complex” on human chromosome 12p12-p13 (Houchins et al., 1991). Thomas Spies and colleagues did the pioneered work to identify NKG2D as an activating immune receptor to stimulate NK cells (Bauer et al., 1999) and costimulate CD8+ T cells (Groh et al., 2001). NKG2D is normally expressed on all NK cells, CD8+ T cells and subsets of γδ T cells, CD4+ T cells and invariant NKT (iNKT) cells (Bauer et al., 1999; Jamieson et al., 2002). However, NKG2D lacks signaling elements within its cytoplasmic domain. In humans, the DNAX-activating protein of 10 kDa (DAP10) has been shown to constitutively and functionally associate with NKG2D to form a hexameric complex structure which can stabilize NKG2D expression and initiate signaling cascades (Wu et al., 1999; Garrity et al., 2005). Upon NKG2D ligand engagement, Tyr-X-X-Meth (YXXM) motif within the cytoplasmic domain of DAP10 recruits Grb2 and PI3K to trigger NK cell effector functions (Upshaw et al., 2006; Wu et al., 1999). In mice, NKG2D can additionally associate with DAP12 containing an immunoreceptor tyrosine-based activation motif (ITAM) which recruits ZAP70 and Syk to activate NK cell cytotoxicity pathways (Lanier et al., 1998; Diefenbach et al., 2002). In cancer patients, surface NKG2D expression on NK or T cells has

been reported significantly lower than that in healthy donors, probably as a consequence of chronic exposure to NKG2D ligand expressing cells or soluble NKG2D ligands (Doubrovina et al., 2003; Lee et al., 2004; Saito et al., 2012; Klöß et al., 2015; Mamessier et al., 2011), leading to an impaired effector function. TGF-β (transforming growth factor beta) was also reported to downregulate NKG2D expression (Park et al., 2011). Nevertheless, the surface expression of NKG2D can be restored by certain stimuli, e.g., incubation with anti-CD3 antibody (Groh et al., 2002) or cytokines (IL-2, IL15) (Wu et al., 2004).

The initial study of NKG2D in CIK cells showed that NKG2D expression is up-regulated upon activation and expansion of these effector cells and demonstrated that NKG2D triggering accounts for the majority of MHC-unrestricted cytotoxicity most likely through DAP10-mediated signaling (Verneris et al., 2004). The expression of DAP-10 in CIK cells is dependent on cytokine stimulation during culture, as only cells cultured in high-dose of IL-2 expressed DAP10 and were cytotoxic (Verneris et al., 2004). The same group also demonstrated that NKG2D is required for the CIK cell-mediated in vivo antitumor activity, and interestingly, found that DAP12 could pair with human NKG2D as well and involve in the activation of CIK cells in a yet to be identified mechanism (Karimi et al., 2005). In addition, consistent with the surface expression, the gene expression of NKG2D in CIK cells gradually increased and peaked at day 14 as shown by the dynamic transcriptomic atlas analysis (Meng et al., 2018).

1.3 NKG2D ligands

NKG2D receptor recognize a diverse range of ligands with differential binding affinities varying from 10^6-10^9 M (Raulet, 2003; Champsaur and Lanier, 2010; Li and Mariuzza, 2014). In humans, NKG2D recognizes family of MHC I Chain-related molecules A and B (MICA and MICB, generally termed MIC) and family of six cytomegalovirus UL16-binding proteins (ULBP1-6) (Eagle and Trowsdale, 2007; El-Gazzar et al., 2013). In mice, NKG2D recognizes retinoic acid early transcript 1 (Rae1α, Rae1β, Rae1γ, Rae1δ, and Rae1ε), histocompatibility 60 (H60a, H60b, and H60c) and mouse UL16-binding protein-like transcript 1 (Mult1) (Cerwenka et al., 2000; Diefenbach et al., 2000; Carayannopoulos et al., 2002; Takada et al.,

2008). All these NKG2D ligands have membrane-distal α1 and α2 extracellular domains which are the sites interacting with the NKG2D receptor (Raulet, 2003). In addition, MICA and MICB proteins also possess a membrane-proximal α3-like domain which is the site responsible for proteolytic shedding (Kaiser et al., 2007), but with no association with β2-microglobulin (Groh et al., 1996).

Although various NKG2D ligands were detected intracellularly in some normal cells, such as airway epithelium and gastrointestinal epithelium (Kraetzel et al., 2008; Hüe et al., 2004; Ghadially et al., 2017), they are generally absent or limited on the surface of normal tissues, but often are induced by cellular stress conditions, including viral infection and cellular transformation (Groh et al., 1998; Groh et al., 2001). The regulation of NKG2D ligand expression is complex, involving in the transcriptional, post-transcriptional, and post-translational levels. Heat shock stress pathway (Venkataraman et al., 2007), DNA damage response ATM (Ataxia telangiectasia, mutated) and ATR (Ataxia telangiectasia and Rad3 related) pathways (Gasser et al., 2005; Gasser and Raulet, 2006), endogenous microRNAs (Stern-Ginossar et al., 2008; Breunig et al., 2017) have been implicated in the regulation or induction of MICA/B.

Among the diverse NKG2D ligands, the MIC family molecules (MICA and MICB) are the best characterized ligands, most prevalently expressed in human tumors. Expression of NKG2D ligands on tumor cells increase their susceptibility to the immune surveillance. However, tumor cells frequently escape the immune surveillance of NKG2D pathways by proteolytic-mediated shedding of NKG2D ligands from tumor cell surface or by exosome-mediated secretion to release the soluble form of NKG2D ligands (Baragano et al., 2014). High levels of circulating soluble MICA/B or ULBP2 have been reported to correlate with poor clinical prognosis in multiple cancer entities, such as renal, colorectal, breast, ovarian, lung, prostate, and blood cancers (Zhao et al., 2015; Zhao et al., 2004; Holdenrieder et al., 2006; Paschen et al., 2009; Yamaguchi et al., 2012; Nuckel et al., 2010). In a recent clinical study, it showed that serum soluble NKG2D ligands may negatively impact clinical outcome of immune checkpoint blockade therapy for melanoma patients (Maccalli et al., 2017).

Several molecules have been shown to correlate with the proteolytic shedding of MICA and MICB, such as disulfide isomerase (ERp5, endoplasmic reticulum protein 5), a disintegrin and metalloproteinase (ADAM) proteins and matrix metalloproteinases (MMPs) (Kaiser et al., 2007; Boutet et al., 2009; Waldhauer et al., 2008; Groh et al., 2002). But it is difficult to specifically block MICA and MICB shedding with small molecule inhibitors since this process is involved in multiple proteases with broad substrate specificities (Boutet et al., 2009; Waldhauer et al., 2008; Groh et al., 2002). Interestingly, some conventional chemotherapeutic drugs (e.g. epirubicin and sorafenib) have been reported to effectively down-regulate the soluble MICA and increase the surface expression of MICA through inhibition of ADAM 10 and ADAM 9 (Kohga et al., 2009; Kohga et al., 2010). One research group led by Dr. Jennifer Wu has long been focusing on the development of anti-MIC antibodies to target and neutralize the soluble MIC in tumor mouse models. They found the antibody-mediated neutralization of soluble MIC had synergistic effects with checkpoint blockade therapies (PD1/PD-L1 and CTLA4 blockade) in melanoma and prostate cancer mouse models (Basher et al., 2020; Zhang et al., 2019; Zhang et al., 2017). Additionally, in order to find a more specific approach for inhibition of MICA/B shedding, Ferrari de Andrade et al. (2018) recently generated monoclonal antibodies (e.g. 7C6) specifically targeting the α3 domain of MICA, the site of proteolytic shedding associated with ERp5 (Kaiser et al., 2007) and found these antibodies prevented loss of cell surface MICA and MICB from human cancer cells without influence on the interaction between NKG2D and the extracellular domains of MICA (α1 and α2). As a result, these antibodies reactivated the NK cell-mediated antitumor immunity through activation of NKG2D and CD16 Fc receptors (Ferrari de Andrade et al., 2018).

1.4 Flow cytometric cytotoxicity assay

In vitro, multiple methodologies can be used for detection of the immune response to target cells. It can be carried out indirectly by the analysis of granules release (perforin, granzymes, or equivalantly degranulation) or cytokines release (IFN-γ, TNF-α) from the effector cell side. Or directly, a more informative way is to quantify the death of targets in coculture with effector cells. Chromium-51 (^{51}Cr)

release assay (CRA) was first developed for this purpose in 1960s (Brunner et al., 1968) and becomes a “gold standard“ for the direct measurement of cell-mediated cytolysis. But the hazardous and disposal problems of this radioactive isotope limit its wide usage, and many other non-radioactive alternatives have been developed, including calcein-AM release assay, MTT assay, lactate dehydrogenase (LDH) release assay and flow cytometric assay (Korzeniewski et al., 1983; Page et al., 1998; Baumgarten, 1986; Blomberg et al., 1986; Papa et al.,1988; Lichtenfels et al., 1994). Among them, flow cytometry-based cytotoxicity assay is widely used showing several advantages, for example, higher sensitivity, and the ability to distinguish between effector and target cells and to detect both populations at the single-cell level.

The general principle of flow cytometric cytotoxicity assay is labeling either effector cells or target cells or both with the cell tracking dye (s) or the cell surface marker (s) to distinguish them from each other, followed by the use of a viability dye to differentiate dead from alive cells. The specific lysis is evaluated either by calculation of the increased percentage of dead target cells or the absolute loss of alive target cells. However, the inconsistence in strategies for gating and lysis calculation is apparent in literatures (Jang et al., 2012; Gillissen et al., 2016; Kandarian et al., 2017; Lorenzo-Herrero et al., 2019; Langhans et al., 2005; Ozdemir et al., 2003). In addition, the concern of cross-staining between effector and target cells due to the spontaneous release and leakage of the labeling dyes (e.g., CFSE (carboxyfluorescein succinimidyl ester)) still remains (Cholujová et al., 2008; Tóth et al., 2017). Despite a clear cutoff between CFSE labeled target cells and unstained effector cells was seen (Cholujová et al., 2008), it is difficult to conclude the absence of cross-contamination in the coculture, because if the effector cells were cross-stained by the leaking CFSE they might have also become CFSE positive thus merging into the CFSE-labeled target population. Thus, the potential contamination between the labeled cells and the neighboring unlabeled cells is yet to be clearly elucidated.

1.5 Aims of the thesis:

CIK cell treatment is one of the promising candidates for ACT, showing some promising results in clinical trials (Zhang and Schmidt-Wolf, 2020). But only a limited number of patients respond to this therapy. A better understanding of the molecular components of CIK cells may aid in developing new strategies to improve the CIK cell-based therapy**.** Since most activating molecules are initially identified in NK or T cells, still much is unknown about their roles in CIK cells. For example, in resting NK cells, the coengagement of NKG2D, 2B4 and LFA-1 is defined as the minimal requirement for the induction of natural cytotoxicity (Bryceson et al., 2009). Although NKG2D is relatively well studied in CIK cells, It remains unclear whether NKG2D engagement alone is sufficient or if it requires additional co-stimulatory signals (e.g. 2B4) to activate CIK cells.

Moreover, the strategy for upregulating MICA/B expression on tumor cells might potentiate the antitumor efficiency of CIK cells against these tumor targets. Recently, a new monoclonal antibody (7C6 mAb) has been established to specifically target the a3 domain of MICA, and reported to inhibit the MICA/B shedding from tumor cells and in turn to stabilize its surface expression (Ferrari de Andrade et al., 2018). We aimed to explore the effect of the newly developed anti-MICA monoclonal antibody on CIK cell-mediated antitumor activity.

In order to evaluate the CIK cell-mediated cytotoxicity in a more accurate and efficient way, we also aimed at improving the already established flow cytometric cytotoxicity assay.

In summary, the aims of this thesis were:

1). To optimize and standardize the flow cytometry cytotoxicity assay;

2). To investigate whether engagement of NKG2D alone is sufficient to trigger and activate CIK cells; and what role 2B4 alone and in combination with NKG2D may play in CIK cells;

3). To test whether the anti-MICA monoclonal antibody (7C6 mAb) can enhance the antitumor activity of CIK cells.

2. Materials and Methods

2.1 Materials

2.1.1 Table 1: Antibodies for cell culture or functional analysis

Antibody	Source	Clone	Identifier #
anti-human CD3	eBioscience	OKT3	16-0037-85
$F(ab')_2$ fragment goat anti-mouse IgG	Jackson ImmunoResearch	polyclonal	115-006-006
purified anti-human NKG2D	Biolegend	1D11	320814
purified anti-human 2B4	eBioscience	C1.7	16-5838-85
purified human IgG1	Biolegend	QA16A12	403501
purified mouse IgG1	Biolegend	MOPC-21	400165
7C6, an anti-MICA a3 domain human monoclonal antibody	kindly provided by Dr. Kai W. Wucherpfennig from Harvard University		

2.1.2 Table 2: Antibodies for FACS analysis

Antibody	Source	Clone	Identifier #
APC anti-human CD3	Biolegend	OKT3	317318
APC anti-human CD4	Biolegend	OKT4	317416
APC anti-human 2B4	Biolegend	C1.7	329511
APC anti-human MICA/B	Biolegend	6D4	320908
APC anti-human NKG2D	Biolegend	1D11	320808
APC anti-human 107a	BD Biosciences	H4A3	560664
APC mouse IgG1	BD Biosciences	MOPC-21	555751
APC mouse IgG1	Biolegend	MOPC-21	400119
APC mouse IgG2a	Biolegend	MOPC-173	400219
BV421 anti-human CD8	Biolegend	RPA-T8	301036
BV421 mouse IgG1	Biolegend	MOPC-21	400157
FITC anti-human CD3	Biolegend	OKT3	317306
FITC $F(ab')_2$ Fragment Goat Anti-Human IgG	Jackson ImmunoResearch	polyclonal	109-096-008
FITC mouse IgG2a	Biolegend	MOPC-173	400209
PE anti-human CD48	Biolegend	BJ40	336707

PE anti-human CD56	Biolegend	5.1H11	362508
PE mouse IgG1	Biolegend	MOPC-21	400113
Recombinant human CD99 Fc chimera protein	R&D Systems		3968-CD-050
Recombinant human ICAM-1/CD54 Fc chimera protein	R&D Systems		720-IC-050

2.1.3 Table 3: Chemicals, reagents, and enzymes

Product	**Source**	**Identifier #**
Accutase	Biolegend	423201
Annexin V Binding Buffer	BD Biosciences	556454
APC Annexin V	Biolegend	640920
BSA	Roth	8076.2
$CaCl_2$	Sigma	21115
CellTrace Violet	Thermo Fisher Scientific	C34557
CFSE	Thermo Fisher Scientific	C34554
Distilled water	Thermo Fisher Scientific	15230097
DMSO - Dimethyl sulfoxide	Roth	A994.2
DuoSet ELISA Ancillary Reagent Kit 2	R&D Systems	DY008
EDTA (0.5 M, PH 8)	Panreac Applichem	A4892
Ethanol ≥99,5 %	Roth	K928.4
FACS flow	BD Biosciences	
FACS clean	BD Biosciences	
FACS shotdown	BD Biosciences	
FACS rinse	BD Biosciences	

FBS	Sigma	F7524
GolgiStop	BD Biosciences	554724
HEPES Buffer 1M	Pan-Biotech	7365-45-9
Hoechst 33258	Cayman Chemical	Cay16756-50
Human MICA DuoSet ELISA	R&D Systems	DY1300
Human TrueStain FcXTM	Biolegend	422301
IFN-γ	ImmunoTools	11343536
IFN gamma kit	Thermo Fisher Scientific	88-7316-86
IL-1β	ImmunoTools	11340013
IL-2	ImmunoTools	11340027
$MgCl_2$	Sigma	M1028
mycoplasma detection kit	Thermo Fisher Scientific	M7006
Pancoll	Pan-Biotech	P04-60500
paraformaldehyde	Boster Bio	AR1068
PBS	Pan-Biotech	P04-36500
PBS tablet	Sigma	P4417
Penicillin-Streptomycin	Gibco	15140122
PMA	Sigma	P8139
PP1	Cayman Chemical	Cay14244-1
Precision Count Beads	Biolegend	424902
RBC lysis buffer	Biolegend	420301
RPMI-1640	Pan-Biotech	P04-16500
Trypan Blue	Thermo Fisher Scientific	15250061
Trypsin EDTA	Thermo Fisher Scientific	25300054
Tween-20	Roth	9127.2
U73122	Cayman Chemical	Cay70740-1
wortmannin	Cayman Chemical	Cay10010591-1
2-Propanol > 99,8%	Roth	6752.4
7AAD	Biolegend	420404

2.1.4 Table 4: Equipments and softwares

BD FACSCanto II	BD Biosciences
Centrifuge	Thermo Fisher Scientific
FACSDiva software	BD Biosciences
FlowJo V10.6 software	BD Biosciences
GraphPad Prism (version 8.0)	GraphPad Prism
IDEAS software	Amnis
ImageStream X Mk II cytometer	Amnis
Incubator	Thermo Fisher Scientific
Laminar flow hood	Thermo Fisher Scientific
Microplate reader	Thermo Fisher Scientific
Microscope	ZEISS
Neubauer chamber	Sigma
Vortex mixer	Velp Scientifica
Water bath	memmert

2.1.5 Table 5: Cell lines

Hela (cervix carcinoma)	DSMZ
K562 (chronic myeloid leukemia)	DSMZ
MDA-MB-231 (breast carcinoma)	DSMZ
P815 (mouse mastocytoma)	ATCC
Raji (Burkitt lymphoma)	DSMZ
SU-DHL-4 (B cell lymphoma)	DSMZ

2.2 Methods

2.2.1 Generation of CIK cells and LAK cells

CIK cells were generated as previously described (Schmidt-Wolf et al., 1991). Peripheral blood mononuclear cells (PBMCs) were isolated from blood of heathy donors (from UKB blood bank) by gradient density centrifugation using Pancoll. PBMCs were seeded at 3 × 10^6/ml in a 75 cm^2 flask with complete culture medium for 2 h and then cells were transferred into a new flask to remove the monocytes, On day 0, 1000 U/ml IFN-γ was added, followed by the addition of 50 ng/ml anti-CD3, 600 U/ml IL-2, and 100 U/mL IL-1β on day 1. Cells were incubated at 37˚C, 5% CO_2, humidified atmosphere and subcultured every 3 days in fresh medium supplied with 600U/ml IL-2 at 0.5-1 × 10^6 cells/ml. After 14-21 days of ex vivo expansion, CIK cells were collected for use.

For LAK cells generation, PBMCs isolated as described above were placed in 75 cm^2 flasks with complete medium in the presence of 600U/ml IL-2 and monocytes were removed by replacing the flasks. LAK cells were used for experiments after 2-5 days of in vitro culture.

2.2.2 Cell lines culture

All tumor cell lines were cultured in complete medium at 37˚C, 5% CO_2, humidified atmosphere. All cell lines were mycoplasma free, as tested by mycoplasma detection kit.

2.2.3 Detection of phenotype and surface receptors on CIK cells or PBMCs

CIK cells or PBMCs were washed and resuspended with cold PBS (phosphate-buffered saline) at a concentration of 1×10^7. 100 µl cell suspension per FACS tube was incubated with 1 µl appropriate markers (FITC-anti-CD3, APC-anti-CD3, PE-anti-CD56, BV421-anti-CD8, APC-anti-NKG2D, APC-anti-2B4, PE-anti-CD48 or corresponding isotype control antibodies) (1:100 dilution) in the dark (4˚C, 20 min). Subsequently, cells were washed with cold PBS twice and incubated with 7AAD (0.5 µg/ml, 10 min, RT (room temperature)) or Hoechst 33258 (0.5 µg/ml, few sec), then measured on FACS Canto II (BD).

In order to get an accurate discrimination of singlets from doublets, the FSC-scaling value on FACSDiva software was always set at 0.7 (in the case of CIK cells or PBMCs), as suggested by Hazen et al. (2018).

2.2.4 Detection of surface ligands on tumor cells

Tumor cells were washed and resuspended with cold PBS at a concentration of 1×10^7. 100 µl cell suspension per FACS tube was incubated with 1 µl appropriate markers (APC-anti-MICA/B, PE-anti-CD48 or corresponding isotype control antibodies) (1:100 dilution) in the dark (4˚C, 20 min). Subsequently, cells were washed with cold PBS twice and incubated with Hoechst 33258 (0.5 µg/ml, few sec), then measured on FACS Canto II.

In some cases where indicated specifically, tumor cells (1×10^5/well) were cultured in 96-well plates (flat bottom for adherent cells, round bottom for suspension cells) at 37˚C, 5% CO_2 in the presence of 7C6 mAb or human IgG1 isotype control antibody at 10 µg/ml. After 24 h of culture, MICA/B on cell surface was detected by FACS. Accutase was used for detaching adherent cells without disturbing the integrity of surface molecule. Prior to the staining process, Fc receptors were blocked with Human TrueStain FcXTM at a final dilution of 1:100.

2.2.5 Flow cytometry-based cytotoxicity assay

Target cells (3×10^6) were labeled with 0.25 µM CFSE in 1 ml PBS for 5-10 min at 37˚C in the dark, followed by three times of washing with 5 ml of culture medium (containing 10% FBS, to quench the excess CFSE dye). Where indicated, LAK cells were labeled with CellTrace Violet (0.25 µM) in 1 ml PBS in a same procedure as target cells were labeled. Then a constant number of target cells were cocultured with effector cells in total of 200 µl medium for 4-20 h at various E/T ratios in 96-well plates (flat bottom for adherent cells, round bottom for suspension cells) at 37˚C 5% CO_2. Target cells cultured alone were used as the basal spontaneous lysis. Cells were gently mixed and spinned down at 800 rpm (revolutions per minute) for 2 min to facilitate E/T (effector/target) binding before being placed in the incubator. At the end of the culture, cells were transfered to FACS tubes (adherent target cells were detached by Accutase) without further washing and stained with 7AAD (0.5

μg/ml, 10 min, RT) or Hoechst 33258 (0.5 μg/ml, few sec), measured by FACS. Sample acquisition time was set for 30 s/tube. Where indicated, the acquisition was set for 1500 bead events for each tube when Precision Count Beads (10 μl/tube) was applied to standardize this assay.

In some experiments where indicated specifically, APC conjugated Annexin V combined with Hoechst 33258 was used to detect the apoptotic populations. CFSE labeled targets were cultured with LAK cells at an E/T ratio of 5:1 for 4 h. At the end of incubation, cells were washed with 2 ml of cold PBS, followed by one more wash with 2 ml of Annexin V Binding Buffer. Pellets were then resuspended with 100 μl of Annexin V Binding Buffer and stained with 1 μl of APC-Annexin V (1:100 dilution) for 10 min at room temperature. As next, cells were stained with Hoechst 33258 (0.5 μg/ml, few sec) and measured by FACS Canto II.

For the P815 redirected cytotoxicity experiments, CFSE-labeled P815 cells were incubated with indicated Abs (IgG1, anti-NKG2D, anti-2B4, anti-CD3) at 5 μg/ml (except anti-CD3, 0.01 μg/ml or 0.05 μg/ml) for 30 min prior to coculture with CIK cells.

For blocking experiments, CIK cells were pre-incubated with 10 μg/ml Abs (IgG1, anti-NKG2D or anti-2B4) for 30 min prior to coculture with target cells.

Where indicated, 7C6 mAb or control IgG1 antibody was added at 10 μg/mL at the beginning of E/T coculture.

Three methods for calculation of specific lysis:

(1). Beads-based calculation:

$$\text{Specific lysis}\ (\%) = \left(\frac{\text{TC} - \text{TE}}{\text{TC}}\right) \times 100$$

TC: absolute number of alive CFSE+ target cells in control tubes (Target alone)

TE: absolute number of alive CFSE+ target cells in coculture tubes (Effector+Target)

$$\text{Absolute cell number} = (\text{cell count} \div \text{beads count}) \times \text{beads volume} \times \text{beads concentration}$$

(2). Cell count-based calculation:

$$\text{Specific lysis } (\%) = (\frac{\text{TC} - \text{TE}}{\text{TC}}) \times 100$$

TC: cell count of alive CFSE+ target cells in control tubes (Target alone)

TE: cell count of alive CFSE+ target cells in coculture tubes (Effector+Target)

Cell count: the cell number recorded in the alive CFSE+ gate

(3). Percentage-based calculation:

$$\text{Specific lysis } (\%) = (\frac{\text{TC} - \text{TE}}{\text{TC}}) \times 100$$

TC: the percentage of alive CFSE+ target cells in control tubes (Target alone)

TE: the percentage of alive CFSE+ target cells in coculture tubes (Effector+Target)

2.2.6 Conjugate assay

Target cells (3×10^6) were labeled with CFSE (0.25 μM) and effector cells (1×10^7) were labeled with CellTrace Violet (0.25 μM) in 1 ml PBS (5-10 min, 37˚C in the dark), followed by washing three times with 5 ml culture medium with 10% FBS. CFSE-labeled target cells (2.5×10^4, 50μl) were co-cultured with Violet-labeled effector cells (50μl) at an E/T ratio of 5:1 specifically in 1.5 ml Eppendorf tubes in the presence of 7AAD (0.5 μg/ml). Cells were gently mixed and centrifuged (200 g, 2 min) to facilitate cell-to-cell contact. After brief incubation (10 min, 37℃ water bath), cells were vortexed (5 sec) to break nonspecific binding, fixed with 1% paraformaldehyde (5 min, RT), and then measured by FACS Canto II.

For the P815 redirected conjugate experiments, CFSE-labeled P815 cells were incubated with indicated Abs (IgG1, anti-NKG2D, anti-2B4) at 5 μg/ml for 30 min prior to coculture with Violet-labeled CIK cells.

For the blocking experiments, Violet-labeled CIK cells were incubated with indicated Abs (IgG1, anti-NKG2D, anti-2B4) at 10 μg/ml for 30 min prior to coculture with CFSE-labeled tumor cells.

Where indicated, CFSE-labeled K562 cells were cocultured with Violet-labeled LAK cells in the absence of EDTA (ethylenediaminetetraacetic acid) or in the

presence of EDTA (2.5mM) either at the beginning or 5 min prior to incubation termination.

2.2.7 Degranulation assay

The standard degranulation assay was performed using a lysosomal marker CD107a.

For cell-mediated stimulation, P815 cells were pre-incubated with the indicated Abs (IgG1, anti-NKG2D, anti-2B4; 5 µg/ml for 30 min) and then co-cultured with CIK cells at an E/T ratio of 5:1 in the presence of APC-anti-CD107a (1:100) and GolgiStop (1:1500) in 96-well U-bottom plates. As next, the cells were centrifuged (800 rpm, 2 min), incubated (5 hours, 37˚C, 5% CO_2).

For plate-bound antibody stimulation, Abs were coated at concentration of 5 µg/ml for 3 hours (37˚C) or overnight (4˚C) on the high-binding 96-well flat-bottom plate. After incubation, PBS was aspirated and CIK cells or PBMCs (2 x 10^5/well) were added with the culture medium (37˚C, 5% CO_2). As next, APC-anti-CD107a (1:100) and GolgiStop (1:1500) were added after 1 hour and further incubation for 4 hours was considered.

Where indicated, CIK cells and tumor cells were plated at a 5:1 E/T ratio in the presence of 7C6 mAb or IgG1 antibody at 10 µg/mL in 96 well plates. Afterward, APC-anti-CD107a antibody (1:100) was added in each well and incubated for 4 h at 37˚C, 5% CO_2. For NKG2D blocking experiments, CIK cells were incubated with anti-NKG2D antibody (clone, 1D11) or IgG1 control antibody at 10 µg/mL 1 h prior to mixing with tumor cells. After 1 h of E/T coculture, GolgiStop was added to each well at a final dilution of 1:1500 and further incubation for 4 hours was considered.

Subsequently, the cells were washed twice with cold PBS and stained with FITC-anti-CD3 and PE-anti-CD56 or BV421-anti-CD8. At the end, the percent CD107a-positive cells within the total population or CD3+CD56- or CD3+CD56+ subpopulation were measured using BD FACS Canto II.

2.2.8 Ligand complex-based adhesion (LC-AA) assay

A ligand complex-based adhesion assay (LC-AA) was performed, as described previously (Urlaub et al., 2017). A base buffer containing PBS (0.5% BSA) with or

without cations (1mM $CaCl_2$ and 2mM $MgCl_2$) was prepared for all the incubation steps. Also, 50 µg/ml recombinant human ICAM-1-Fc chimera and F(ab)2 fragments of goat anti-human Fcγ fragment (160 µg/ml FITC-labeled) were mixed (cation-free buffer, 30 min, RT) to prepare ICAM-1-Fc complexes. CD99-Fc was used as a negative control for gating instead of ICAM-1-Fc. CIK cells were incubated (10 min) with all primary Abs at the concentration of 2 µg/ml (except anti-CD3, 0.5 µg/ml), followed by washing and resuspension of the cells in the buffer and ICAM-1-Fc complex (dilution 1:20). The cross-linking with a secondary goat anti-mouse antibody (5 µg/ml) was performed at 37℃ water bath (10 min). The stimulation controls were performed by adding PMA (10 nM). Afterwards, the cells were gently mixed and fixed by the addition of paraformaldehyde (final concentration 1%). Where indicated, the cells were preincubated with inhibitors separately (30 µM PP1, 100 nM wortmannin, 2.5 µM U73122) for 30 min (37℃), and these inhibitors were retained in the medium during the stimulation process. Lastly, the quantifications were performed using FACS Canto II.

2.2.9 Imaging flow cytometry

For imaging flow cytometric experiments, K562 cells and LAK cells were labeled as described in "**2.2.6**". CFSE-labeled K562 cells (2×10^5) were cocultured with Violet-labeled LAK cells at 5:1 E/T ratio for 4 h. At the end of coculture, cells were incubated with 7AAD (0.5 µg/ml, in the dark, 10 min) and then measured on an ImageStream X MarkII cytometer. Data were analyzed using the IDEAS software.

2.2.10 ELISA

2.2.10.1 IFN-γ secretion

For plate-bound antibody stimulation, Abs were coated at concentration of 5 µg/ml overnight (4˚C) on the high-binding 96-well flat-bottom plate. After incubation, PBS was aspirated and CIK cells (1 x 10^6/well) were added with the culture medium (200 µl) and incubated for 24 h (37˚C, 5% CO_2).

For tumor cell stimulation, CIK cells were co-cultured with Hela cells or MDA-MB-231 cells (5 x 10^4/well) at a ratio of 20:1 for 24 h in 96-well flat bottom plates in the presence of PBS or 7C6 mAb or IgG1 antibody at 10 µg/mL.

At the end of culture, the cell-free supernatant was collected to perform sandwich IFN-γ ELISA, according to the manufacturer's instructions.

2.2.10.2 MICA Shedding

Hela cells (3 x 10^4/well) and MDA-MB-231 cells (4 x 10^4/well) were cultured in 48-well plates with 200 µL complete medium for 48 h in the presence of PBS or 7C6 mAb or IgG1 antibody at 10 µg/mL. At the end of culture, the cell-free supernatant was harvested and the level of soluble MICA was determined by sandwich MICA ELISA, according to the manufacturer's instructions.

2.2.11 Statistical analysis

FACS data sets were analyzed using FlowJo V10.6 software. Statistical analyses were performed using GraphPad Prism v.8.0. The data groups were compared using unpaired two-tailed t test or one-way or two-way analysis of variance (ANOVA) with Turkey’s or Bonferroni’s post-hoc test. P-values < 0.05 were considered significant differences and are marked: * < 0.05; ** < 0.01; **** < 0.0001; ns = not significant.

3. Results

3.1 Study 1: Improvements in flow cytometric cytotoxicity assay

3.1.1 Introduction

Cytotoxicity assay was a major method to assess the in vitro effectiveness of CIK cells against target cells in this study. Given the hazardous and disposal problems of radioactive ^{51}Cr, we did not consider this “gold standard” CRA in this study. Initially, MTT and LDH assays were performed, but showing relatively low sensitivity and fluctuant results. This may be due to the enzymatic reaction by both effector and target cells in the coculture, more apparently when effector cells are in a poor state. Among other alternatives, the flow cytometric assay seemed to be an appropriate choice for the purpose of this study with multiple advantages, such as, the avoidance of radioactive compounds, the ability of distinguishing effector from target cells, the detection of cytotoxicity at the single-cell level and evaluation of all stages of the cytotoxic process (Zaritskaya et al., 2010).

After reviewing the literature in which flow cytometry cytotoxicity assay was utilized, we found apparent inconsistence in these studies, regarding the cell labeling, gating, lysis calculation and whether using calibration beads or not (Jang et al., 2012; Gillissen et al., 2016; Kandarian et al., 2017; Lorenzo-Herrero et al., 2019; Langhans et al., 2005; Ozdemir et al., 2003). More importantly, the fluorescent dyes (e.g. CFSE) for cell staining have been reported to spontaneously release and leak from the initial labeling (Cholujová et al., 2008; Tóth et al., 2017). Although one early study showed a clear discrimination between CFSE labeled target cells and unstained effector cells, it is difficult to conclude the absence of cross-staining because if the effector cells were cross-contaminated by the leaking CFSE they might have become CFSE positive and merged into the originally CFSE-labeled target population (Cholujová et al., 2008). Therefore, the potential cross-staining between effector and target cells in this assay is still yet to be completely elucidated.

In our preliminary experiments, LAK cells showed relatively better consistency in cytotoxicity between batches from different donors, while the cytotoxicity of CIK

cells appeared to be donor-dependent. In addition, LAK cells were ready for use in a short-term culture (2-5 days). Thus, in order to address the above mentioned issues and establish a reliable flow cytometric assay in a fast pace, LAK cells were used in this chapter.

3.1.2 Results

3.1.2.1 No cross-staining between labeled target and effector cells after 4-hour incubation

As shown in Fig. 1A, the CFSE intensity markedly decreased after 4-hour culture (MdFI (median fluorescence intensity), 4h vs 0h, 16702 ± 29.7 vs 50941 ± 631.5, respectively), indicating that over the course of incubation the spontaneous release of CFSE occurred. Fig. 1B shows that the intensity of CFSE in dead cells also declined as compared to the alive population (MdFI, dead vs alive, 9847 ± 24.5 vs 17113 ± 136.2, respectively), indicating that the disruption of cell membrane integrity could lead to the efflux of this dye. Both outcomes imply that some free CFSE presented in the environment of co-culture might cause the secondary staining of surrounding effector cells as concerned by others (Chahroudi et al., 2003; Ozdemir et al., 2003).

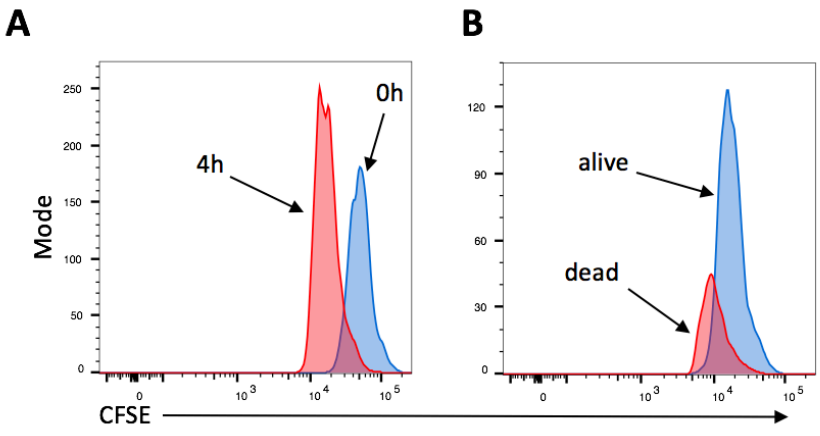

Figure 1. CFSE intensity in K562 cells decreased over the coculture time or after being challenged by effector cells. CFSE-labeled K562 cells were incubated alone (A) or with LAK cells (B) for 4 hours at a 5:1 E/T ratio. Following incubation with 7AAD at the end of culture, samples were measured by FACS Canto II flow cytometer. **(A)** Comparisons of the CFSE intensity of K562 cells between the beginning and end of 4-hour culture. **(B)** Comparisons of the CFSE intensity

between dead and living target cells after 4-hour coculture with LAK cells. Data are depicted in histograms and are representative of at least three independent experiments.

To address this concern, we combined another CellTrace dye Violet to label the effector cells. If, in this condition, a secondary staining happened there would be some double positive cells expressing both green and violet dyes. As shown in Fig. 2A (control), indeed some double positive cells were observed after 4-hour incubation, 11.1% CFSE+Violet+ cells within the CFSE+ K562 cells. However, this population nearly disappeared when EDTA was added either at the start or at the end of the coculture (Fig. 2A, EDTA 0 h and 4 h, respectively). Knowing the nature of effector cells response to targets, it is clear that they need to be in contact with each other to start all the subsequent events, including activation of effector cells, cytotoxic granules release, that will lead to the apoptotic cell death. Therefore, these double positive cells seem more likely to be the conjugation of effector and target cells as the calcium chelator EDTA was shown to be able to prevent the cell-cell contact. Fig. 2B further supported the conjugate formation as these double positive events were much larger than CFSE+Violet- cells in size (MdFI of FSC-A, 116715 ± 1376 vs 75243 ± 258.7, respectively).

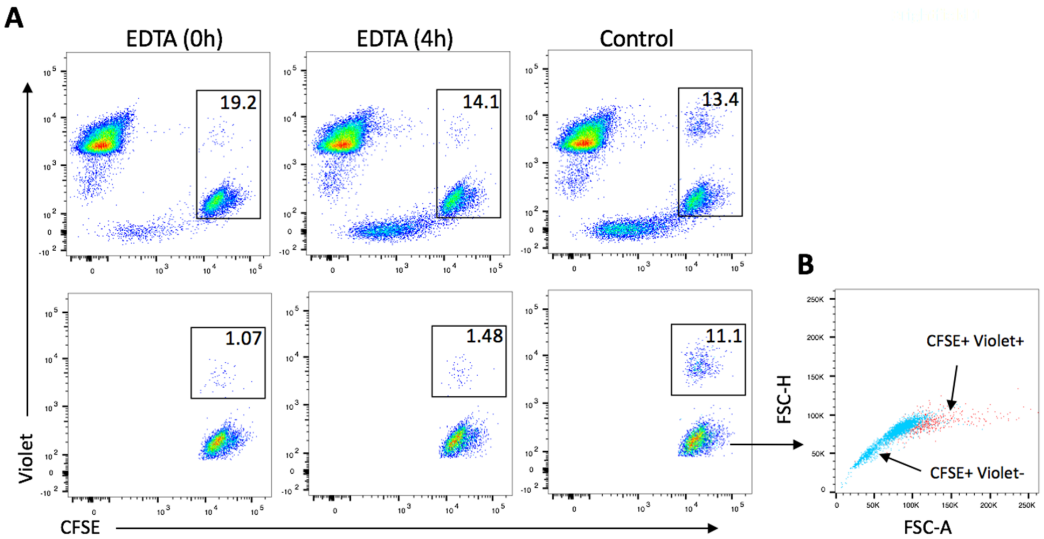

Figure 2. Double positive events are present in E/T coculture but disppear in the presence of EDTA. CFSE-labeled K562 cells were incubated with Violet-labeled LAK cells for 4 hours at a 5:1 E/T ratio in the absence of EDTA (control) or

in the presence of EDTA (2.5 mM) at the start (EDTA 0 h) or at the end of 4-hour culture (EDTA 4 h). Following incubation with 7AAD at the end of culture, samples were measured on FACS Canto II. **(A)** CFSE+ K562 cells (upper panel) in indicated groups were gated out based on the target alone to eliminate debris, CFSE+Violet+ double positive events (bottom panel) were gated within the corresponding CFSE+ K562 cells from the upper panel. **(B)** The double positive cells in red color from the control group in 'A' (bottom plot) fell into the doublet area in an FSC-A vs FSC-H plot. Number represents the percentage of the gated population. Data are representative of three independent experiments.

To further confirm the conjugate formation, the coculture of CFSE-labeled K562 cells and Violet-labeled LAK cells were examined on an imaging flow cytometry system. As shown in Fig. 3, all double positive events were clearly visualized as E/T conjugation in two different colors.

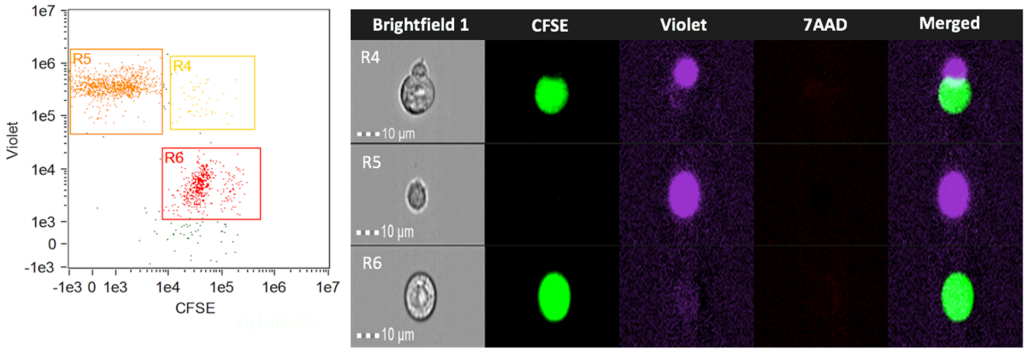

Figure 3. Double positive events are E/T conjugate. CFSE-labeled K562 cells were incubated with Violet-labeled LAK cells for 4 hours at a 5:1 E/T ratio. After staining with 7AAD at the end of culture, samples were measured on a ImageStream X MarkII cytometer. CFSE+Violet+ conjugate composition (R4) was visualized by an imagery system.

Taken together, these data indicate that the CFSE either from the spontaneous release or from the leakage by membrane-compromised target cells was unable to secondarily stain the neighboring effector cells, thus guaranteeing a clear discrimination between effector and target cells in this flow-based cytotoxicity assay.

3.1.2.2 Improvements in the gating strategy for precise gating of alive target cells

Since we performed the cytotoxicity assay without further washing step after coculture, all the events could be well preserved from the original wells. As compared to effector cells cultured alone (Fig. 4A), CFSE+ target cells were distributed clearly and distinctly into three areas (Fig. 4C and Fig. 4D, a. alive, b. dead, c. debris), with a significant increase in percentage of both dead cells and debris in the E/T coculture while decrease in living cells as compared to target cells alone (Fig. 4B). Even the debris (probably including the apoptotic body, but herein referred to as generic "debris") showed relatively recognizable CFSE signal compared to effector cells. However, due to the loss of CFSE intensity in dead targets and autofluorescence in dead effectors (Fig. 4C), the overlap of dead (dying) events from CFSE-labeled K562 cells and effector cells made the cutoff between them slightly unclear.

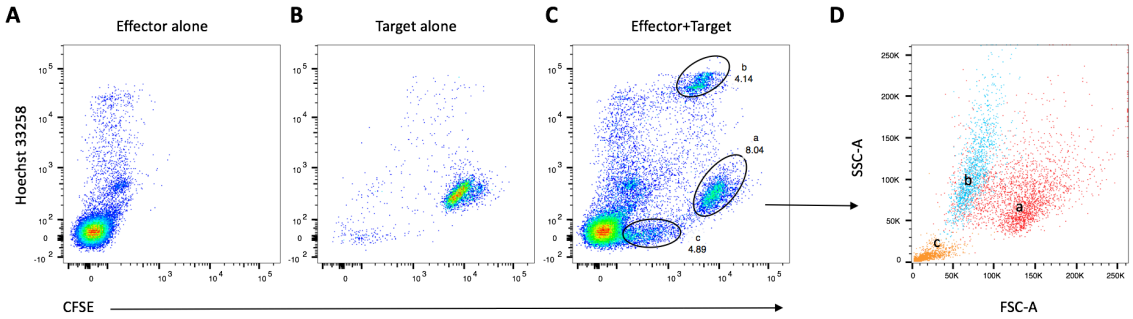

Figure 4. Distribution of CFSE+ K562 cells in coculture with LAK cells. CFSE-labeled K562 cells were incubated alone or with LAK cells for 4 h at 5:1 E/T ratio. Cells were added with Hoechst 33258 at the end of culture and measured on FACS Canto II. **(A)** LAK cells cultured alone without target cells. **(B)** CFSE-labeled K562 cells cultured alone without LAK effector cells. **(C)** CFSE-labeled K562 cells cocultured with LAK cells, divided into alive cells (a), dead cells (b), debris (c). **(D)** a, b, c in 'C' were rebuilt in a FSC vs SSC dot plot. Number represents the percentage of corresponding population.

In order to get a clear separation between target and effector cells, we utilized a fluorochrome-free channel PerCP (peridinin-chlorophyll-protein) vs CFSE where the autofluorescence from effector cells would distribute equally into these two detectors as shown in Fig. 5A.

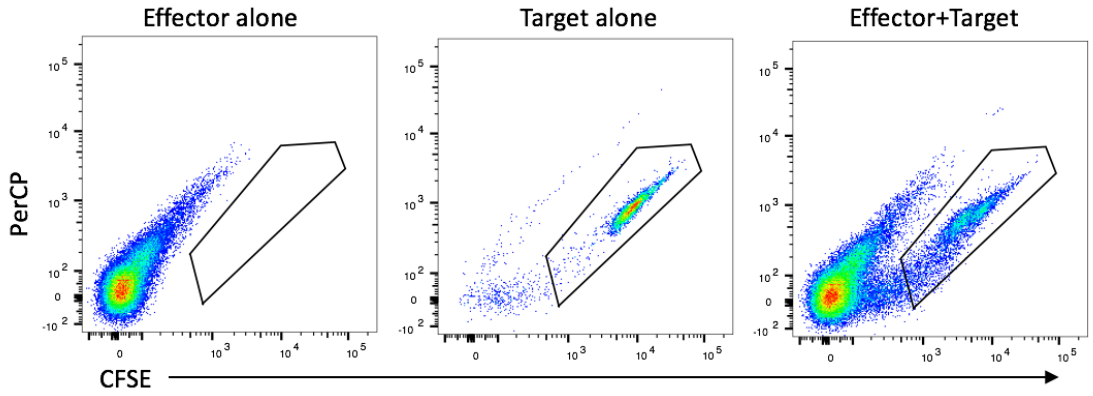

Figure 5. Discrimination of effector and target cells in coculture. CFSE-labeled K562 cells were cultured alone or with LAK cells at 5:1 E/T ratio for 4 hours. At the end of culture, cells were stained with Hoechst 33258 without washing and measured on FACS Canto II. The gate was drawn based on both effector alone and target alone in a fluorescence-free channel PerCP vs CFSE plot.

Following the selection of the CFSE+ K562 cells, the most frequently used CFSE vs Hoechst 33258 dot plot (Fig. 6A) was applied to gate the living or dead cells. The specific lysis calculation is typically determined based on this final gating. Interestingly, when we looked at the living population in Fig. 6A (right) in a FSC-H vs Hoechst 33258 plot, there were some cells out of the gate (Fig. 6B, right) based on the gating in target alone (Fig. 6B, left). These out-gated cells showed a decrease in the intensity of FSC-H but remained CFSE signal as high as cells in living gate. On the basis of the above observation that cells with compromised cell membrane would be stained positively with Hoechst 33258 and lose some CFSE intensity. We inferred that these out-gated cells might be undergoing some early stages of cell death like early apoptosis in which challenged cells could keep the integrity of cell membrane while suffer other biological alterations like in morphology or translocation of phosphatidylserine.

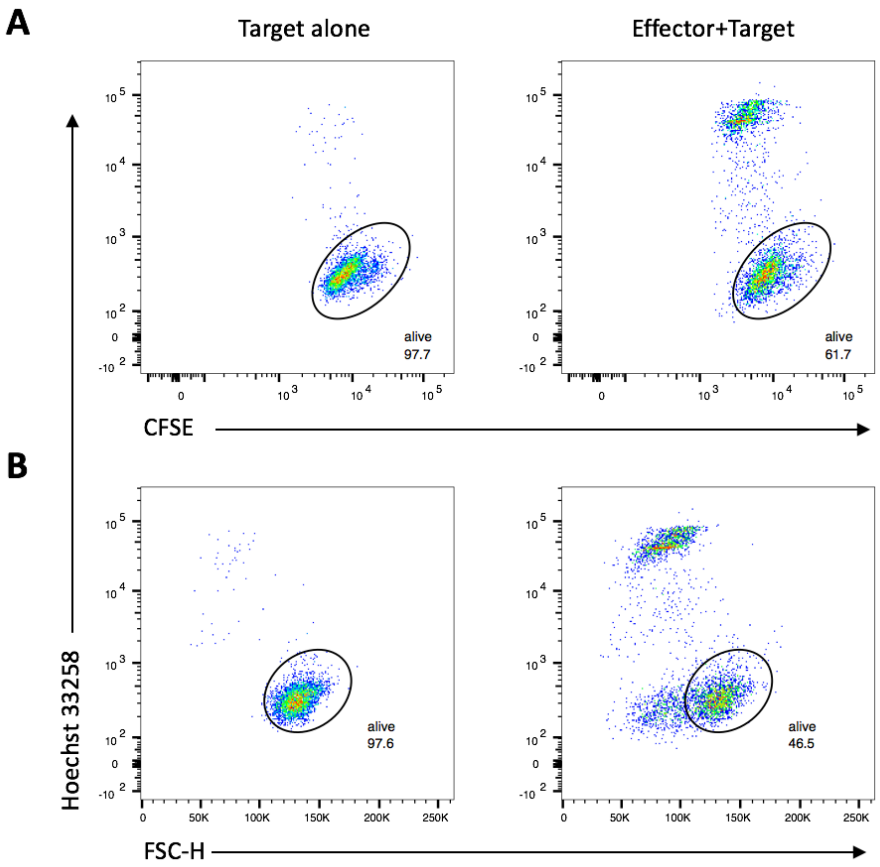

Figure 6. Differences in distribution of alive target cells between FSC-H vs Hoechst 33258 and CFSE vs Hoechst 33258 plots. CFSE-labeled K562 cells were cultured alone or with LAK cells at 5:1 E/T ratio for 4 hours. At the end of culture, cells were stained with Hoechst 33258 and measured on FACS Canto II. **(A)** CFSE vs Hoechst 33258 plot depicts the gating of alive CFSE-labeled K562 population in cocultured with effectors (right) based on target alone (left). **(B)** FSC-H vs Hoechst 33258 plot depicts the gating of alive CFSE-labeled K562 population in cocultured with effectors (right) based on target alone (left). Number represents the percentage of alive cells.

In order to address this issue, cells were washed at the end of 4-hour coculture and stained with APC-Annexin V and Hoechst 33258 to detect early apoptotic cells. Target cells alone served as controls. Following the elimination of effector cells (shown in Fig. 5), CFSE+ targets were displayed in both CFSE vs Hoechst 33258 plot (Fig. 7A and 7B, left plots) and FSC-H vs Hoechst 33258 plot (Fig. 7A and 7B, middle plots). Based on the gating in target alone (Fig. 7A, middle), the events (b) were discriminated from gate a. Following the gating in target alone (Fig. 7A, right),

90% of the out-gated events (b) were shown to be early apoptotic cells (Fig. 7B, right) with a distinguishable shrinkage in size as presented in Fig. 7C.

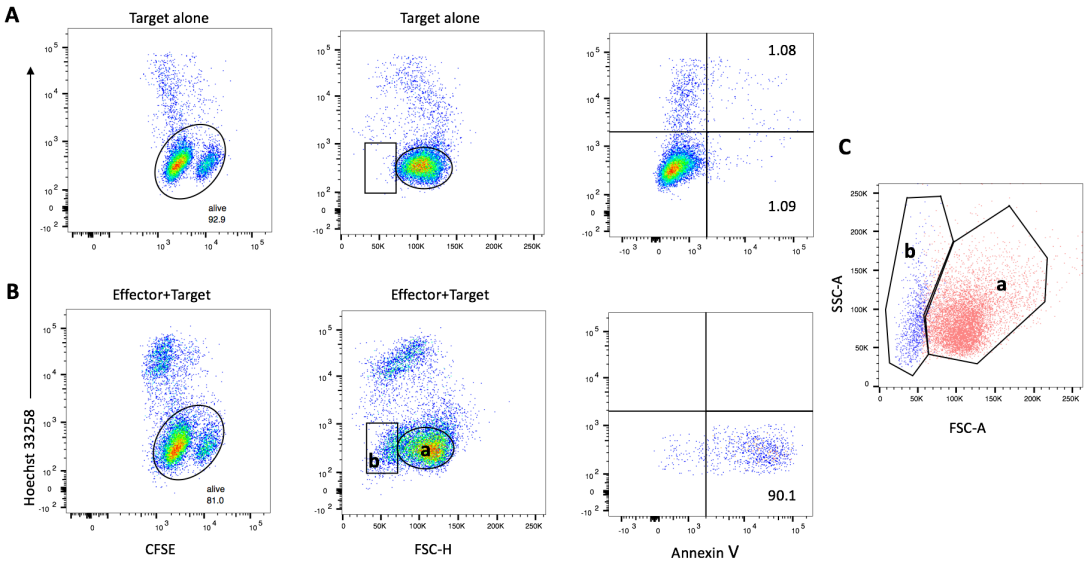

Figure 7. The early apoptotic target cells are distinguished by an FSC-H vs Hoechst 33258 plot or an FSC vs SSC plot. CFSE-labeled K562 cells were cultured alone or with LAK cells at a 5:1 E/T ratio for 4 hours. Early apoptotic target cells were measured by flow cytometry following staining with APC-Annexin V and Hoechst 33258 and elimination of effector cells and debris. **(A)** Living gate shown in a Hoechst 33258 vs CFSE or vs FSC-H plot (left, middle), apoptotic cells shown in a Hoechst 33258 vs Annexin V plot (right). **(B)** Based on the gating shown in 'A' (middle), 90.1% of the cells in 'b' out of the living gate 'a' (middle) were early apoptotic events (right). **(C)** the two populations (a, b) shown in 'B' are displayed in an FSC vs SSC plot.

Taken together, these data suggest that the most commonly used plot CFSE vs Hoechst 33258 might not be accurate enough to gate out the living population. It would be necessary to combine other dot plots which may indicate the morphological change of early apoptotic targets cells, such as FSC vs Hoechst 33258 plot or SSC vs FSC plot. Base on the above data, an example of the gating was set and shown in Fig. 8.

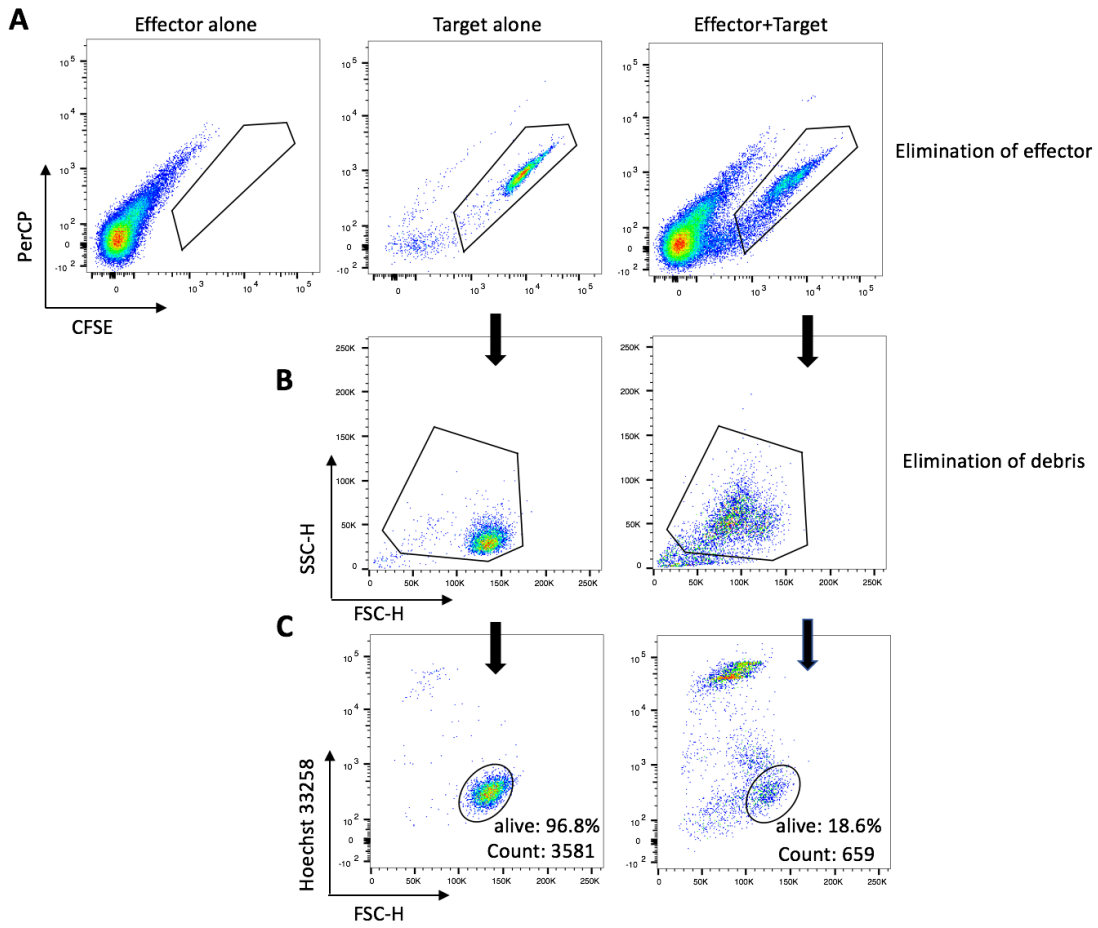

Figure 8. Gating strategy. CFSE-labeled K562 cells were cultured alone or with LAK cells at 10:1 E/T ratio for 4 hours. At the end of culture, cells were stained with Hoechst 33258 without washing and measured by FACS Canto II. **(A)** The top panel depicts the elimination of CFSE negative effector cells based on a fluorochrome-free PerCP channel vs CFSE plot. **(B)** The center panel depicts the debris exclusion in FSC-A vs SSC-A plot. **(C)** The bottom panel shows the alive gate based on the gating in target alone control.

3.1.2.3 Cytotoxicity is overestimated if only effector cells are labeled in flow cytometric assay

Since a certain amount of E/T conjugates were observed in Fig. 2 and Fig. 3, the lysis appears to be overevaluated if only effector cells were labeled due to the loss of part of viable targets in E/T conjugate. To test this assumption, K562 and LAK cells were labeled with two dyes and treated as previously described in Fig. 3, with the exception of addition of two higher E/T ratios (10:1 and 20:1). Fig. 9A shows that nearly all E/T conjugates were alive events. In addition, a trend of increase in

E/T conjugate was seen as the E/T ratio rose (Fig. 9B). Under this condition, target cells could be gated out by either selecting CFSE positive non-debris population (Fig. 9C, bottom left) or Violet negative non-debris population (Fig. 9C, bottom middle). Based on the gating in target cells alone (Fig. 9C, upper right), expectedly, either the percentage or cell count of alive target cells in Violet negative non-debris population was lower than that in CFSE positive non-debris population (Fig. 9C, upper left and middle), thus leading to significantly overestimated values at varied E/T ratios (Fig. 9D). This was due to the exclusion of E/T conjugate as seen in Fig. 9C (bottom middle and right).

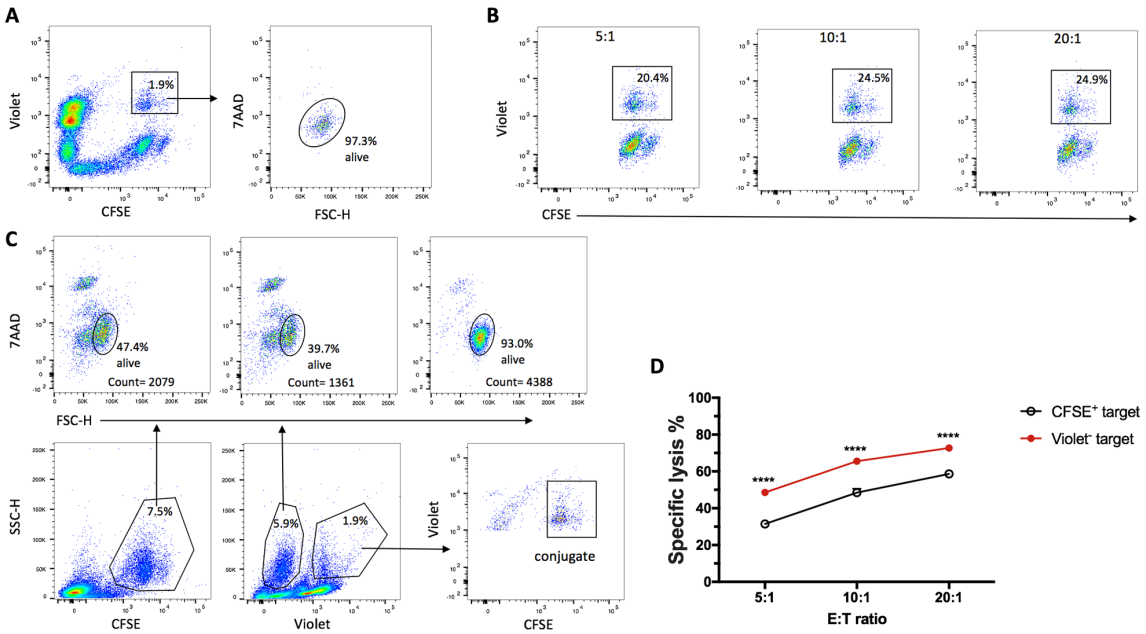

Figure 9. Overestimated cytotoxicity by analysing the Violet negative target cells due to the loss of part of viable targets in conjugates. CFSE-labeled K562 cells were incubated with Violet-labeled LAK cells for 4 hours at indicated E/T ratios. Following the addition of 7AAD at the end of culture, cells were measured by a FACS Canto II. **(A)** Nearly all conjugates were alive cells, data shown at 5:1 E/T ratio. **(B)** The trend of increase in E/T conjugate as the E/T ratio elevated. **(C)** Two different ways to gate target cells, CFSE+ target (left panel) and Violet- target (middle panel), data shown at 10:1 E/T ratio. Upper right plot shows the target alone control and lower right plot shows the conjugates excluded from Violet- target cells. **(D)** Cytotoxicity based on Violet- target was significantly higher than that based on CFSE+ target at indicated E/T ratios. Data are presented as mean +/- SD of triplicate measurements and one presentative from experiments with two donors.

3.1.2.4 A good correlation in the lysis calculation between the cell Count-based method and beads-based method

After 4-hour culture with effector cells, CFSE+ K562 target cells showed a significant increase in debris as well as in dead cells (Fig. 4C). Normally, the debris would be excluded in the final gating for lysis calculation. As a consequence, the specific lysis calculated by the percentage-based method would be actually lower than in reality. But the counting beads has been long used to solve this problem by calculating the absolute number of remaining living cells (Ozdemir et al., 2003; Jedema et al., 2004; Ozdemir et a., 2007). Based on the absolute number of living cells in the target alone, the real loss of target cells and lysis percent could be obtained. Of interest, as we examined the formula of beads-based lysis calculation we found that if a constant number of beads are collected for each tube, we can just take out all the beads values from the formula and leave the cell count values alone. This was herein referred to as cell count-based calculation in this study. The concentration of beads in each sample is supposed to be the same since the volume of added beads and suspended cells are identical in each tube. Therefore, a fixed time for acquisition could theoretically collect a same number of beads in each sample.

To verify this hypothesis, 30 seconds of the stopping time for acquisition and 10 µl of beads (total number, 10000) in each tube was devised. Beads count was found similar after 30-second of collection for each tube (mean 1373, range from 1178-1581). As shown in Fig. 10A, in line with our speculations, the specific lysis calculated by cell count was shown to be well parallel at each corresponding E/T ratio to that calculated by beads while remained higher than percentage-based lysis. With the E/T ratio increased, more target cells were shown to be lost (Fig. 10B).

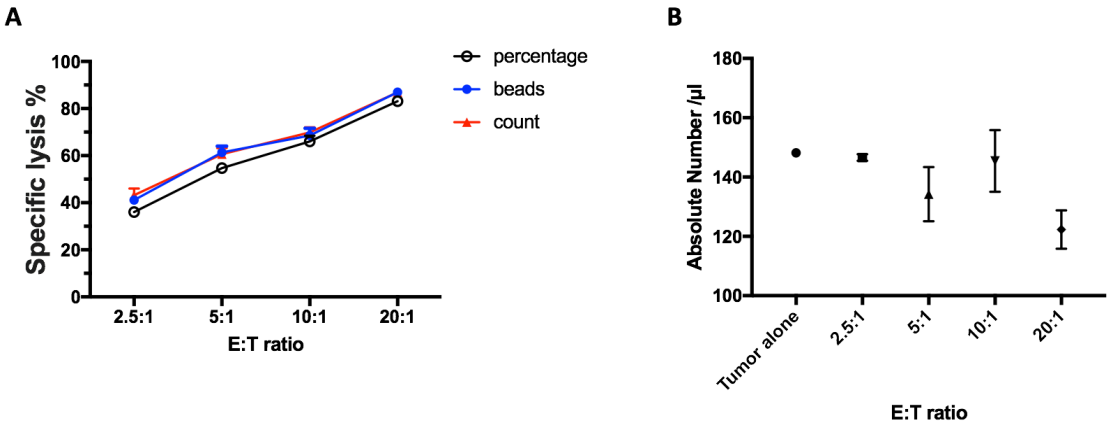

Figure 10. Comparison of specific lysis between varied calculation methods. **(A)** CFSE-labeled K562 cells were cultured alone or with LAK cell at indicated E/T ratios for 4 hours. Specific lysis was calculated through indicated methods following staining with Hoechst 33258 and acquiring each sample for 30 seconds by flow cytometer. Gating was performed according to the strategy in Fig. 8. **(B)** The absolute number (/µl) of CFSE+ K562 cells in indicated conditions. Data are from the experiments shown in 'A'. Data are presented as mean +/-SD of triplicate measurements and one representative of three independent experiments.

Next, we examined if varied recording durations would make a difference in the cell-count based lysis evaluation. K562 cells were labeled with CFSE and cocultured with LAK cells at a 10:1 of E/T ratio. In parallel, target cells alone were used as basal lysis. Following 4-hour of incubation, cells were stained with Hoechst 33258 and measured immediately on the cytometer. The stopping time on the acquisition dashboard was set to 15 sec, 30 sec, and 60 sec. As shown in Fig. 11, there was no significant difference in the specific lysis between various recording durations.

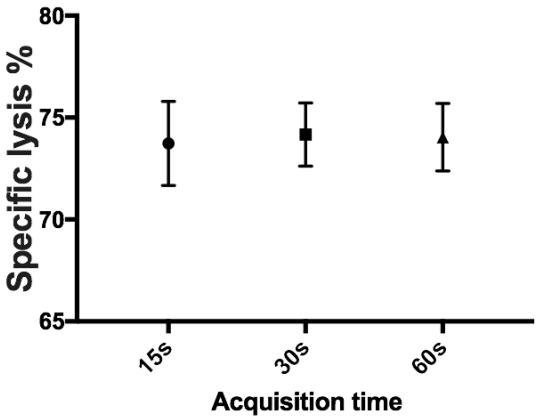

Figure 11. Comparison of the specific lysis between different sample acquisition time. CFSE-labeled K562 cells were cultured alone or with LAK cell at a 10:1 of E/T ratio for 4 hours. Specific lysis was calculated by the count-based method following staining with Hoechst 33258 and collecting each sample for indicated acquisition time by flow cytometer. Data are presented as mean +/-SD of triplicate measurements and one representative of three independent experiments.

Together, these data indicate that the cell-count based approach is well correlated with beads-based in evaluating cytotoxicity. However, it is important to minimize variations between samples by keeping the concentration of cells and volume of wells as identical as possible. With a good consistency in well volumes and cell concentrations, we found that the threshold rate of samples in triplicate acquiring on cytometer runs at a relatively constant level. Therefore, the threshold rate can be considered as a way of quality control during the sample collection. If the rates between the same sample conditions considerably fluctuate, thorough vortexing is needed to reach stable rates. Additionally, total number of events should be similar between tubes of the same condition. Furthermore, in order to keep a stable sample pressure, appropriate FACS tubes should be used to avoid any inconsistency caused by the unstable acquisition.

3.1.3 Discussion

CFSE is able to stably label molecules within cells, with each cell division resulting in a sequential halving of fluorescence (Quah et al., 2007). Initially, carboxyfluorescein diacetate succinimidyl ester (CFDASE) which is non-fluorescent, is highly membrane permeant and can rapidly flux across the plasma

membrane. Once inside a cell it reacts with intracellular esterases resulting highly fluorescent CFSE with a reduced membrane permeability. The succinimidyl ester of CFSE allows it to react with amino groups to form a highly stable covalent bond that gives rise to the carboxifluorescein (CF) compounds, namely CFR1 and CFR2. The former is able to exit via plasma membrane or is rapidly degraded, while the latter forms highly stable fluorescent molecules that remain inside the cells for months. Following cell division, CFR2 is diluted between the daughter cells. High concentrations of CFSE can be toxic to cells and should be avoided. According to previous reports (Quah et al., 2007; Lecoeur et al., 2001), 0.25 μM of CFSE was used in this study and turned out to be effective in labeling with more than 95% post-staining alive cells.

In early studies (Cholujová et al., 2008; Tóth et al., 2017), CFSE was shown to be released spontaneously from CFSE-labeled cells, especially during early time points within 3 or 4 hours following initial labeling. In accord with this finding, we also showed a significant decrease in CFSE intensity after 4-hour culture and when the target killed by effector cells. According to the above description of CFSE labeling process, there are three compounds capable of freely fluxing across plasma membrane (CFDASE, CFSE, CFR1) which might result in the contamination of other unstained neighboring cells. In order to address this problem, Gao et al. (2010) used CFSE to label target cells and anti-CD8b antibody to mark the effector cells. They found that CFSE+ gate was contaminated by small numbers of $CD8^+$ effector cells, most apparent at high E/T ratios and demonstrated that the use of dyes such as CFSE to stain target cells have potential to introduce a certain degree of error. Similarly, we also observed a small fraction of double positive events after Violet-stained effector cells were cocultured with CFSE-labeled target cells. This population, however, was subsequently shown to be the E/T aggregation rather than the cross-staining as these double positive events remarkably decreased in the presence of EDTA and were further visually confirmed by imaging flow cytometry. In fact, the dual labeling of effector and target cells with two dyes is widely used in the conjugate formation assay to detect the binding ability of both. Therefore, these data demonstrate that there is no cross-contamination between the CSFE-labeled target cells and Violet-labeled LAK cells.

Of note, these conjugates which all were found to be alive cells (Fig. 9A) would generally be excluded if effector instead of target cells were labeled in this assay as previously published by others (Benson et al., 2010; Jang et al., 2012), leading to a possible overestimated lysis calculation because of the loss of these viable conjugated targets (Fig. 9C and 9D). These complexes were tightly bound and hardly broken even under vigorous vortexing and pipetting, with a trend of increase at higher E/T ratios (Fig. 9B). Additionally, nearly all conjugates were formed by one single target cell and effector cell (s) as observed by imaging flow cytometry. Herein, labeling target cells is suggested in this assay, or in the case of only effector cells need to be labeled adding EDTA at the end of culture can avoid the overestimation of results.

As shown in Fig. 4C and 4D, the CFSE+ events are clearly divided into three fractions (alive, dead and debris). It is noteworthy that not all the Hoechst 33258 negative events within CFSE+ cells are living targets. The debris with diminished CFSE is also negative for the dead/live dye. In an early study (shown in its Supplementary Figure 1) (Cao et al., 2010), the debris seemed to be gated into the living population which probably led to an underestimate in cytotoxicity. Following the debris exclusion as shown in our Fig. 8, the alive and dead cells were clearly distinguishable by plotting CFSE against Hoechst 33258. Of interest, when these events were viewed in the FSC-H vs Hoechst 33258 plot or FSC-A vs SSC-A plot (Fig. 7B and 7C), a third population with diminished FSC value appeared, indicating the alteration in the cell size. It is well known that the apoptosis can be induced by the perforin/granzyme pathway within minutes up to few hours (Voskoboinik et al., 2015; Jedema et al., 2004). During the early process of apoptosis (Elmore, 2007), cell shrinkage and externalization of phosphatidylserine residues on the outer plasma membrane occur along with other alterations in morphology such as blebbing and nuclear fragmentation while cell membrane remains intact. Combining the cell-permeable dye Hoechst 33258 with the specific marker for phosphatidylserine APC-Annexin V, the population with lower FSC value in Fig. 7B and 7C was demonstrated to be representative of early apoptotic cells. These cells would eventually become the Hoechst 33258 positive cells over a certain period of time. Therefore, the combination of additional plots with FSC parameter would allow

a more accurate evaluation in cytotoxicity by distinguishing these potential apoptotic events. Although there were also some early apoptotic events in the rest of living cells in Fig. 7B (data not shown), the mono-dye (cell-permeable) for marking dead cells seems sufficient in cytotoxicity assessment with the consideration of feasibility and efficiency (no washing, no extra staining, no event loss at the end of E/T culture). Only in the case where no significant difference is found in the lysis between experimental groups and controls, the combination of the Annexin V would be helpful to check if there are any early apoptotic cells.

The loss of targets (debris) lysed by effector cells made the specific lysis calculated by percentage lower than that calculated by beads. Although the percentage-based method showed less variations and would not be largely affected by the count of recorded events, it holds a major limitation-underestimating cytotoxicity (Godoy-Ramirez et a., 2005). This issue might be especially apparent when effector cells are more cytotoxic or treated with certain interventions. Hence, beads application in the flow cytometry-based cytotoxicity assay is usually preferable (Jedema et al., 2004; Ozdemir et a., 2007; Cao et al., 2010). Herein, we showed that the lysis evaluation based on cell count had similar values to that calculated by beads when the samples were collected in a fixed time. In fact, since the concentration of target cells and volume of cell suspension in each tube are equivalent, sample acquisition in a fixed time enables specific lysis calculation to be done using the cell count recorded in the E/T coculture tube and target alone tube. When beads are used, slight variations in bead counting between tubes seem inevitable probably due to changes in the flux or beads handling or vanishing bead phenomenon (Brando et al., 2001). Thus, using the fixed stopping time parameter appears to have a greater stability than the use of beads in standardizing this flow cytometry-based assay.

Laura et al. (2020) recently presented a quantitative method for cell-mediated cytotoxicity studies, preserving the effector cell function with minimal sample manipulation. In terms of cytotoxicity assessment, if combined with the method presented here by using a fixed stopping time for sample acquisition, some precious blood samples might be saved without being added into the controls for getting an absolute cell count.

In contrast to the CRA, the flow cytometry-based approach has one shortage in sample recording. Unlike the relatively fast recording of the supernatant of samples by a gamma counter in CRA, it would take a bit longer to record the samples one by one on flow cytometer. Herein, we showed that the consistency of the specific lysis was greatly preserved between varied recording times. Thus, shortening collection time in this assay to 15 seconds is possible.

In conclusion, we confirm in study 1 that no cross-staining occurs between the effector and target cells after 4 h of coculture. Moreover, the gating strategy can be improved by plotting CFSE against FSC to discriminate some early apoptotic events. In addition, sample acquisition in a fixed time can be used as an alternative to counting beads in standardizing the flow cytometry cytotoxicity assay with a greater stability. With a good quality control, the acquisition time for each sample can be shortened to 15 sec, thus making this work to be done efficiently, especially in the case of larger sample sizes. Collectively, the findings presented here make the flow cytometric cytotoxicity assay more accurate, efficient, and cost-effective, thus guaranteeing the performance of cytotoxicity assessment in the subsequent studies of this thesis.

3.2 Study 2: NKG2D engagement alone suffices to activate CIK cells while 2B4 only provides limited coactivation

3.2.1 Introduction

CIK cells are heterogeneous population of lymphocytes comprised of a majority of CD3+CD56- T cells, CD3+CD56+ cells and a minor fraction of CD3-CD56+ NK cells (Schmidt-Wolf et al., 1991). In comparison to LAK cells, CIK cells exhibit a higher proliferation rate and possess superior in vivo antitumor activity (Lu et al., 1994). Though CIK cells resemble NK-like T cells, in contrast to classical invariant natural killer T (iNKT) cells, they consist of a high proportion of CD8 cells with a heterogeneous Vβ repertoire (Verneris et al., 2002). With phenotypic and functional similarities to T cells and NK cells, CIK cells are endowed with potent cytotoxicity against a broad range of tumors (solid and hematologic origins) in both MHC-restricted and MHC-unrestricted manners (Jäkel et al., 2014; Schmeel et al., 2014; Pievani et al., 2011).

It is well established that the cytotoxic lymphocytes kill the target cells by releasing the contents of the secretory lysosomes at the immune synapse (a process called degranulation). Besides, the interaction of LAF-1 on effector cells with its ligands-ICAMs on target cells contributes to stable adhesion, immunological synapse formation, polarization of lytic granules and subsequent killing of the target cell. In agreement with this, an early study showed that stimulation by the CIK recognition structure in concert with LFA-1 could lead to granule-dependent cytolysis (Mehta et al., 1995). Subsequently, some activating NK receptors were detected as recognition structures of CIK cells, including NKG2D, DNAM-1, NKp30, CD16 (Pievani et al., 2011; Verneris et al., 2004; Cappuzzello et al., 2016). Notably, NKG2D is considered among them to be the main contributor to the MHC-unrestricted cytolysis of CIK cells against various types of tumor (Verneris et al., 2004; Lu et al., 2012; Yin et al., 2017), probably through the DAP-10-mediated signaling (Verneris et al., 2004; Karimi et al., 2005).

NKG2D is primarily a C-type lectin-like receptor capable of activating NK cells and co-stimulating CD8+ T cells (Bauer et al., 1999; Groh et al., 2001). In humans, the NKG2D receptor recognizes a number of ligands (MICA/B, ULBP1-6) that are

usually absent (or present in low amounts) on the surface of normal cells but are induced or upregulated by various stress signals (e.g., infection, transformation, DNA damage) (Raulet et al., 2013), thus making them more susceptible to the immune system. It is well established that blocking the NKG2D receptor on CIK cells can partially reduce cytolytic activity against NKG2D-bearing tumor cells (Pievani et al., 2011; Verneris et al., 2004; Lu et al., 2012; Yin et al., 2017). Therefore, it would be of interest to know if NKG2D ligation alone can lead to the activation of CIK cells, since the interaction of NKG2D, 2B4, and LFA-1 has been defined as a minimum requirement for the induction of natural cytotoxicity (Bryceson et al., 2009). As with NKG2D, 2B4 (CD244) is another well-characterized NK cell activation receptor that belongs to the lymphocyte signaling activation molecule (SLAM) family (Nakajima et al., 2000). To our knowledge, the peculiar role of 2B4 in CIK cells still remains unknown.

Considering this, herein, we aimed to investigate 1) whether engagement of NKG2D alone is sufficient to trigger and activate CIK cells, 2) what role 2B4 alone and in combination with NKG2D may play in the activation of CIK cells.

3.2.2 Results

3.2.2.1 NKG2D and 2B4 expression levels elevate over time in CIK culture

As reported by others (Garni-Wagner et al., 1993), nearly all CD3-CD56+ NK cells from PBMCs expressed NKG2D and 2B4 (Fig. 12A, upper histograms). Since the majority of CD3+CD56+ cytotoxic cells in CIK cultures were derived from CD3+CD56- T cells (Lu et al., 1994), we analyzed the expression of NKG2D and 2B4 on CD3+CD56- T cells (on day 0). In contrast to NK cells, only part of CD3+CD56- T cells expressed NKG2D (32.0% ± 24.5%) and 2B4 (38.7% ± 17.0%) (Fig.12A, lower histograms). Interestingly, after 14 days of ex vivo expansion, not only the percentage of CD3+C56+ cells increased (51.2% ± 12.7%), but also the expression of NKG2D (92.9% ± 9.0%) and 2B4 (86.7% ± 4.4%) (Fig. 12B). In addition, both receptors were expressed on approximately all CD3+CD56+ cells in mature CIK culture (99.7%, 97.9%, respectively).

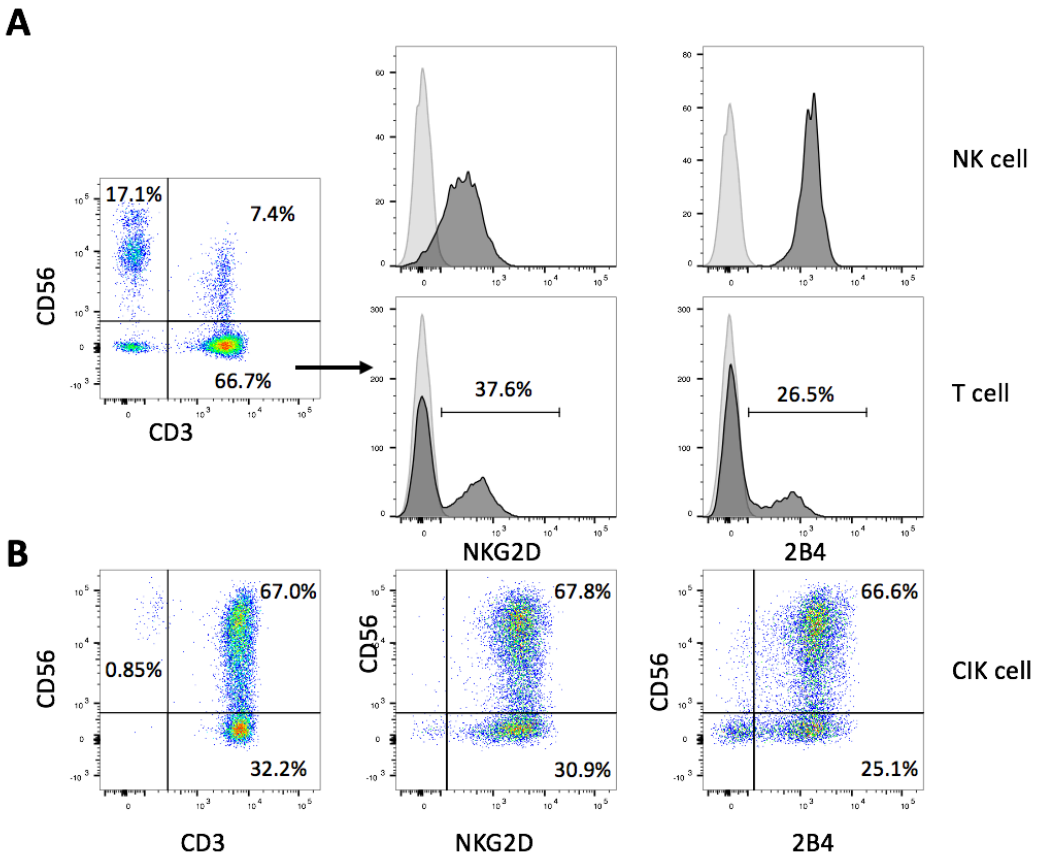

Figure 12. NKG2D and 2B4 expression levels elevate over time in CIK culture. NKG2D and 2B4 expression of cells were measured by flow cytometry after staining with FITC-CD3, PE-CD56, APC-NKG2D or APC-2B4 antibodies. **(A)** Histograms showing the expression of NKG2D and CD244 on CD3+CD56- T cells (lower panel) and CD3-CD56+ NK cells (upper panel) from PBMCs on day 0. **(B)** FACS dot plots showing the elevated expression of NKG2D (98.7%) and 2B4 (91.7%) on mature CIK cells (on day 14). The figure shows data from one representative from 4 donors.

3.2.2.2 Blockade of NKG2D but not 2B4 attenuates the CIK cell-mediated cytotoxicity and E/T conjugate formation

MICA/B was expressed on part of K562 cells but absent on Raji cells (Fig. 13A). Expectedly, blockade of NKG2D on CIK cells with anti-NKG2D resulted in a reduction in both cytotoxicity and E/T conjugate formation in K562 cells but not in Raji cells (Fig. 13B and 13C).

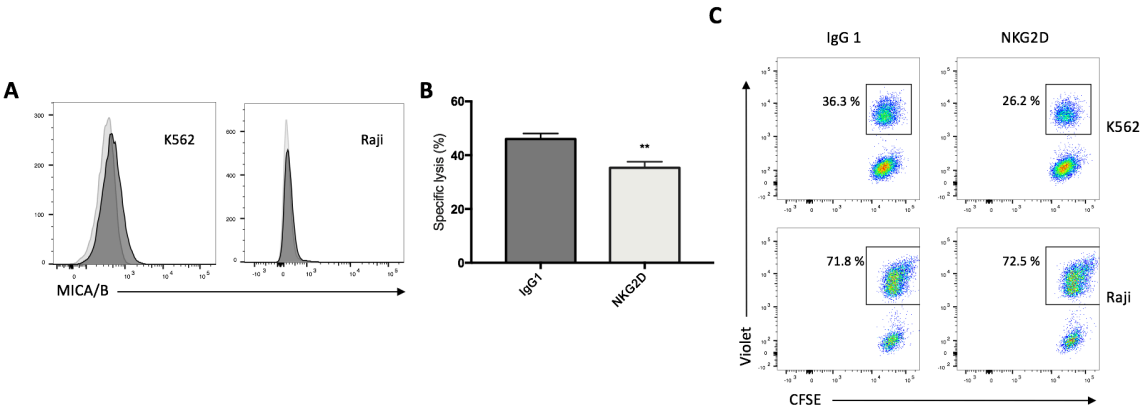

Figure 13. NKG2D blocking reduces the cytotoxicity and E/T conjugate formation. (A) FACS histograms demonstrating the presence of MICA/B on K562 cells and absence on Raji cells. **(B)** FACS-based cytotoxicity performed on CFSE-labeled K562 cells by preincubation of CIK cells with IgG1 isotype control or anti-NKG2D (10 µg/ml, E/T ratio of 20:1). **(C)** Conjugate assay on CFSE-labeled K562 cells (upper plots) or Raji cells (lower plots) by preincubation of Violet-labeled CIK cells with IgG1 isotype control or anti-NKG2D (10 µg/ml, E/T ratio of 5:1). Plots show the percentage of CFSE+ Violet+ double positive cells within the CFSE+ target gate. These results are one representative of three independent experiments. Data are shown as mean ± SD of triplicates per condition and one representative of three independent experiments. ** $p < 0.01$ calculated by unpaired two-tailed t test.

Conversely, CD48 (the ligand of 2B4) was expressed on all SU-DHL-4 and CIK cells (Fig. 14A), but no decline in cytotoxicity and E/T conjugation was observed when CIK cells were preincubated with anti-2B4 (Fig. 14B and 14C). Together, these results suggest that NKG2D (not 2B4) is directly implicated in CIK cell-mediated cytotoxicity and E/T conjugate formation.

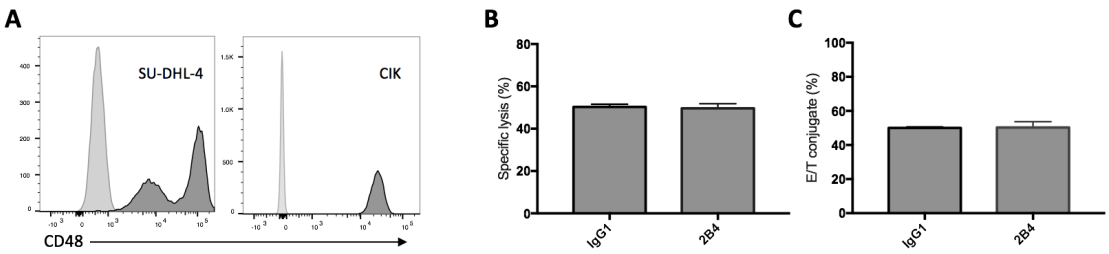

Figure 14. Blockade of 2B4 has no impact on CIK cell-mediated cytotoxicity and E/T conjugate formation. (A) FACS histograms demonstrating the presence of CD48 on all SU-DHL-4 cells and CIK cells. **(B)** FACS-based cytotoxicity (E/T ratio, 20:1) performed on CFSE-labeled SU-DHL-4 cells by preincubation of CIK cells with IgG1 isotype or anti-2B4 (10 µg/ml). **(C)** Conjugate assay against CFSE-

labeled SU-DHL-4 cells by preincubation of Violet-labeled CIK cells with IgG1 isotype control or anti-2B4 (10 µg/ml, E/T ratio of 5:1). Data are shown as mean ± SD of triplicates per condition and one representative of three independent experiments.

3.2.2.3 Engagement of NKG2D (not 2B4) increases the CIK cell-mediated cytotoxicity, degranulation and E/T binding against P815 cells

To further investigate the possible association of NKG2D and 2B4 in CIK cells, the mouse mastocytoma cell line (P815), which expresses the Fc receptor on the surface that can easily recognize and bind the Fc fragment of respective antibodies (e.g. anti-NKG2D, anti-2B4) was used in the current experimental setup. Compared to the IgG1 treatment (Fig. 15), lysis was significantly increased when anti-NKG2D was preloaded on P815 cells, while it remained unchanged as anti-2B4 was loaded. Of note, no additional improvement in lysis occurred when NKG2D and 2B4 were combined in contrast to NKG2D ligation alone. Moreover, anti-CD3, which showed high sensitivity and lysis rate as a positive control did not further increase lysis when being co-incubated (CD3 and NKG2D; CD3 and 2B4).

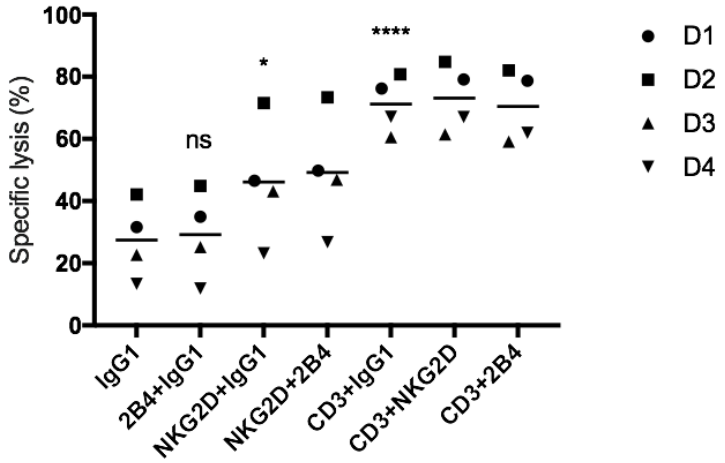

Figure 15. NKG2D (not 2B4) increases the CIK cell-mediated cytotoxicity. The redirected cytolysis assay against murine P815 cells (preloaded with indicated Abs at 5 µg/ml, except for anti-CD3 at 0.05 µg/ml) was performed on FACS at an E/T ratio of 20:1 for 6-8 hours. Data are represented as mean ± SD of triplicates per condition and one representative of three independent experiments. * < 0.05, ****p < 0.0001 calculated by one-way or two-way ANOVA, Bonferroni's post-hoc test.

To better know whether NKG2D or 2B4 can synergize with CD3, the concentration of anti-CD3 was reduced to 0.01 μg/ml to get a lower basal lysis. As shown in Fig. 16, again 2B4 alone or in combination with CD3 led to no further improvement in cytolysis, while NKG2D alone or combined with CD3 resulted in significant enhancement. However, the improvement in cytotoxicity in combination of NKG2D and CD3 appears to be an additive effect rather than a synergy. Data are one representative of three independent experiments with 3 donor-derived CIK cells. Therefore, these data suggest that both NKG2D and 2B4 do not synergize with CD3 in CIK cell-mediated cytotoxicity.

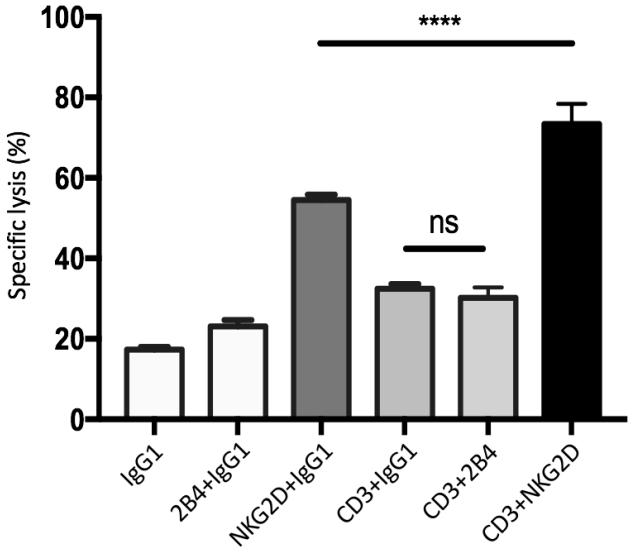

Figure 16. Both NKG2D and 2B4 fail to synergize with CD3 in CIK cell-mediated cytotoxicity. The redirected cytolysis assay against murine P815 cells (preloaded with indicated Abs at 5 μg/ml, except for anti-CD3 at 0.01 μg/ml) was performed on FACS at an E/T ratio of 20:1 for 6-8 hours. Data are represented as mean ± SD of triplicates per condition and one representative of three independent experiments. ****$p < 0.0001$ calculated by one-way ANOVA, Bonferroni's post-hoc test.

Next, P815 cell redirected degranulation and E/T conjugation assays were performed to further confirm the roles of NKG2D and 2B4. As seen in Fig. 17A and 17B, ligation of NKG2D significantly increased the degranulation and E/T conjugate formation, whereas 2B4 alone or in combination with NKG2D had minor to no effect.

These results are in agreement with the data from the previous P815 redirected cytotoxicity experiments.

Taken together, we confirm that NKG2D is an activating receptor on CIK cells that can promote cytotoxicity, E/T conjugate formation and degranulation. In contrast, 2B4 ligation appears to weakly induce cytotoxicity of CIK cells and does not contribute to E/T conjugation and degranulation. And NKG2D provides no synergy in CIK cell-mediated cytotoxicity, degranulation and E/T conjugation with 2B4. In addition, both NKG2D and 2B4 do not costimulate CD3.

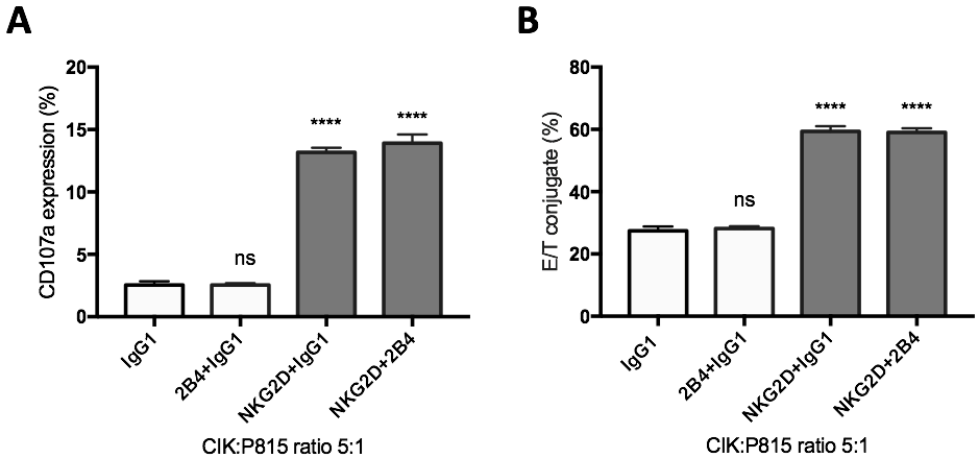

Figure 17. NKG2D (not 2B4) increases the CIK cell-mediated degranulation and E/T binding against P815 cells. (A) The percentage of CD107a on CIK cells was determined after coculture with antibody-loaded P815 cells (all Abs at 5 µg/ml) at an E/T ratio of 5:1 for 5 hours. **(B)** Conjugate assay was performed against antibody-loaded P815 cells (all Abs at 5 µg/ml) at an E/T ratio of 5:1. All the experiments were performed on FACS and the data are represented as mean ± SD of triplicates per condition and one representative of three independent experiments. ns = not significant, ****p < 0.0001 calculated by one-way ANOVA, Bonferroni's post-hoc test.

3.2.2.4 NKG2D contributes alone to degranulation, IFN-γ secretion and LFA-1 activation, whereas 2B4 only provides synergistic effect in activation of LFA-1

It is worth mentioning that even in the absence of any antibodies, CIK cells were still able to form a tight conjugation with P815 cells and induce cytotoxicity, suggesting that P815 cells themselves can be recognized and killed by CIK cells.

Therefore, the impact of these yet to be known P815-CIK intrinsic interactions is difficult to exclude from our data. To circumvent this potential interference, monoclonal antibodies against these receptors (NKG2D, 2B4, CD3) by a plate-bound method or by cross-linking with a rabbit anti-mouse antibody were used to define the relative contribution of NKG2D and 2B4 in degranulation, IFN-γ secretion and LFA-1 activation.

Fig. 18A shows that NKG2D alone was effective enough to induce degranulation while 2B4 alone lacked this ability and led to no further improvement in combination with NKG2D. As expected, CD3+CD56+ subpopulation accounted for the majority of degranulated cells that responded to anti-NKG2D (Fig. 18B).

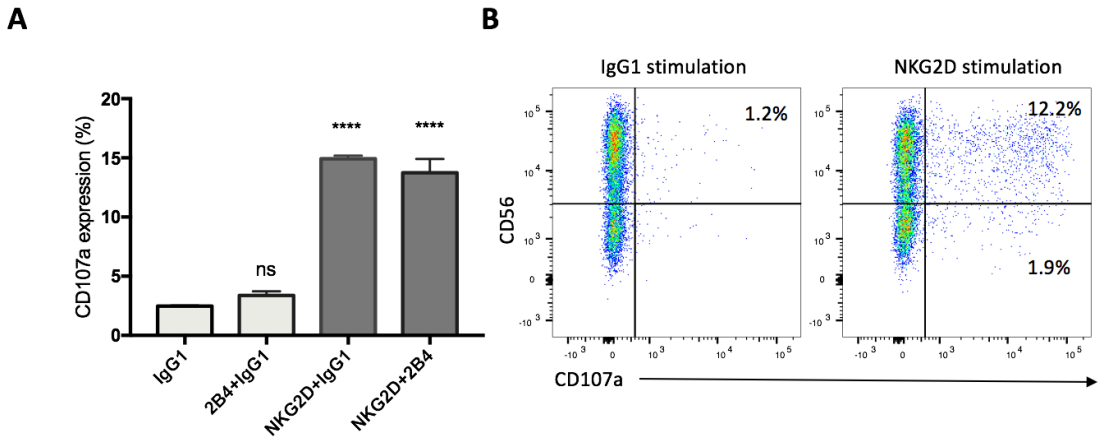

Figure 18. NKG2D (not 2B4) contributes alone to the degranulation of CIK cells. CIK cells were stimulated by indicated plate-bound Abs (5μg/ml) in the presence of APC-anti-CD107a (1:100) and GolgiStop (1:1500) for 5 hours. At the end of culture, cells were stained with PE-anti-CD56, FITC-anti-CD3, followed by the addition of Hoechst 33258 and measured on FACS. **(A)** The percentage of CD107a in response to indicated Ab stimulations. **(B)** FACS dot plots showing the representative degranulation of different CIK subsets in response to IgG1 or NKG2D stimulation. The data are represented as mean ± SD of triplicates per condition and one representative of three independent experiments. ns = not significant, ****p < 0.0001 calculated by one-way ANOVA, Bonferroni's post-hoc test.

Since NK cells were reported to respond well to the NKG2D and 2B4 stimulations, the same assay used in CIK cells was performed for PBMCs as an additional positive control. As shown in Fig. 19, engagement of either NKG2D or 2B4 induced a modest degranulation, and NKG2D exhibited a better response. In contrast to CIK

cells, NKG2D ligation in CD3-CD56+ NK cells produced a markedly synergistic effect with 2B4. Consistent with the literatures (Bryceson et al., 2006), $CD56^{low}$ NK cells were the major degranulated population. Data from two donors are shown.

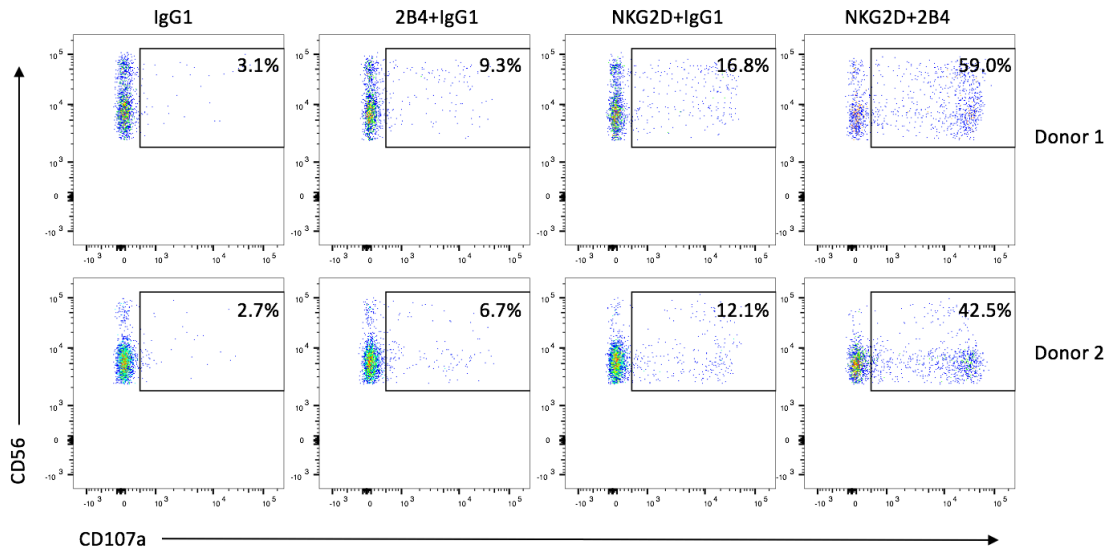

Figure 19. Strong synergy in degranulation is induced by the combination of NKG2D and 2B4 in NK cells. PBMCs were stimulated by indicated plate-bound Abs (5μg/ml) in the presence of APC-anti-CD107a (1:100) and GolgiStop (1:1500) for 5 hours. At the end of culture, cells were stained with PE-anti-CD56, FITC-anti-CD3, followed by the addition of Hoechst 33258 and measured on FACS. Dot plots showing the percentage of CD107a degranulation of CD3-CD56+ NK population from two donors in response to indicated Ab stimulations.

Next, IFN-γ secretion was examined. As seen in Fig. 20, NKG2D ligation alone was able to induce the IFN-γ secretion of CIK cells, while 2B4 alone failed to do so. In addition, no further secretion was observed when NKG2D and 2B4 were coengaged.

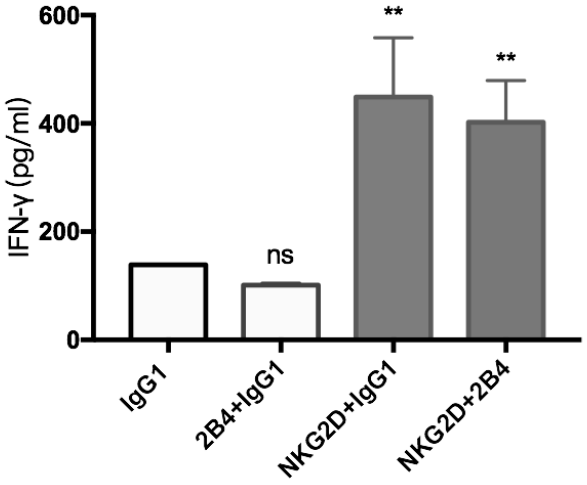

Figure 20. NKG2D (not 2B4) induces the IFN-γ secretion of CIK cells. After 20-hours of stimulation by indicated plate-bound Abs, IFN-γ secretion from CIK cells was quantified using supernatant by sandwich ELISA. The data are represented as mean ± SD of triplicates per condition and one representative of three independent experiments. ns = not significant, ** < 0.01 calculated by one-way ANOVA, Bonferroni's post-hoc test.

Considering the activation of LFA-1 being influenced by the inside-out signals from other activating receptors in NK cells (Urlaub et al., 2017; Enqvist et al., 2015), LC-AA was performed to examine the effect of NKG2D and 2B4 individually and in combination on the activation of LFA-1 in mature CIK cells. In the absence of any stimulation, only a few LFA-1 molecules were found active on the surface of CIK cells (Fig. 21A). NKG2D alone was able to induce LFA-1 activation, and some synergy occurred when it was combined with 2B4, whereas 2B4 ligation solely failed to induce any activation. Additionally, NKG2D or 2B4 in combination with anti-CD3 did not significantly improve the LFA-1 activation. In line with an early report (Urlaub et al., 2017), we also observed contrasting results with resting NK cells, i.e., 2B4 ligation resulted in a stronger activation of LFA-1 compared to NKG2D ligation (Fig. 21B).

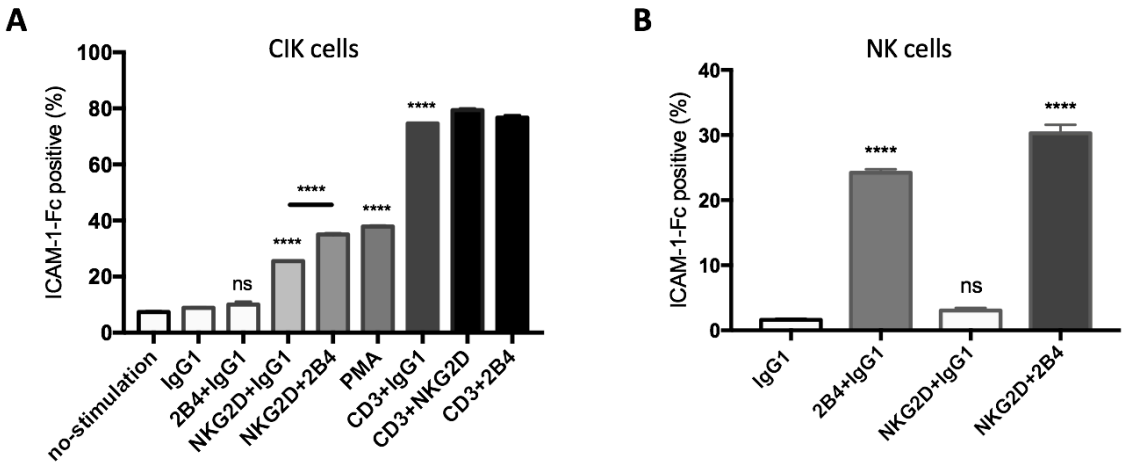

Figure 21. NKG2D alone is able to induce LFA-1 activation of CIK cell, whereas 2B4 provides synergistic signals. (A) CIK cells were unstimulated or stimulated with PMA or indicated Abs in pairwise combination or combined with IgG1 isotype control. Following the crosslink of the receptors with goat F(ab)2 anti-mouse IgG, the activation of LFA-1 was measured by staining with ICAM-1-Fc complexes. **(B)** Freshly isolated PBMCs were treated as described in 'A' with indicated Ab stimulations. For identifying NK cells in PBMCs, cells were stained with anti-CD3-APC and anti-CD56-PE after ICAM-1-Fc complexes staining. All the experiments were performed on FACS and data are represented as mean ± SD of triplicates per condition and one representative of three independent experiments. ns = not significant, ****p < 0.0001 calculated by one-way ANOVA, Bonferroni's post-hoc test.

Together, engagement of NKG2D alone is sufficient not only to induce degranulation and IFN-γ secretion but also activation of LFA-1 in CIK cells. While 2B4 provides only synergistic signal in activation of LFA-1.

3.2.2.5 PI3K, PLC-γ, and Src involve in the NKG2D-mediated LFA-1 activation in CIK cells

In NK cells, PI3K, PLC-γ, and Src related signaling pathways have been reported to be associated with NKG2D (or 2B4)-mediated activation (Urlaub et al., 2017; Upshaw et al., 2006; Kim et al., 2010). Therefore, to enhance the findings presented above, three inhibitors: wortmannin (PI3K pathway), PP1(Src pathway), and U73122 (PLC-γ pathway) were used to interfere with these known signaling pathways in the current experimental settings. As seen in Fig. 22, all of these inhibitors strongly block the activation of LFA-1 induced by NKG2D alone and in combination with 2B4. This suggests that, similar to NK cells, these specific

signaling pathways (PI3K, PLC-γ, and Src) also play a role in NKG2D- or NKG2D/2B4-induced LFA-1 activation in CIK cells.

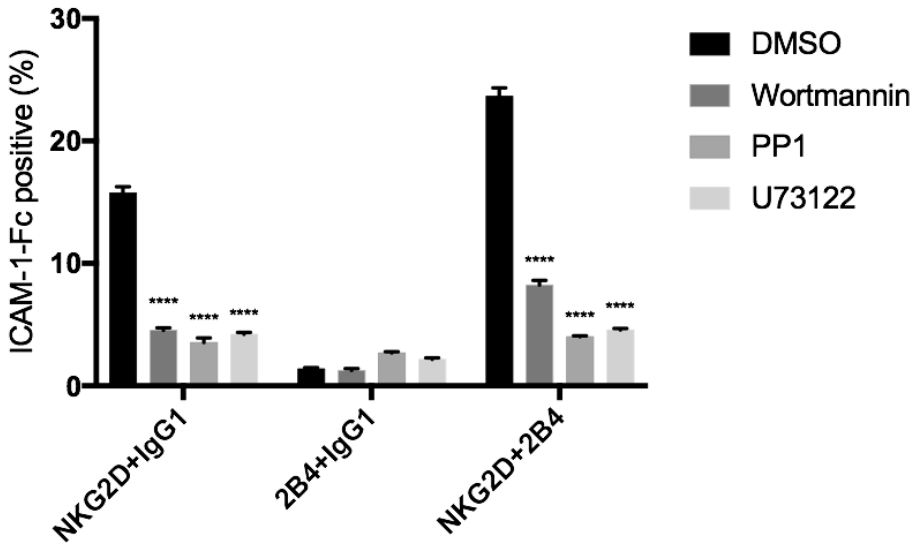

Figure 22. Signaling inhibition by chemical inhibitors to block LFA-1 activation. CIK cell preincubated with various signalling inhibitors (DMSO control, wortmannin [PI3K inhibitor], PP1 [Src kinase inhibitor], U73122 [phospholipase C-γ inhibitor]), stimulated with anti-NKG2D, anti-2B4 or both (1 μg/ml) by crosslinking the receptors with goat F(ab)2 anti-mouse IgG. The activation level of LFA-1 was measured by staining with ICAM-1-Fc complexes. The data are represented as mean ± SD of triplicates per condition and one representative of three independent experiments. ****$p < 0.0001$ calculated by two-way ANOVA, Bonferroni's post-hoc test.

3.2.3 Discussion

In study 2, we investigated the role of NKG2D and 2B4 individually or in combination in CIK cell related activities. Consistent with previous reports (Mehta et al., 1995; Verneris et al., 2004), the percentage of CD3+CD56+ CIK cells and the expression of NKG2D were significantly increased during the 14-day culture. Of note, as the CIK cells matured, they also exhibited higher 2B4 expression. One previous study failed to detect 2B4 on CIK cells (Dai et al., 2016), however, the use of different clones for the 2B4 marker could be a possible reason for this discrepancy. To ensure consistency in current study, we stained cells with a common clone (C1.7) against 2B4, as it was used in most of NK associated studies

(Kim et al., 2010; Valiante et al., 1993; Bryceson et al., 2006). As expected, all NK cells expressed 2B4 when the phenotype of freshly isolated PBMCs was analysed, thus confirming its expression on CIK cells.

As expected, the blockade of NKG2D partially attenuated the cytolysis and E/T conjugate against K562 cells. Additionally, redirecting P815 cells against NKG2D led to a significant increase in CIK cell-mediated cytotoxicity, E/T conjugate formation, and degranulation. In agreement with previous studies (Verneris et al., 2004; Karimi et al., 2005), these data support that NKG2D acts as an activating receptor for CIK cells and also imply that it may provide signals to activate LFA-1 on CIK cells which can enhance the E/T contact.

To further determine whether ligation of NKG2D alone is sufficient to activate CIK cells, monoclonal antibodies against NKG2D by the plate-bound method or by cross-linking with a secondary antibody were used. We demonstrate that NKG2D engagement is sufficient to induce degranulation and IFN-γ secretion from CIK cells on its own. Here, it is important to mention that the effect of NKG2D ligation on degranulation varied between CIK subgroups and, in particular, the CD3+CD56+ subgroup accounted for the majority of degranulated cells. This is in agreement with an early study showing that CD3+CD56+ cells are the most effective population of bulk CIK cells (Lu et al., 1994). The cytolytic activity of CIK cells is dependent on the cell-to-cell contact as Mehta et al. (1995) demonstrated that the killing could be completely blocked by anti-LFA-1 antibody. However, in the present study, active LFA-1 were found virtually undetectable on CIK cells during ex vivo expansion. Normally, LFA-1 has varying avidities and affinities for its ligand ICAMs, depending on the conformation and clustering of LFA-1 and modifications in them have been shown to be influenced by the inside-out signals from other activating receptors in T and NK cells (Urlaub et al., 2017; Enqvist et al., 2015; Gronholm et al., 2011). Consistent with this, we showed that LFA-1 could also be activated by the engagement of other molecules on CIK cells. More specifically, NKG2D engagement alone was able to induce the LAF-1 activation on mature CIK cells through similar signaling pathways (PI3K, PLC-γ, and Src) to NK cells (Urlaub et al., 2017; Upshaw et al., 2006; Kim et al., 2010). Of interest, it was reported that the resting NK cells barely responded to single NKG2D stimulation, whereas IL-2-

activated NK cells responded well (Bryceson et al., 2006; Bauer et al., 1999). Therefore, we speculate that the responsiveness of CIK cells to the NKG2D engagement might be attributed to the presence of IL-2 in CIK culture, as it was previously shown that only cells cultured in high-dose IL-2 expressed DAP10 and were cytotoxic (Verneris et al., 2004) and the incubation with cytokine could make effector cells more susceptible to the subsequent activating receptor stimulation (Urlaub et al., 2017). Taken together, the study presented here highlights that NKG2D alone is adequate enough to activate CIK cells, inducing degranulation, IFN-γ secretion and LFA-1 activation.

It is worth mentioning that although ligation of other receptors can induce activation of LFA-1, making it more active toward its ICAM ligands, still a higher rate of E/T conjugation may not always reflect a better immune response. To some extent, this can be seen in Fig. 13C, where the NK-resistant Raji cells formed a significantly higher E/T binding rate compared to the NK-sensitive K562 cells. On broader aspect, this may be explained by the dynamic regulatory process of E/T conjugation (involving both attachment and detachment systems), where an activating signal not only promotes E/T contact but also accelerates the dissociation (Springer et al., 2012).

Strikingly, the scenario appears to be different in 2B4 compared to NKG2D, with no effect of 2B4 blockade on cytotoxicity and E/T conjugate against SU-DHL-4 cells, and no increase in the redirected cytotoxicity, degranulation and E/T binding against 2B4-loaded P815 cells. Similarly, in the experiments using the plate-bound stimulation or by crosslinking receptors with a secondary antibody, 2B4 alone was not sufficient enough to modulate activities of CIK cells, hence was incapable of inducing the degranulation, IFN-γ secretion and LFA-1 activation. It can be assumed that a chronic exposure to neighboring CD48+ CIK cells (during ex vivo expansion) might make 2B4+ CIK cells more fatigued to react on secondary stimulation. One early study (Chen et al., 2004) reported that the 2B4-mediated signal in NK cells was defined solely by the tyrosine-based motifs in the cytoplasmic domain of 2B4 and it was not appreciably influenced by the transmembrane and extracellular segments of 2B4. This may also occur in CIK cells and further studies are needed. In most cases of the current study, 2B4 stimulation failed to produce

synergistic signals to NKG2D, except in the activation of LFA-1, suggesting that the synergy of NKG2D and 2B4 indeed exists in CIK cells but it is confined to certain functional responses (e.g. LFA-1 activation).

Contrary to previous findings that NKG2D provides strong synergistic effects with 2B4 in NK cells and costimulatory signals with the TCR-CD3 complex in CD8 cytotoxic T cells (Urlaub et al., 2017; Bryceson et al., 2006; Groh et al., 2001), we showed that NKG2D provides limited synergy with 2B4 but no significant costimulation with CD3 in activating CIK cells. There were similar results presented by Verneris MR et al (Verneris et al., 2004), which also showed that NKG2D did not produce synergy with CD3 in P815 redirected cytotoxicity. Despite the fact that CIK cells share phenotypic and functional characteristics with NK and T cells, a divergence in receptor function can be assumed. In one early study, NKG2D appeared not to provide additional activation of iNKT cells when combined with anti-CD3 stimulation (Kuylenstierna et al., 2011). Likewise, 2B4 alone failed to induce the degranulation of iNKT cells (Kuylenstierna et al., 2011). In this regard, ex vivo expanded CIK cells seem to function in a similar manner to the classical iNKT cells with deficiencies in 2B4 stimulation and costimulation of CD3 with NKG2D. A complete understanding of the interaction between these molecules is warranted, as aforementioned, NKG2D produces strong synergy with 2B4 in NK cells and costimulatory signals with the TCR-CD3 complex in T cells, providing the opportunity to improve the CD3ζ-based CAR construct for NK or T cells by integration of NKG2D or 2B4 (Li et al., 2018; Baumeister et al., 2019). Recently, CAR-CIK cells have also been explored with some encouraging results, however further validation will be required to draw conclusions (Schlimper et al., 2012; Merker et al., 2017; Magnani et al., 2020). Given the divergence in receptor function between CIK cells and NK (or T) cells as presented in the current study, the CAR structure for CIK cells may need to be established independently to maximize their functional potential.

In conclusion, the work presented in study 2 demonstrates that the engagement of NKG2D alone is sufficient to activate CIK cells without additional costimulatory signals, thereby strengthening the idea of targeting the NKG2D axis may improve the antitumor activity of CIK cells. In addition, CIK cells appear to function similarly

to the classical iNKT cells with deficiencies in 2B4 stimulation and in costimulation of CD3 with NKG2D, but exhibit divergences in receptor function compared to NK and T cells.

3.3 Study 3: Enhancement of antitumor activity of CIK cells by antibody-mediated inhibition of MICA shedding

3.3.1 Introduction

In study 2, we demonstrated that engagement of NKG2D receptor alone is sufficient to activate CIK cells without additional costimulatory signals. Next we asked whether upregulation of MICA/B expression on tumor cells could significantly enhance the antitumor activity of CIK cells.

In human, NKG2D receptor recognizes diverse ligands, including MICA, MICB, ULBP1-6 (Eagle and Trowsdale, 2007; El-Gazzar et al., 2013). These ligands rarely express on normal tissues, instead prevalently present on tumors of epithelial origin, for instance ovarian cancer, colorectal cancer and breast cancer and so on (Madjd et al., 2007; McGilvray et al., 2009; McGivary et al., 2010; de Kruijf et al., 2012). It is well accepted that NKG2D ligands are regulated through cellular stress pathways, including heat shock stress pathway (Venkataraman et al., 2007), DNA damage response ATM and ATR pathways (Gasser et al., 2005; Gasser and Raulet, 2006), endogenous microRNAs (Stern-Ginossar et al., 2008; Breunig et al., 2017). Therefore, NKG2D ligands can be induced under cellular stress conditions, e.g., viral infection and cellular transformation (Groh et al., 1998; Groh et al., 2001).

Expression of NKG2D ligands on tumor cells increase their vulnerability to the immune system. However, tumor cells frequently escape the immune surveillance of NKG2D pathways by loss of NKG2D ligand expression through proteolytic shedding or exosome secretion (Baragano et al., 2014). Several molecules have been reported to correlate with the proteolytic shedding of MICA/B, such as ERp5 and ADAM proteins and MMPs (Kaiser et al., 2007; Boutet et al., 2009; Waldhauer et al., 2008; Groh et al., 2002). Based on the fact that the membrane-proximal α3 domain of MICA/B is the site of proteolytic shedding (Kaiser et al., 2007), a new monoclonal antibody (7C6 mAb) has been recently developed to specifically target the MICA a3 domain and shown the ability to inhibit MICA/B shedding and stabilize their surface expression (Ferrari de Andrade et al., 2018).

In study 3, we aimed to investigate the effects of 7C6 antibody-mediated inhibition of MICA shedding on the antitumor acitivity of CIK cells.

3.3.2 Results

3.3.2.1 NKG2D expression and phenotype of CIK cells

After 14 days of ex vivo expansion, the bulk CIK cells were a heterogeneous population comprised of CD3+CD56+ cells (31.3% ± 11.2%), CD3+CD56- T cells (65.6% ± 8.9%), and a small percentage of CD3-CD56+ NK cells (2.8% ± 4.4%) (Fig. 23, one representative data from four donors). In particular, the percentage of CD8+ cells in CD3+CD56+ subset was slightly higher than that in CD3+CD56- T cells (83.0% ± 12.4% vs 79.5% ± 5.7%, respectively). Additionally, most of cells expressed NKG2D (90.7% ± 2.0%). As shown in Fig. 23B and Fig. 23C, NKG2D expressed on all CD8+ cells either within CD3+CD56+ subset or CD3+CD56- T cells.

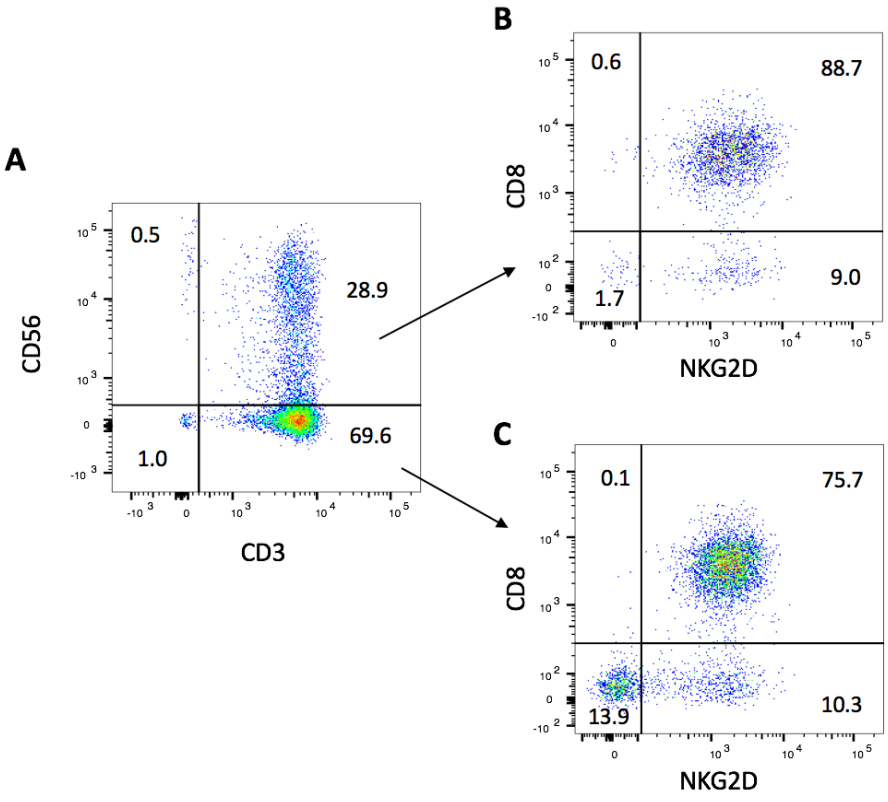

Figure 23. Phenotyping and NKG2D expression on mature CIK cells. Phenotype and NKG2D expression of CIK cells on day 14 were measured on FACS after staining with FITC-CD3, PE-CD56, BV421-CD8 and APC-NKG2D antibodies. Dead cells were excluded by 7AAD. **(A)** The percentage of various subsets of bulk CIK cells. **(B)** The expression of CD8 and NKG2D within CD3+CD56+ population.

(C) The expression of CD8 and NKG2D within CD3+CD56- population. Numbers represent the percentage (%) of individual gating. Data are one representative of CIK cells from four donors.

3.3.2.2 Inhibition of MICA shedding and stabilization of surface MICA/B expression on tumor cells by 7C6 antibody

Compared with the control IgG1 antibody treatment, MICA shedding from Hela cells in the presence of 7C6 antibody was strongly inhibited (Fig. 24A, 1081.9 ± 69.1 pg/mL vs. 613.4 ± 48.6 pg/mL, respectively) and in turn the surface MICA/B expression was significantly increased (Fig. 24B, MdFI, 2644.5 ± 29.0 vs. 3367.7 ± 40.7, respectively). Similar results were observed when MDA-MB-231 cells used as targets, less shedding of MICA (Fig. 24A, 819.6 ± 17.6 pg/mL vs. 352.8 ± 24.7 pg/mL, respectively) and increased surface MICA/B expression (Fig. 24B, MdFI, 592.3 ± 64.0 vs. 968.7 ± 70.2, respectively) were shown in the presence of 7C6 antibody in contrast to IgG1 group. In Fig. 24B and Fig. 24C, nearly a three-fold increase in MICA/B expression on K562 cells was observed after treatment with 7C6 antibody versus IgG1 control. However, no MICA shedding from K562 cells was detected (Fig. 24D). As reported by others (Cluxton et al., 2019), K562 cells did shed MICB rather than MICA. Thus, the increase in surface MICA/B expression on K562 cells following 7C6 antibody treatment is more likely led by the inhibition of MICB shedding. Consistent with the previous study (Ferrari de Andrade et al., 2018), we here showed that 7C6 antibody is able to inhibit the shedding of MICA from MICA/B-bearing tumor cells, resulting in a substantial increase of the cell surface density of MICA.

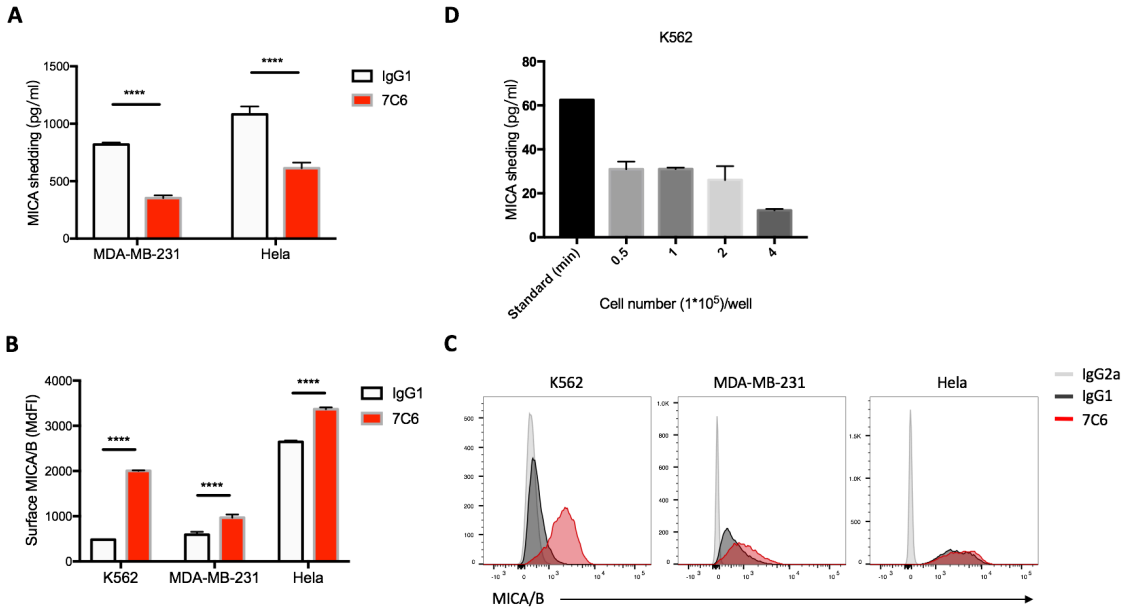

Figure 24. 7C6 mAb inhibits MICA shedding and increases the cell surface density of MICA/B. (A) Human Hela cervical and MDA-MB-231 breast cancer cell lines were treated with 7C6 or IgG1 control antibody at 10 µg/mL for 48 h. Shed MICA was quantified in the supernatant by sandwich ELISA. Data are mean ± SD of triplicate measurements; data are one representative of three independent experiments. ****p < 0.0001 calculated by two-way ANOVA, Bonferroni's post-hoc test. **(B)** K562, Hela, and MDA-MB-231 cells were treated with 7C6 or IgG1 control antibody at 10 µg/mL for 24 h. Surface MICA/B expression was measured by flow cytometry following staining with APC-conjugated 6D4 antibody; median fluorescence intensities (MdFI) are shown. Data are mean ± SD of triplicate measurements; data are one representative of three independent experiments. ****p < 0.0001 calculated by two-way ANOVA, Bonferroni's post-hoc test. **(C)** Histograms depict the surface level of MICA/B following treatment with 7C6 (red) or IgG1 control (black). IgG2a (grey) was the staining isotype control. Data are part of the experiment shown in 'B'. **(D)** Indicated number of K562 cells were incubated with 7C6 mAb or IgG1 control antibody at 10 µg/mL for 48 h. Shed MICA was quantified in the supernatant by sandwich ELISA. Data are mean ± SD of duplicate measurements and one representative of three independent experiments. Black bar indicates the sensitivity of this ELISA kit with a minimum detectable concentration of 62.5 pg/mL.

3.3.2.3 7C6 mAb enhances the cytotoxicity of CIK cells in an NKG2D-dependent way

Next, flow cytometric cytotoxicity was performed. As shown in Fig. 25, the cytolysis of CIK cells against indicated tumor targets was significantly enhanced by the addition of 7C6 mAb, as compared to the IgG1 control treatment. For example,

81.3 ± 3.4% vs 46.6 ± 6.7% of K562 cells, 72.3 ± 1.0% vs. 46.3 ± 3.6% of MDA-MB-231 cells and 77.4 ± 4.6% vs. 38.8 ± 10.7% of Hela cells were killed at 10:1 E/T ratio.

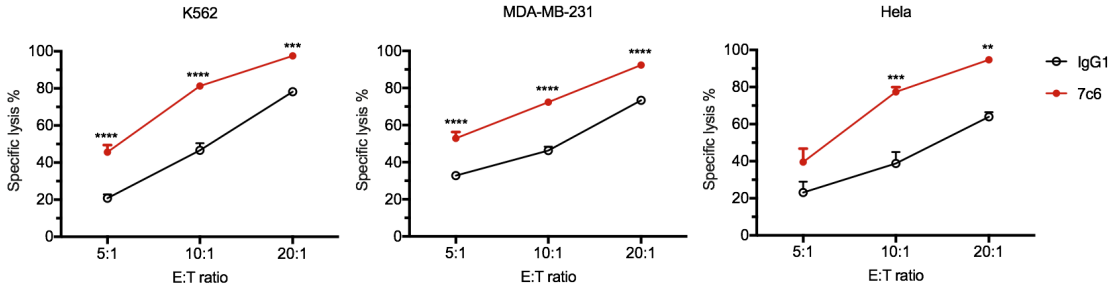

Figure 25. 7C6 mAb increases cytotoxicity of CIK cells against tumor targets. Cytotoxicity of CIK cells against indicated tumor cell lines in the presence of 7C6 or isotype control IgG1 antibody (10 μg/ml) was performed by FACS. Data are mean ± SD of triplicates per condition and one representative of three independent experiments. **p < 0.01, ***p < 0.001, ****p < 0.0001 calculated by two-way ANOVA, Bonferroni's post-hoc test.

As expected, the enhancement of cytolysis was completely inhibited by preincubation of CIK cells with NKG2D blocking antibody (clone, 1D11) to the basal level as that treated with 1D11 in the presence of IgG1 control (Fig. 26), suggesting that the 7C6-mediated improvement of cytotoxicity is dependent on the NKG2D axis.

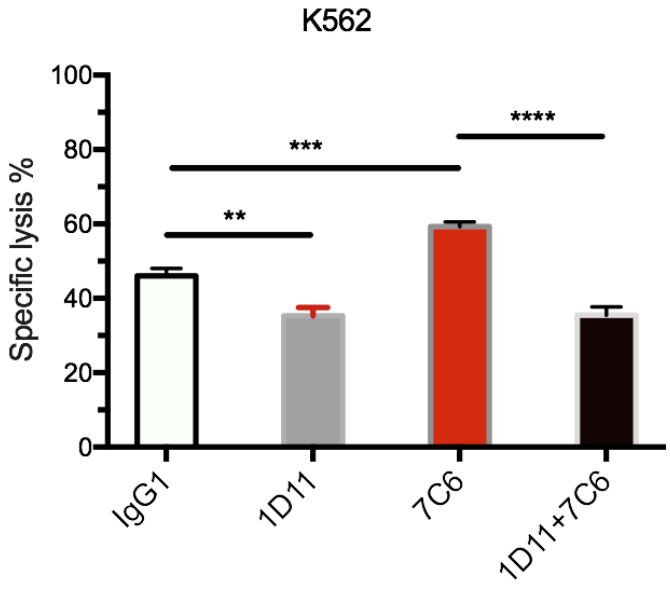

Figure 26. The 7C6-mediated enhancement of cytotoxicity is completely inhibited by NKG2D blockade. Cytotoxicity of CIK cells (preincubated with 1D11 or IgG1 antibody, at 10 μg/ml) against K562 cells in the presence of 7C6 or isotype control IgG1 antibody (10 μg/ml) was performed by FACS. Data are mean ± SD of triplicates per condition and one representative of three independent experiments. **p < 0.01, ***p < 0.001, ****p < 0.0001 calculated by one-way ANOVA, Bonferroni's post-hoc test.

Next, we examined the effect of 7C6 mAb on cytokine release of CIK cells. As seen in Fig. 27A and Fig. 27B, the IFN-γ secretion of CIK cells against Hela and MDA-MB-231 cells was significantly increased in the presence of 7C6 mAb as compared with that treated with isotype IgG1, while no effect on CIK cells in the absence of target cells.

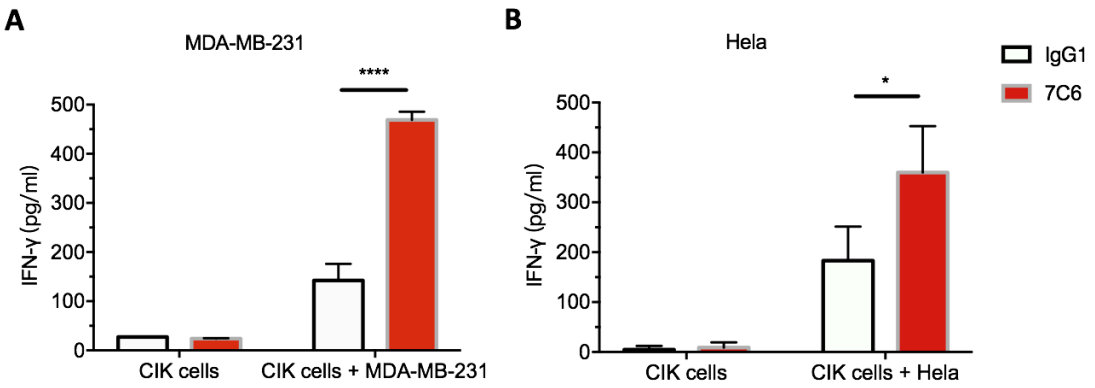

Figure 27. 7C6 mAb increases IFN-γ secretion of CIK cells against tumor targets. Following culture of CIK cells alone or with indicated tumor cells for 24 h at a 20:1 of E:T ratio in the presense of 7C6 or IgG1 antibody, IFN-γ production in the supernatant was detected by sandwich ELISA. **(A)** IFN-γ secretion of CIK cells against MDA-MB-231 cells. **(B)** IFN-γ secretion of CIK cells against Hela cells. Data are mean ± SD of triplicates per group, representative of three independent experiments. *p < 0.01, ****p < 0.0001 calculated by two-way ANOVA, Bonferroni's post-hoc test.

Taken together, these data demonstrate that 7C6 mAb can significantly promote the CIK-mediated cytotoxicity and IFN-γ secretion against these tumor targets, exclusively through the NKG2D pathway.

3.3.2.4 7C6 mAb enhances the degranulation of CIK cells, with the involvement of both CD3+CD56+ and CD3+CD56- subsets

To further investigate the effect of 7C6 mAb on CIK cell-mediated antitumor activity, the CD107a degranulation assay was performed. As seen in Fig. 28, the degranulation of CIK cells against both K562 cells and Hela cells was significantly improved in the presence of 7C6 mAb in contrast to the IgG1 treatment (32.8 ± 1.7% vs. 21.8 ± 1.1%, 40.4 ± 2.7% vs. 28.5 ± 0.8%, respectively). Expectedly, masking CIK cells with NKG2D blocking antibody (clone, 1D11) strongly inhibited this effect, which was brought close to the value treated with IgG1 control alone.

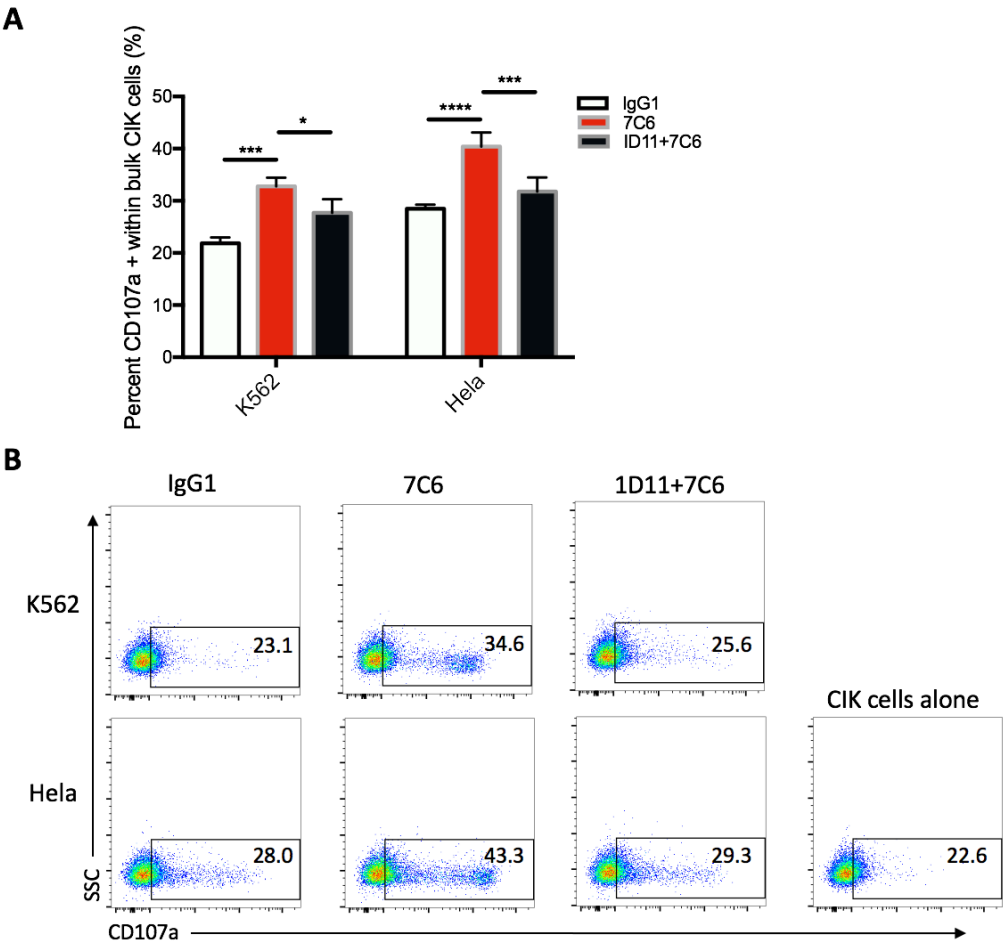

Figure 28. 7C6 mAb increases the degranulation of CIK cells against tumor targets. CIK cells pretreated with 1D11 or IgG1 antibody at 10 μg/mL (1 hour prior to coculture) were co-incubated with indicated tumor cells at 5:1 E/T ratio in the presence of 7C6 mAb or IgG1 antibody at 10 μg/mL for 5 hours. APC-anti-CD107a (1:100) was added at the start of coculture. Degranulation was determined by FACS. **(A)** Bargraph showing the percentage of CD107a expression on bulk CIK cells against K562 or Hela cells in indicated conditions. Data are mean ± SD of triplicates, representative of three independent experiments. *$p < 0.05$, ***$p < 0.001$, ****$p < 0.0001$ calculated by two-way ANOVA, Bonferroni's post-hoc test. **(B)** Dot plots showing the representative CD107a expression on bulk CIK cells against K562 cells (upper panel) and Hela cells (lower panel), numbers represent the percentage of gated population.

Similar effects were also observed when CD3+CD56+ and CD3+CD56− subsets of CIK cells were further analyzed. The CD107a expression on both subsets against Hela cells (Fig. 29) or K562 cells (Fig. 30) was significantly upregulated when 7C6 mAb was added in the culture. Of note, the enhancement in degranulation was nearly offset by blocking NKG2D receptor of CIK cells prior to coculture with tumor

cells. Interestingly, CD3+CD56+ cells exhibited a better response to the treatment of 7C6 mAb than the CD3+CD56- counterpart against Hela cells (Fig. 29) or against K562 cells (Fig. 30).

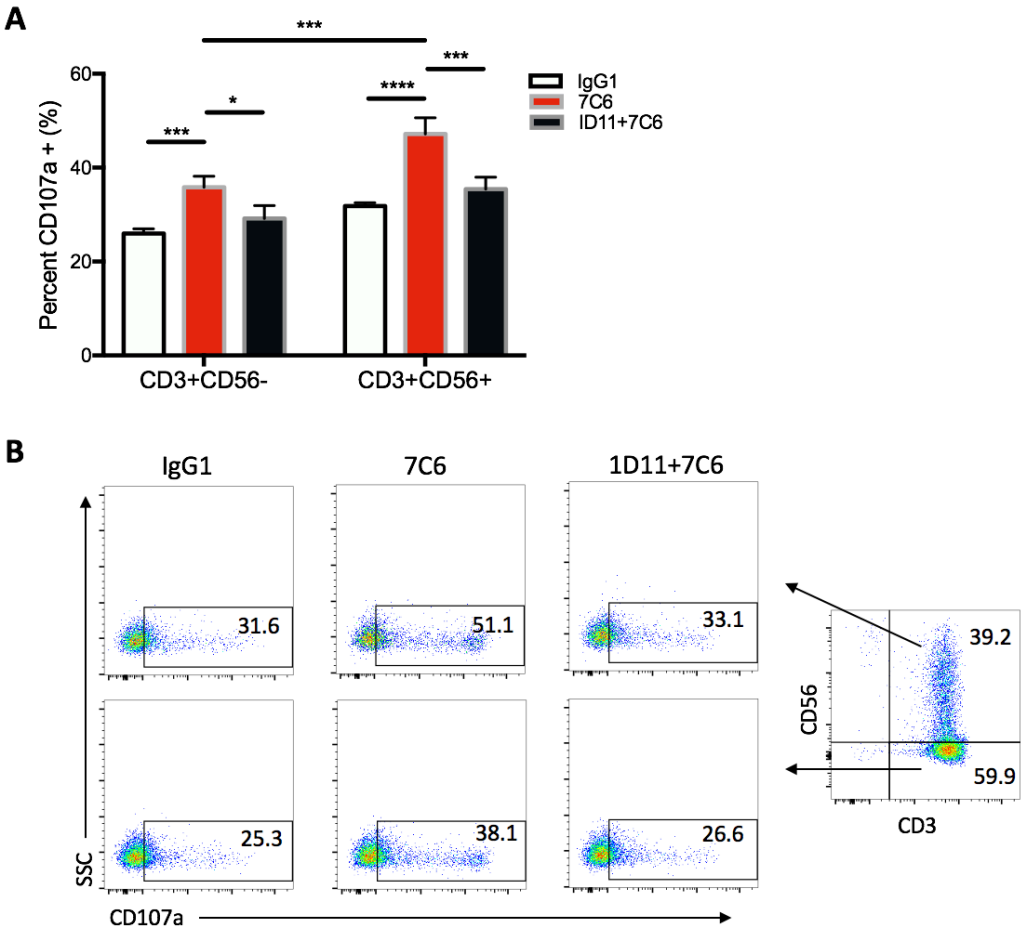

Figure 29. 7C6 mAb increases the degranulation of subsets of CIK cells against Hela cells. CIK cells pretreated with 1D11 or IgG1 antibody at 10 µg/mL (1 hour prior to coculture) were co-incubated with Hela cells at 5:1 E/T ratio in the presence of 7C6 mAb or IgG1 antibody at 10 µg/mL for 5 hours. APC-anti-CD107a (1:100) was added at the start of coculture. Degranulation of subsets of CIK cells was determined on FACS by staining cells with FITC-CD3 and PE-CD56 antibodies. **(A)** Bargraph showing the percentage of CD107a expression on CD3+CD56- and CD3+CD56+ subsets against Hela cells in response to indicated conditions. Data are mean ± SD of triplicates, representative of three independent experiments. *$p < 0.05$, ***$p < 0.001$, ****$p < 0.0001$ calculated by two-way ANOVA, Bonferroni's post-hoc test. **(B)** Dot plots showing the representative CD107a expression on CD3+CD56+ cells (upper panel) and CD3+CD56- cells (lower panel), numbers represent the percentage of gated population.

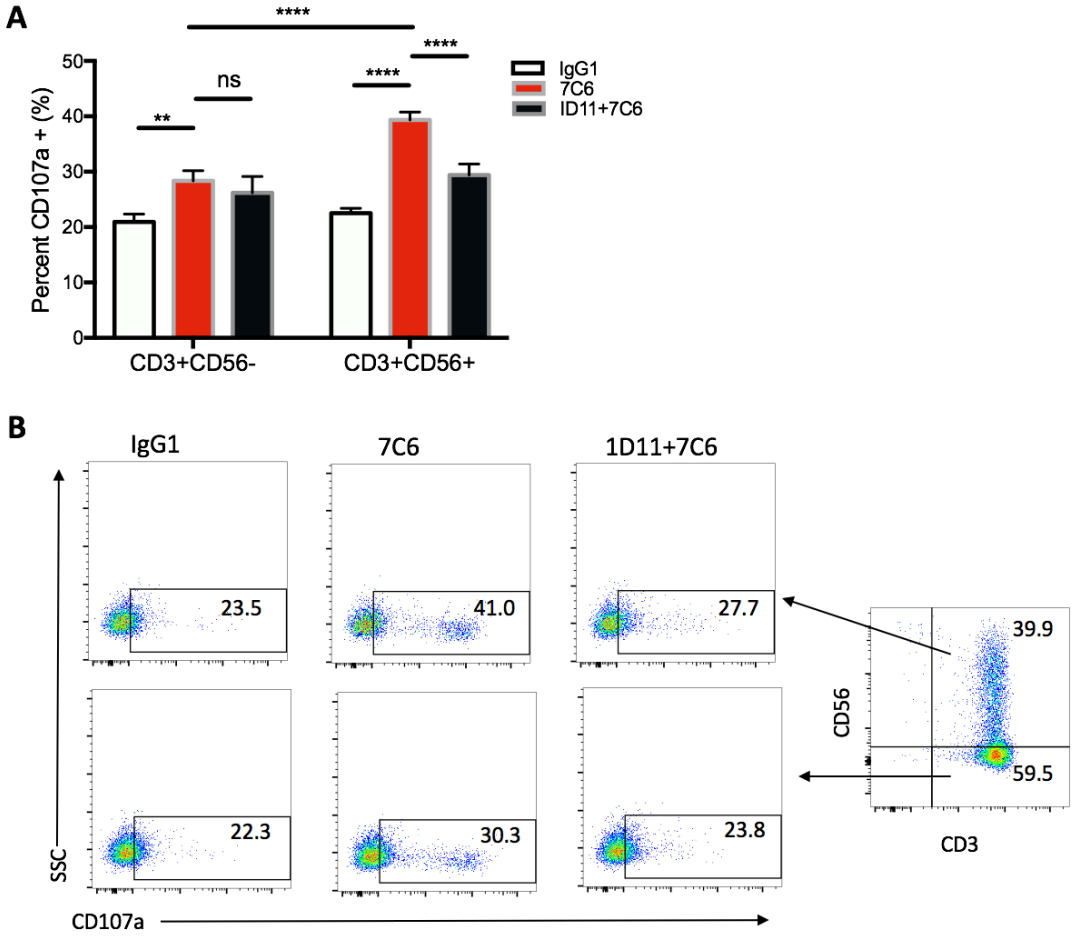

Figure 30. 7C6 mAb increases the degranulation of subsets of CIK cells against K562 cells. CIK cells pretreated with 1D11 or IgG1 antibody at 10 µg/mL (1 hour prior to coculture) were co-incubated with K562 cells at 5:1 E/T ratio in the presence of 7C6 mAb or IgG1 antibody at 10 µg/mL for 5 hours. APC-anti-CD107a (1:100) was added at the start of coculture. Degranulation of subsets of CIK cells was determined on FACS by staining cells with FITC-CD3 and PE-CD56 antibodies. **(A)** Bargraph showing the percentage of CD107a expression on CD3+CD56- and CD3+CD56+ subsets against Hela cells in response to indicated conditions. Data are mean ± SD of triplicates, representative of three independent experiments. *p < 0.05, ***p < 0.001, ****p < 0.0001 calculated by two-way ANOVA, Bonferroni's post-hoc test. **(B)** Dot plots showing the representative CD107a expression on CD3+CD56+ cells (upper panel) and CD3+CD56- cells (lower panel), numbers represent the percentage of gated population.

Altogether, these data indicate that the presence of 7C6 mAb in the effector/target coculture can promote the degranulation of CIK cells, and both CD3+CD56+ and CD3+CD56- subpopulations are involved in this activation while CD3+CD56+ cells exhibit a better response. In addition, the strong inhibition of the

enhancement in degranulation by NKG2D blocking suggests the NKG2D system is the major signaling involved in this activity.

3.3.3 Discussion

In study 3, we used a novel antibody which is able to specifically target α3 domain of MICA and MICB molecules while sparing the NKG2D binding site α1 and α2 domains (Ferrari de Andrade et al., 2018). In agreement with the previous report (Ferrari de Andrade et al., 2018), our study show that anti-MICA specific antibody strongly inhibited the loss of MICA from the tumor membrane surface and substantially preserved the density of MICA/B. As proposed, this might be the consequence of the competitive binding of MICA antibody to the α3 domain which could leave less space for ERp5 and protease to execute the shedding.

NKG2D can be induced in the presence of IL-2, regardless of the dosage during the ex vivo CIK expansion, but only cells cultured in high doses of IL-2 gained expression of the adapter protein DAP10 and were cytotoxic (Verneris et al., 2004). In the current study, the CD3+CD56+ subpopulation was shown to have the highest expression of NKG2D, this may facilitate it to be the main effective effectors in the bulk CIK cells. In the presence of 7C6 mAb, a significant increase in cytotoxicity, IFN-γ secretion and degranulation of CIK cells was observed against tumor cells as compared to IgG1 control antibody. As expected, the effect on the augmentation in cytotoxicity and degranulation was nearly completely inhibited by pretreatment of CIK cells with NKG2D blocking antibody. These indicate no or little involvement of other molecules except for the NKG2D receptor in the 7C6-driven enhancement of CIK cell killing against target cells in our current experimental settings. The Fc segment of 7C6 mAb is of human IgG1 origin which is replaced from the parental anti-MICA α3 mouse IgG2b antibody. Therefore, 7C6 mAb is able to additionally induce the ADCC (antibody-dependent cellular cytotoxicity) effect in human NK cells by engaging the CD16 Fc receptor (Ferrari de Andrade et al., 2018). However, this does not appear to be the case for CIK cells in the current study since NKG2D blockade nearly completely inhibited the effect induced by 7C6 mAb. Of course, the data shown here can only represent the CIK cells from a small sample size (10 donors). it cannot be concluded that there is no engagement of CD16 in the 7C6-

mediated enhancement of cytotoxicity of CIK cells. Because CD16 expression on CIK cells was reported to be donor-dependent and could mediate the ADCC activity as well (Cappuzzello et al., 2016). We assume that ADCC can be induced by 7C6 mAb if a certain amount of CD16 is present on CIK cells, but this needs further investigation by screening CIK cells with high expression of CD16.

It is well known that CD3+CD56+ CIK subset has a lower capacity of proliferation but a more robust antitumor activity compared with the CD3+CD56- subset, which is considered as precursor cells of CD3+CD56+ cells (Lu et al., 1994; Nishimura et al., 2008). Consistent with this, a significant increase in degranulation was observed in both subpopulations after treatment of 7C6 antibody while CD3+CD56+ cells remained a higher degranulation rate than its counterpart. Comparison to the results in previous chapter showing that CD3+CD56- T cells barely responded to the NKG2D stimulation in degranulation, here this chapter showed that the upregulation of MICA/B by 7C6 mAb is be able to trigger and activate both CD3+CD56+ and CD3+CD56- T subsets of CIK cells. The discrepancy in the response of CD3+CD56- T cells between these two chapters may be due to the differences in the source of stimulation. In chapter 2, it was a mAb-mediated stimulation (anti-NKG2D antibody, 1D11), which may not be able to completely mimic the activation process induced by a physiologic ligand (the membrane bound ligand engagement). Another possible reason could be a synergistic effect induced by the 7C6-mediated upregulation of MICA/B and other receptor-ligand engagements, while in chapter 2 only limited molecules were tested for the combinatory effect with NKG2D ligation. Of interest, in previous studies (Ferrari de Andrade et al., 2018; Ferrari de Andrade et al., 2020), only NK cells rather than CD8 T cells were shown to be essential for the therapeutic activity of 7C6 mAb against cancer metastases. This may be explained by the roles of NKG2D in NK and T cells, in which NKG2D engagement can directly activate NK cells whereas it can only costimulate CD8 T cells with the association of TCR engagement (Bauer et al., 1999; Groh et al., 2001). Hence, we further showed that the ex vivo expanded CD8+ T cells behave differently from the primary CD8+ T cells. This was especially apparent in the experiments using K562 cells as targets, we could say 7C6 mAb augmented the degranulation of expanded CD8+ CIK cells in an NKG2D-dependent and MHC-unrestricted manner, since

K562 cells lack the expression of HLA class I and class II molecules (Hirano et al., 1996).

This enhancement of 7C6-mediated cytolytic activity appears to be due to the increase in surface MICA/B expression, although decrease in shed MICA may also be a relevant contributing factor. Contention remains regarding the function of soluble NKG2D ligands. Some studies have shown that the existence of soluble MICA/B in the serum could degrade and internalize NKG2D expressed on NK or CD8+ T cells leading to tumor escape from immune response (Groh et al., 2002). Others have considered the soluble MICA/B just competitively bound to the NKG2D receptor on these effectors (Raulet et al., 2013). Opposite to those, soluble Mult1 (a NKG2D ligand in mouse) has been found to promote NK cells activation and tumor rejection (Deng et al., 2015). One likely explanation is that Mult1 possesses higher affinity than MICA/B to NKG2D receptor. In addition, the downregulation of NKG2D under condition of high level of soluble MICA/B might also be induced by cytokines like TGF-β (Clayton et al., 2008). However, the downregulation of NKG2D can be reversed by either stimulation with anti-CD3 antibody (Groh et al., 2002) or cytokines such as IL-2 and IL-15 (Wu et al., 2004). Interestingly, a recent study showed that the anti-α3 domain-specific MICA antibody could completely reverse the soluble MICA-mediated NK cell suppression in a Fc-dependent manner (Du et al., 2019).

NKG2D expression on NK or T cells in some cancer patients was shown to be impaired (Groh et al., 2002; Huergo-Zapico et al., 2014) and abnormal NK cell function/activity in patient with different malignancies was also reported (Konjevic et al., 2012). If administration of 7C6 mAb is proved safe in patients, adoptive CIK cell therapy therefore may provide a potent combination partner with anti-MICA/B antibody-mediated immunotherapy.

4. Discussion

4.1 Aims and main findings

As one of promising candidates of adoptive immunotherapy, CIK cell therapy has shown some encouraging results in clinical trials for treatment of both solid and blood malignancies (Zhang and Schmidt-Wolf, 2020). With multiple advantages, such as the convenient and inexpensive expansion capability, good safety profile with low incidence of GVHD in allogeneic cancer patients, CIK cell therapy may provide more benefits to those patients with early stage of cancers when the tumor load is low. Additionally, a better understanding of the role of molecular components in CIK cells may also aid in developing new strategies for improving their antitumor efficacy. The main aim of this thesis is to improve the antitumor activity of CIK cells by targeting the NKG2D axis.

Firstly, in order to evaluate the in vitro cytotoxicity of CIK cells in a more accurate and efficient way, we aimed to optimize and standardize the already established flow cytometric cytotoxicity assay. In **study 1**, we demonstrate that under our experimental condition, there was no cross-contamination between the labeled target cells and effector cells. Furthermore, effector cell labeling alone in this assay should be avoided, due to overestimated cytolysis as a consequence of exclusion of viable targets in effector-target aggregates. In addition, the gating strategy could be improved by plotting CFSE vs FSC to discriminate some early apoptotic events without additional apoptosis markers (e.g. Annexin V). More importantly, we found an alternative to the use of calibration beads in standardizing the flow cytometry assay. Instead of using beads, sample acquisition in a fixed time was shown to have the same effect on the lysis evaluation as beads application but exhibit a greater stability. We also compared various stopping acquisition time, and found no impact of acquisition duration on the lysis calculation, thus, making a shorter sample acquisition possible. Taken together, these findings allow us to perform the flow cytometric cytotoxicity assay in a more accurate, efficient, and cost-effective way. This improved method was applied throughout the whole thesis.

In **study 2**, we aimed to investigate the individual and cumulative contribution of NKG2D and 2B4 in the activation of CIK cells. Besides performing the blocking experiments and P815-based redirected experiments, we crosslinked the receptors on CIK cells by immobilized antibodies or a secondary antibody. We demonstrated: a) NKG2D (not 2B4)

is implicated in CIK cell-mediated cytotoxicity, E/T conjugate formation and degranulation, b) NKG2D alone is adequate enough to induce degranulation, IFN-γ secretion and LFA-1 activation in CIK cells, while 2B4 only provides limited synergy with NKG2D (e.g. in LFA-1 activation), c) NKG2D was unable to costimulate CD3. Contrary to previous studies where NKG2D showed strong synergistic effects with 2B4 in NK cells and costimulatory signals with the TCR-CD3 complex in CD8 cytotoxic T cells (Groh et al., 2001; Urlaub et al., 2017; Bryceson et al., 2006), the divergence in the role of NKG2D between CIK cells and NK (or T) cells can be assumed. Nevertheless, here we showed that NKG2D engagement alone suffices to activate CIK cells, thereby strengthening the idea of targeting the NKG2D axis may enhance the cytotoxicity of CIK cells against NKG2D ligand-expressing tumor cells.

In **study 3**, we aimed to investigate the effect of anti-MICA antibody on the antitumor activity of CIK cells. In this work, we used an monoclonal antibody (7C6 mAb) which was previously reported to specifically target the α3 domain of MICA/B and inhibit the ligand shedding from tumor cells. In agreement with that study (Ferrari de Andrade et al., 2018), we here showed that 7C6 mAb strongly inhibited the loss of MICA by MICA/B-bearing tumor cell lines (Hela, MDA-MB-231) and increased its surface expression. The underlying mechanism by which 7C6 mAb prevents the shedding of MICA remains unclear, but it is proposed that the competitive binding of MICA antibody to the α3 domain might leave less space for ERp5 and protease to execute the shedding. In the current study, the stabilization of MICA/B on tumor cells by 7C6 mAb made them more sensitive to CIK cells, leading to a significant increase in cytotoxicity, degranulation and IFN-γ secretion. These effects were proven to be mediated through NKG2D pathway since the augment in these activities were brought back to the basal levels when NKG2D receptor was blocked. Notably, both CD3+CD56- and CD3+CD56+ CIK subpopulations were accountable to the enhancement in degranulation after 7C6 mAb treatment while CD3+CD56+ cells remained the highest contribution. Collectively, these data indicate that the 7C6-mediated inhibition of MICA shedding can stabilize the ligand expression and significantly potentiate the antitumor activity of CIK cells.

In summary, we demonstrate that NKG2D engagement solely is sufficient to activate CIK cells and the upregulation of NKG2D ligands on tumor cells allows CIK cells to kill

them more efficiently. Therefore, targeting the NKG2D axis is a promissing approach to improve the antimumor activity of CIK cells.

4.2 Future perspectives

In this thesis, we demonstrate that NKG2D ligation alone is able to activate CIK cells and the upregulation of NKG2D ligands on tumor cells makes them more vulnerable to CIK cells. This may also apply to other situations where NKG2D ligands are induced or upregulated, for instance chemotherapy or radiotherapy. Chemotherapy and radiotherapy have been reported to induce or upregulate the NKG2D ligands on tumor cells, mostly through an ATM and/or ATR mediated DNA damaging pathways (Gasser et al., 2005). Weiss et al. (2018) showed that temozolomide (TMZ) or irradiation (IR) could induce NKG2D ligands in vitro and in vivo in glioblastoma models, and glioblastoma patient samples had increased levels of NKG2D ligands after therapy with TMZ and IR. This enhanced the immunogenicity of glioma cells in a NGK2D-dependent manner and the survival benefit afforded by TMZ or IR relied on an intact NKG2D system and was decreased upon inhibition of the NKG2D pathway (Weiss et al., 2018). Based on these data, the combination of CIK therapy with the conventional chemoradiotherapy might be a promising approach to potentiate the therapeutic effects for cancer patients. Indeed, evidence from one phase III clinical trial shows that the addition of autologous CIK cells immunotherapy to standard chemoradiotherapy with TMZ improved the progression-free survival for glioblastoma patients without significant adverse events (Kong et al., 2017). But it remains unclear whether the NKG2D pathway had played a significant role in the concomitant therapy since this study did not examine the NKG2D ligand expression on the tumor. Given the NKG2D-mediated cytotoxicity of CIK cells and the inducibility of NKG2D ligands by chemoradiotherapy, the evaluation of the level of NKG2D ligand (e.g. MICA/B) before and after chemoradiotherapy may have relevant implications on the survival rate or the prognosis prediction, as shown by Yu et al. (2015) demonstrating that gastric carcinoma patients with high expression of MICA had longer disease-free survival and overall survival in the adjuvant chemotherapy plus CIK group. Therefore, future preclinical and clinical studies with more detailed information about the NKG2D system will help us better understand the potential of combinatory treatment of CIK cells with the traditional chemotherapy and/or radiotherapy.

By using anti-CD3 antibody as a positive control in this thesis, CD3 ligation showed much stronger effect in CIK cell activation than the other two stimuli (NKG2D and 2B4), suggesting that CIK cells can be well tolerated and function efficiently from moderate to strong stimuli. And also it indicates that the cytoplasmic domain (CD3-ζ) of CD3 receptor is a dominant activating signaling domain for CIK cells. Therefore, triggering this signaling domain may make full use of the cytotoxic potential of CIK cells. One of the possibilities is incorporating CIK cells with a genetically modified CD3-ζ-based CAR. CD3-ζ is preferably used as the main signaling domain for most CAR-T or CAR-NK cell studies. To date, four CD19-directed CAR-T cell products have been approved by the US Food and Drug Administration (FDA) for the treatment of B cell malignancies (Maude et al., 2014; Mullard, 2017; Chan et al., 2021). Nonetheless, CAR-modified T-cells have a number of limitations: 1) The generation of an autologous product for each individual patient is logistically cumbersome and restrictive for widespread clinical use; 2) The manufacturing of CAR T-cells often takes several weeks, making it impractical for patients with rapidly advancing disease; 3) it is not always possible to generate clinically relevant doses of CAR T-cells from heavily pre-treated patients. Therefore, other alternatives are needed to overcome these limitations. Most recently, the first clinical trial using CD19-CAR-CIK cells for the treatment of relapsed B-ALL patients after allogeneic HSCTs has shown promising results (Magnani et al., 2020). In this study, 6 out of 7 patients who received one infusion of high doses of CAR CIK cells experienced CR, more impressively, with only grade 1-2 CRS, but no GVHD and neurotoxicity. Several other preclinical studies also reported that antigen directed CAR-CIK cells exhibit superior antitumor capability than unmodified CIK cells (Leuci et al., 2020; Magnani et al., 2018; Leuci et al., 2018; Merker et al., 2017; Du et al., 2016; Oelsner et al., 2016; Pizzitola et al., 2014; Schlimper et al., 2012). However, the CAR constructs used in these studies are initially designed for CAR-T cells. Since divergences in receptor function between CIK cells and NK (or T) cells have been observed in the current thesis, the CAR structure for CIK cells may need to be customized and optimized to maximize their functional potential. As shown in one early study, CIK cells armed with CD28-ζ CAR outperformed those engineered with CD28-OX40-ζ CAR which is commonly used as a “super stimulation“ in CAR-T cells (Hombach et al., 2013). In the same study, the activation-induced cell death (AICD) of CIK cells was induced by the CAR-mediated stimulation and could not be rescued by either CD28 or OX40

costimulation (Hombach et al., 2013). In CAR-T cells, incorporation of 4-1BB shows higher levels of the anti-apoptotic proteins BCL-2 and BCL-XL, and a metabolic profile that may enhance memory formation (Kawalekar et al., 2016; Li et al., 2018). Therefore, constructing 4-1BB as a costimulatory domain of CAR-CIK cells may protect cells from AICD and prolong the survival of CIK cells and further enhance the antitumor efficacy.

Although NKG2D failed to costimulate CD3 in CIK cell-mediated cytotoxicity as shown in the present thesis, it seems that the CD3-ζ-based CAR is strong enough to trigger CIK cells and a better antitumor response may be obtained by incorporation of other costimulatory domains which can promote the expansion and survival of CAR-CIK cells. In addition, given the wide overexpression of NKG2D ligands in various tumor types, incorporation of NKG2D as an ectodomain of CAR construct may provide a broader antitumor spectrum for CAR-CIK cells. Since the allogeneic CIK cell therapy has been proven safe and well tolerated, together with the advantage of convenient and inexpensive expansion capability, CIK cells provide an attractive alternative to T-cells for CAR engineering as an off-the-shelf product.

5. Abstract

CIK cells are an ex vivo expanded heterogeneous cell population with an enriched NK-T phenotype (CD3+CD56+). Due to the convenient and inexpensive expansion capability, together with low incidence of GVHD in allogeneic cancer patients, CIK cells are a promising candidate for immunotherapy. It is well known that NKG2D plays an important role in CIK cell-mediated antitumor activity, thus upregulation of NKG2D ligands on tumor cells might elevate the immune response of CIK to these tumor targets. However, it still remains unclear whether NKG2D engagement alone is sufficient or if it requires additional co-stimulatory signals (e.g. 2B4) to activate CIK cells. In order to address these issues and assess the in vitro cytotoxicity of CIK cells in a more accurate and efficient way, we first established an improved flow cytometric cytotoxicity assay based on prior studies. Instead of using calibration beads, a fixed acquisition time can be utilized to standardize the flow cyometric assay with similar efficiency but higher stability. Furthermore, the sample acquisition can be shortened to 15 sec for each tube, thereby making this methodology more cost-effective and efficient. Next, we investigated the individual and cumulative contribution of NKG2D and 2B4 to the activation of CIK cells. Unlike resting NK cells, we found NKG2D engagement alone is sufficient to activate CIK cells, inducing deganulation, IFN-γ secretion and LFA-1 activation, while 2B4 alone failed to elicit these activities and only provides synergistic effect on LFA-1 activation with NKG2D. Unexpectedly, NKG2D was unable to costimulate CD3 in the cytotoxicity of CIK cells. These data indicate the divergences in the role of NKG2D between CIK cells and NK (or T) cells. Nevertheless, we demonstrate that NKG2D alone suffices to activate CIK cells, thus strenghthening the idea of targeting the NKG2D axis may promote the antitumor efficacy of CIK cells. To this end, we further investigated whether the upregulaton of NKG2D ligands on tumor targets can incease the sensitivity of CIK cells. By using an anti-MICA α3 domain monoclonal antibody (7C6 mAb), which was shown to specifically inhibit the MICA shedding and stabilize its surface density on tumor cells (Hela and MDA-MB-231), we found that the CIK cell-mediated antitumor activities (including cytotoxicity, degranulation, IFN-γ secretion) were substantially enhanced. The effect was mostly modulated through NKG2D axis as NKG2D blocking offset the 7C6-driven enhancement in these activities. Collectively, the findings presented in this thesis demonstrate that

targeting the NKG2D axis is a promissing approach to improve the antimumor activity of CIK cells, suggesting that the combinatory treatment of CIK cells with other therapeutic modalities which are able to induce or upregulate NKG2D ligands holds great potential to improve the clincial response of cancer patients.

6. List of figures

7. List of tables

8. References

Baker J, Verneris MR, Ito M, Shizuru JA, Negrin RS. Expansion of cytolytic CD8(+) natural killer T cells with limited capacity for graft-versus-host disease induction due to interferon gamma production. Blood 2001; 97(10): 2923-2931

Baragano Raneros A, Suarez-Alvarez B, Lopez-Larrea C. Secretory pathways generating immunosuppressive NKG2D ligands: New targets for therapeutic intervention. Oncoimmunology 2014; 3:e28497

Basher F, Dhar P, Wang X, Wainwright DA, Zhang B, Sosman J, Ji Z, Wu JD. Antibody targeting tumor-derived soluble NKG2D ligand sMIC reprograms NK cell homeostatic survival and function and enhances melanoma response to PDL1 blockade therapy. J Hematol Oncol 2020; 13(1): 74

Bauer S, Groh V, Wu J, Steinle A, Phillips JH, Lanier LL, Spies T. Activation of NK cells and T cells by NKG2D, a receptor for stress-inducible MICA. Science 1999; 285(5428): 727-729

Baumeister SH, Murad J, Werner L, Daley H, Trebeden-Negre H, Gicobi JK, Schmucker A, Reder J, Sentman CL, Gilham DE, Lehmann FF, Galinsky I, DiPietro H, Cummings K, Munshi NC, Stone RM, Neuberg DS, Soiffer R, Dranoff G, Ritz J, Nikiforow S. Phase I Trial of Autologous CAR T Cells Targeting NKG2D Ligands in Patients with AML/MDS and Multiple Myeloma. Cancer Immunol Res 2019; 7(1): 100-112

Baumgarten H. A cell ELISA for the quantitation of leukocyte antigens. Requirements for calibration. J Immunol Methods 1986; 94(1-2): 91-98

Benson DM, Jr., Bakan CE, Mishra A, Hofmeister CC, Efebera Y, Becknell B, Baiocchi RA, Zhang J, Yu J, Smith MK, Greenfield CN, Porcu P, Devine SM, Rotem-Yehudar R, Lozanski G, Byrd JC, Caligiuri MA. The PD-1/PD-L1 axis modulates the natural killer cell

versus multiple myeloma effect: a therapeutic target for CT-011, a novel monoclonal anti-PD-1 antibody. Blood 2010; 116(13): 2286-2294

Blomberg K, Granberg C, Hemmila I, Lovgren T. Europium-labelled target cells in an assay of natural killer cell activity. I. A novel non-radioactive method based on time-resolved fluorescence. J Immunol Methods 1986; 86(2): 225-229

Boutet P, Aguera-Gonzalez S, Atkinson S, Pennington CJ, Edwards DR, Murphy G, Reyburn HT, Vales-Gomez M. Cutting edge: the metalloproteinase ADAM17/TNF-alpha-converting enzyme regulates proteolytic shedding of the MHC class I-related chain B protein. J Immunol 2009; 182(1): 49-53

Brando B, Gohde W, Jr., Scarpati B, D'Avanzo G, European Working Group on Clinical Cell A. The "vanishing counting bead" phenomenon: effect on absolute CD34+ cell counting in phosphate-buffered saline-diluted leukapheresis samples. Cytometry 2001; 43(2): 154-160

Breunig C, Pahl J, Kublbeck M, Miller M, Antonelli D, Erdem N, Wirth C, Will R, Bott A, Cerwenka A, Wiemann S. MicroRNA-519a-3p mediates apoptosis resistance in breast cancer cells and their escape from recognition by natural killer cells. Cell Death Dis 2017; 8(8): e2973

Brunner KT, Mauel J, Cerottini JC, Chapuis B. Quantitative assay of the lytic action of immune lymphoid cells on 51-Cr-labelled allogeneic target cells in vitro; inhibition by isoantibody and by drugs. Immunology 1968; 14(2): 181-196

Bryceson YT, Ljunggren HG, Long EO. Minimal requirement for induction of natural cytotoxicity and intersection of activation signals by inhibitory receptors. Blood 2009; 114(13): 2657-2666

Cao LF, Krymskaya L, Tran V, Mi S, Jensen MC, Blanchard S, Kalos M. Development and application of a multiplexable flow cytometry-based assay to quantify cell-mediated cytolysis. Cytometry A 2010; 77(6): 534-545

Cappel C, Huenecke S, Suemmerer A, Erben S, Rettinger E, Pfirrmann V, Heinze A, Zimmermann O, Klingebiel T, Ullrich E, Bader P, Bremm M. Cytotoxic potential of IL-15-activated cytokine-induced killer cells against human neuroblastoma cells. Pediatr Blood Cancer 2016; 63(12): 2230-2239

Cappuzzello E, Tosi A, Zanovello P, Sommaggio R, Rosato A. Retargeting cytokine-induced killer cell activity by CD16 engagement with clinical-grade antibodies. Oncoimmunology 2016; 5(8): e1199311

Carayannopoulos LN, Naidenko OV, Fremont DH, Yokoyama WM. Cutting edge: murine UL16-binding protein-like transcript 1: a newly described transcript encoding a high-affinity ligand for murine NKG2D. J Immunol 2002; 169(8): 4079-4083

Cerwenka A, Bakker AB, McClanahan T, Wagner J, Wu J, Phillips JH, Lanier LL. Retinoic acid early inducible genes define a ligand family for the activating NKG2D receptor in mice. Immunity 2000; 12(6): 721-727

Chahroudi A, Silvestri G, Feinberg MB. Measuring T cell-mediated cytotoxicity using fluorogenic caspase substrates. Methods 2003; 31(2): 120-126

Champsaur M, Lanier LL. Effect of NKG2D ligand expression on host immune responses. Immunol Rev 2010; 235(1): 267-285

Chan JD, Lai J, Slaney CY, Kallies A, Beavis PA, Darcy PK. Cellular networks controlling T cell persistence in adoptive cell therapy. Nat Rev Immunol 2021; Online ahead of print

Chan JK, Hamilton CA, Cheung MK, Karimi M, Baker J, Gall JM, Schulz S, Thorne SH, Teng NN, Contag CH, Lum LG, Negrin RS. Enhanced killing of primary ovarian cancer by

retargeting autologous cytokine-induced killer cells with bispecific antibodies: a preclinical study. Clin Cancer Res 2006; 12(6): 1859-1867

Chen R, Relouzat F, Roncagalli R, Aoukaty A, Tan R, Latour S, Veillette A. Molecular dissection of 2B4 signaling: implications for signal transduction by SLAM-related receptors. Mol Cell Biol 2004; 24(12): 5144-5156

Chen Y, Lin J, Guo ZQ, Lin WS, Zhou ZF, Huang CZ, Chen Q, Ye YB. MHC I-related chain a expression in gastric carcinoma and the efficacy of immunotherapy with cytokine-induced killer cells. Am J Cancer Res 2015; 5(10): 3221-3230

Cholujova D, Jakubikova J, Kubes M, Arendacka B, Sapak M, Ihnatko R, Sedlak J. Comparative study of four fluorescent probes for evaluation of natural killer cell cytotoxicity assays. Immunobiology 2008; 213(8): 629-640

Clayton A, Mitchell JP, Court J, Linnane S, Mason MD, Tabi Z. Human tumor-derived exosomes down-modulate NKG2D expression. J Immunol 2008; 180(11): 7249-7258

Cluxton CD, Spillane C, O'Toole SA, Sheils O, Gardiner CM, O'Leary JJ. Suppression of Natural Killer cell NKG2D and CD226 anti-tumour cascades by platelet cloaked cancer cells: Implications for the metastatic cascade. PLoS One 2019; 14(3): e0211538

Dai C, Lin F, Geng R, Ge X, Tang W, Chang J, Wu Z, Liu X, Lin Y, Zhang Z, Li J. Implication of combined PD-L1/PD-1 blockade with cytokine-induced killer cells as a synergistic immunotherapy for gastrointestinal cancer. Oncotarget 2016; 7(9): 10332-10344

de Kruijf EM, Sajet A, van Nes JG, Putter H, Smit VT, Eagle RA, Jafferji I, Trowsdale J, Liefers GJ, van de Velde CJ, Kuppen PJ. NKG2D ligand tumor expression and association with clinical outcome in early breast cancer patients: an observational study. BMC Cancer 2012; 12: 24

Deng W, Gowen BG, Zhang L, Wang L, Lau S, Iannello A, Xu J, Rovis TL, Xiong N, Raulet DH. Antitumor immunity. A shed NKG2D ligand that promotes natural killer cell activation and tumor rejection. Science 2015; 348(6230): 136-139

Diefenbach A, Jamieson AM, Liu SD, Shastri N, Raulet DH. Ligands for the murine NKG2D receptor: expression by tumor cells and activation of NK cells and macrophages. Nat Immunol 2000; 1(2): 119-126

Diefenbach A, Tomasello E, Lucas M, Jamieson AM, Hsia JK, Vivier E, Raulet DH. Selective associations with signaling proteins determine stimulatory versus costimulatory activity of NKG2D. Nat Immunol 2002; 3(12): 1142-1149

Doubrovina ES, Doubrovin MM, Vider E, Sisson RB, O'Reilly RJ, Dupont B, Vyas YM. Evasion from NK cell immunity by MHC class I chain-related molecules expressing colon adenocarcinoma. J Immunol 2003; 171(12): 6891-6899

Du C, Bevers J, 3rd, Cook R, Lombana TN, Rajasekaran K, Matsumoto M, Spiess C, Kim JM, Ye Z. MICA immune complex formed with alpha 3 domain-specific antibody activates human NK cells in a Fc-dependent manner. J Immunother Cancer 2019; 7(1): 207

Du SH, Li Z, Chen C, Tan WK, Chi Z, Kwang TW, Xu XH, Wang S. Co-Expansion of Cytokine-Induced Killer Cells and Vgamma9Vdelta2 T Cells for CAR T-Cell Therapy. PLoS One 2016; 11(9): e0161820

Durrieu L, Lemieux W, Dieng MM, Fontaine F, Duval M, Le Deist F, Haddad E. Implication of different effector mechanisms by cord blood-derived and peripheral blood-derived cytokine-induced killer cells to kill precursor B acute lymphoblastic leukemia cell lines. Cytotherapy 2014; 16(6): 845-856

Eagle RA, Trowsdale J. Promiscuity and the single receptor: NKG2D. Nat Rev Immunol 2007; 7(9): 737-744

Edinger M, Cao YA, Verneris MR, Bachmann MH, Contag CH, Negrin RS. Revealing lymphoma growth and the efficacy of immune cell therapies using in vivo bioluminescence imaging. Blood 2003; 101(2): 640-648

El-Gazzar A, Groh V, Spies T. Immunobiology and conflicting roles of the human NKG2D lymphocyte receptor and its ligands in cancer. J Immunol 2013; 191(4): 1509-1515

Elmore S. Apoptosis: a review of programmed cell death. Toxicol Pathol 2007; 35(4): 495-516

Enqvist M, Ask EH, Forslund E, Carlsten M, Abrahamsen G, Beziat V, Andersson S, Schaffer M, Spurkland A, Bryceson Y, Onfelt B, Malmberg KJ. Coordinated expression of DNAM-1 and LFA-1 in educated NK cells. J Immunol 2015; 194(9): 4518-4527

Ferrari de Andrade L, Kumar S, Luoma AM, Ito Y, Alves da Silva PH, Pan D, Pyrdol JW, Yoon CH, Wucherpfennig KW. Inhibition of MICA and MICB Shedding Elicits NK-Cell-Mediated Immunity against Tumors Resistant to Cytotoxic T Cells. Cancer Immunol Res 2020; 8(6): 769-780

Ferrari de Andrade L, Tay RE, Pan D, Luoma AM, Ito Y, Badrinath S, Tsoucas D, Franz B, May KF, Jr., Harvey CJ, Kobold S, Pyrdol JW, Yoon C, Yuan GC, Hodi FS, Dranoff G, Wucherpfennig KW. Antibody-mediated inhibition of MICA and MICB shedding promotes NK cell-driven tumor immunity. Science 2018; 359(6383): 1537-1542

Finke S, Trojaneck B, Lefterova P, Csipai M, Wagner E, Kircheis R, Neubauer A, Huhn D, Wittig B, Schmidt-Wolf IG. Increase of proliferation rate and enhancement of antitumor cytotoxicity of expanded human CD3+ CD56+ immunologic effector cells by receptor-mediated transfection with the interleukin-7 gene. Gene Ther 1998; 5(1): 31-39

Franceschetti M, Pievani A, Borleri G, Vago L, Fleischhauer K, Golay J, Introna M. Cytokine-induced killer cells are terminally differentiated activated CD8 cytotoxic T-EMRA lymphocytes. Exp Hematol 2009; 37(5): 616-628 e612

Gammaitoni L, Giraudo L, Leuci V, Todorovic M, Mesiano G, Picciotto F, Pisacane A, Zaccagna A, Volpe MG, Gallo S, Caravelli D, Giacone E, Venesio T, Balsamo A, Pignochino Y, Grignani G, Carnevale-Schianca F, Aglietta M, Sangiolo D. Effective activity of cytokine-induced killer cells against autologous metastatic melanoma including cells with stemness features. Clin Cancer Res 2013; 19(16): 4347-4358

Garni-Wagner BA, Purohit A, Mathew PA, Bennett M, Kumar V. A novel function-associated molecule related to non-MHC-restricted cytotoxicity mediated by activated natural killer cells and T cells. J Immunol 1993; 151(1): 60-70

Garrity D, Call ME, Feng J, Wucherpfennig KW. The activating NKG2D receptor assembles in the membrane with two signaling dimers into a hexameric structure. Proc Natl Acad Sci U S A 2005; 102(21): 7641-7646

Gasser S, Orsulic S, Brown EJ, Raulet DH. The DNA damage pathway regulates innate immune system ligands of the NKG2D receptor. Nature 2005; 436(7054): 1186-1190

Gasser S, Raulet DH. Activation and self-tolerance of natural killer cells. Immunol Rev 2006; 214: 130-142

Ghadially H, Brown L, Lloyd C, Lewis L, Lewis A, Dillon J, Sainson R, Jovanovic J, Tigue NJ, Bannister D, Bamber L, Valge-Archer V, Wilkinson RW. MHC class I chain-related protein A and B (MICA and MICB) are predominantly expressed intracellularly in tumour and normal tissue. Br J Cancer 2017; 116(9): 1208-1217

Gillissen MA, Yasuda E, de Jong G, Levie SE, Go D, Spits H, van Helden PM, Hazenberg MD. The modified FACS calcein AM retention assay: A high throughput flow cytometer based method to measure cytotoxicity. J Immunol Methods 2016; 434: 16-23

Godoy-Ramirez K, Makitalo B, Thorstensson R, Sandstrom E, Biberfeld G, Gaines H. A novel assay for assessment of HIV-specific cytotoxicity by multiparameter flow cytometry. Cytometry A 2005; 68(2): 71-80

Grimm EA, Mazumder A, Zhang HZ, Rosenberg SA. Lymphokine-activated killer cell phenomenon. Lysis of natural killer-resistant fresh solid tumor cells by interleukin 2-activated autologous human peripheral blood lymphocytes. J Exp Med 1982; 155(6): 1823-1841

Groh V, Bahram S, Bauer S, Herman A, Beauchamp M, Spies T. Cell stress-regulated human major histocompatibility complex class I gene expressed in gastrointestinal epithelium. Proc Natl Acad Sci U S A 1996; 93(22): 12445-12450

Groh V, Rhinehart R, Randolph-Habecker J, Topp MS, Riddell SR, Spies T. Costimulation of CD8alphabeta T cells by NKG2D via engagement by MIC induced on virus-infected cells. Nat Immunol 2001; 2(3): 255-260

Groh V, Steinle A, Bauer S, Spies T. Recognition of stress-induced MHC molecules by intestinal epithelial gammadelta T cells. Science 1998; 279(5357): 1737-1740

Groh V, Wu J, Yee C, Spies T. Tumour-derived soluble MIC ligands impair expression of NKG2D and T-cell activation. Nature 2002; 419(6908): 734-738

Gronholm M, Jahan F, Marchesan S, Karvonen U, Aatonen M, Narumanchi S, Gahmberg CG. TCR-induced activation of LFA-1 involves signaling through Tiam1. J Immunol 2011; 187(7): 3613-3619

Guo W, Xing C, Dong A, Lin X, Lin Y, Zhu B, He M, Yao R. Numbers and cytotoxicities of CD3+CD56+ T lymphocytes in peripheral blood of patients with acute myeloid leukemia and acute lymphocytic leukemia. Cancer Biol Ther 2013; 14(10): 916-921

Hazen AL, Bushnell T, Haviland DL. The importance of area scaling with FACS DIVA software. Methods 2018; 134-135: 130-135

Helms MW, Prescher JA, Cao YA, Schaffert S, Contag CH. IL-12 enhances efficacy and shortens enrichment time in cytokine-induced killer cell immunotherapy. Cancer Immunol Immunother 2010; 59(9): 1325-1334

Hirano N, Takahashi T, Takahashi T, Ohtake S, Hirashima K, Emi N, Saito K, Hirano M, Shinohara K, Takeuchi M, Taketazu F, Tsunoda S, Ogura M, Omine M, Saito T, Yazaki Y, Ueda R, Hirai H. Expression of costimulatory molecules in human leukemias. Leukemia 1996; 10(7): 1168-1176

Holdenrieder S, Stieber P, Peterfi A, Nagel D, Steinle A, Salih HR. Soluble MICA in malignant diseases. Int J Cancer 2006; 118(3): 684-687

Hombach AA, Rappl G, Abken H. Arming cytokine-induced killer cells with chimeric antigen receptors: CD28 outperforms combined CD28-OX40 "super-stimulation". Mol Ther 2013; 21(12): 2268-2277

Hontscha C, Borck Y, Zhou H, Messmer D, Schmidt-Wolf IG. Clinical trials on CIK cells: first report of the international registry on CIK cells (IRCC). J Cancer Res Clin Oncol 2011; 137(2): 305-310

Houchins JP, Yabe T, McSherry C, Bach FH. DNA sequence analysis of NKG2, a family of related cDNA clones encoding type II integral membrane proteins on human natural killer cells. J Exp Med 1991; 173(4): 1017-1020

Hoyle C, Bangs CD, Chang P, Kamel O, Mehta B, Negrin RS. Expansion of Philadelphia chromosome-negative CD3(+)CD56(+) cytotoxic cells from chronic myeloid leukemia patients: in vitro and in vivo efficacy in severe combined immunodeficiency disease mice. Blood 1998; 92(9): 3318-3327

Hue S, Mention JJ, Monteiro RC, Zhang S, Cellier C, Schmitz J, Verkarre V, Fodil N, Bahram S, Cerf-Bensussan N, Caillat-Zucman S. A direct role for NKG2D/MICA interaction in villous atrophy during celiac disease. Immunity 2004; 21(3): 367-377

Huergo-Zapico L, Acebes-Huerta A, Gonzalez-Rodriguez AP, Contesti J, Gonzalez-Garcia E, Payer AR, Villa-Alvarez M, Fernandez-Guizan A, Lopez-Soto A, Gonzalez S. Expansion of NK cells and reduction of NKG2D expression in chronic lymphocytic leukemia. Correlation with progressive disease. PLoS One 2014; 9(10): e108326

Introna M, Borleri G, Conti E, Franceschetti M, Barbui AM, Broady R, Dander E, Gaipa G, D'Amico G, Biagi E, Parma M, Pogliani EM, Spinelli O, Baronciani D, Grassi A, Golay J, Barbui T, Biondi A, Rambaldi A. Repeated infusions of donor-derived cytokine-induced killer cells in patients relapsing after allogeneic stem cell transplantation: a phase I study. Haematologica 2007; 92(7): 952-959

Introna M, Franceschetti M, Ciocca A, Borleri G, Conti E, Golay J, Rambaldi A. Rapid and massive expansion of cord blood-derived cytokine-induced killer cells: an innovative proposal for the treatment of leukemia relapse after cord blood transplantation. Bone Marrow Transplant 2006; 38(9): 621-627

Introna M, Lussana F, Algarotti A, Gotti E, Valgardsdottir R, Mico C, Grassi A, Pavoni C, Ferrari ML, Delaini F, Todisco E, Cavattoni I, Deola S, Biagi E, Balduzzi A, Rovelli A, Parma M, Napolitano S, Sgroi G, Marrocco E, Perseghin P, Belotti D, Cabiati B, Gaipa G, Golay J, Biondi A, Rambaldi A. Phase II Study of Sequential Infusion of Donor Lymphocyte Infusion and Cytokine-Induced Killer Cells for Patients Relapsed after Allogeneic Hematopoietic Stem Cell Transplantation. Biol Blood Marrow Transplant 2017; 23(12): 2070-2078

Itoh K, Shiiba K, Shimizu Y, Suzuki R, Kumagai K. Generation of activated killer (AK) cells by recombinant interleukin 2 (rIL 2) in collaboration with interferon-gamma (IFN-gamma). J Immunol 1985; 134(5): 3124-3129

Jakel CE, Schmidt-Wolf IG. An update on new adoptive immunotherapy strategies for solid tumors with cytokine-induced killer cells. Expert Opin Biol Ther 2014; 14(7): 905-916

Jamieson AM, Diefenbach A, McMahon CW, Xiong N, Carlyle JR, Raulet DH. The role of the NKG2D immunoreceptor in immune cell activation and natural killing. Immunity 2002; 17(1): 19-29

Jang YY, Cho D, Kim SK, Shin DJ, Park MH, Lee JJ, Shin MG, Shin JH, Suh SP, Ryang DW. An improved flow cytometry-based natural killer cytotoxicity assay involving calcein AM staining of effector cells. Ann Clin Lab Sci 2012; 42(1): 42-49

Jedema I, van der Werff NM, Barge RM, Willemze R, Falkenburg JH. New CFSE-based assay to determine susceptibility to lysis by cytotoxic T cells of leukemic precursor cells within a heterogeneous target cell population. Blood 2004; 103(7): 2677-2682

Jiang N, Qiao G, Wang X, Morse MA, Gwin WR, Zhou L, Song Y, Zhao Y, Chen F, Zhou X, Huang L, Hobeika A, Yi X, Xia X, Guan Y, Song J, Ren J, Lyerly HK. Dendritic Cell/Cytokine-Induced Killer Cell Immunotherapy Combined with S-1 in Patients with Advanced Pancreatic Cancer: A Prospective Study. Clin Cancer Res 2017; 23(17): 5066-5073

Kaiser BK, Yim D, Chow IT, Gonzalez S, Dai Z, Mann HH, Strong RK, Groh V, Spies T. Disulphide-isomerase-enabled shedding of tumour-associated NKG2D ligands. Nature 2007; 447(7143): 482-486

Kandarian F, Sunga GM, Arango-Saenz D, Rossetti M. A Flow Cytometry-Based Cytotoxicity Assay for the Assessment of Human NK Cell Activity. J Vis Exp 2017; 126):
Karimi M, Cao TM, Baker JA, Verneris MR, Soares L, Negrin RS. Silencing human NKG2D, DAP10, and DAP12 reduces cytotoxicity of activated CD8+ T cells and NK cells. J Immunol 2005; 175(12): 7819-7828

Kawalekar OU, O'Connor RS, Fraietta JA, Guo L, McGettigan SE, Posey AD, Jr., Patel PR, Guedan S, Scholler J, Keith B, Snyder NW, Blair IA, Milone MC, June CH. Distinct Signaling of Coreceptors Regulates Specific Metabolism Pathways and Impacts Memory Development in CAR T Cells. Immunity 2016; 44(2): 380-390

Kim HM, Lim J, Kang JS, Park SK, Lee K, Kim JY, Kim YJ, Hong JT, Kim Y, Han SB. Inhibition of human cervical carcinoma growth by cytokine-induced killer cells in nude mouse xenograft model. Int Immunopharmacol 2009; 9(3): 375-380

Kim HM, Lim J, Park SK, Kang JS, Lee K, Lee CW, Lee KH, Yun MJ, Yang KH, Han G, Kwon SW, Kim Y, Han SB. Antitumor activity of cytokine-induced killer cells against human lung cancer. Int Immunopharmacol 2007; 7(13): 1802-1807

Kim HM, Lim J, Yoon YD, Ahn JM, Kang JS, Lee K, Park SK, Jeong YJ, Kim JM, Han G, Yang KH, Kim YJ, Kim Y, Han SB. Anti-tumor activity of ex vivo expanded cytokine-induced killer cells against human hepatocellular carcinoma. Int Immunopharmacol 2007; 7(13): 1793-1801

Kim HS, Das A, Gross CC, Bryceson YT, Long EO. Synergistic signals for natural cytotoxicity are required to overcome inhibition by c-Cbl ubiquitin ligase. Immunity 2010; 32(2): 175-186

Kloss S, Chambron N, Gardlowski T, Arseniev L, Koch J, Esser R, Glienke W, Seitz O, Kohl U. Increased sMICA and TGFbeta1 levels in HNSCC patients impair NKG2D-dependent functionality of activated NK cells. Oncoimmunology 2015; 4(11): e1055993

Kohga K, Takehara T, Tatsumi T, Ishida H, Miyagi T, Hosui A, Hayashi N. Sorafenib inhibits the shedding of major histocompatibility complex class I-related chain A on hepatocellular carcinoma cells by down-regulating a disintegrin and metalloproteinase 9. Hepatology 2010; 51(4): 1264-1273

Kohga K, Takehara T, Tatsumi T, Miyagi T, Ishida H, Ohkawa K, Kanto T, Hiramatsu N, Hayashi N. Anticancer chemotherapy inhibits MHC class I-related chain a ectodomain shedding by downregulating ADAM10 expression in hepatocellular carcinoma. Cancer Res 2009; 69(20): 8050-8057

Kong DS, Nam DH, Kang SH, Lee JW, Chang JH, Kim JH, Lim YJ, Koh YC, Chung YG, Kim JM, Kim CH. Phase III randomized trial of autologous cytokine-induced killer cell immunotherapy for newly diagnosed glioblastoma in Korea. Oncotarget 2017; 8(4): 7003-7013

Konjevic G, Jurisic V, Jovic V, Vuletic A, Mirjacic Martinovic K, Radenkovic S, Spuzic I. Investigation of NK cell function and their modulation in different malignancies. Immunol Res 2012; 52(1-2): 139-156

Korzeniewski C, Callewaert DM. An enzyme-release assay for natural cytotoxicity. J Immunol Methods 1983; 64(3): 313-320

Kraetzel K, Stoelcker B, Eissner G, Multhoff G, Pfeifer M, Holler E, Schulz C. NKG2D-dependent effector function of bronchial epithelium-activated alloreactive T-cells. Eur Respir J 2008; 32(3): 563-570

Kuylenstierna C, Bjorkstrom NK, Andersson SK, Sahlstrom P, Bosnjak L, Paquin-Proulx D, Malmberg KJ, Ljunggren HG, Moll M, Sandberg JK. NKG2D performs two functions in invariant NKT cells: direct TCR-independent activation of NK-like cytolysis and co-stimulation of activation by CD1d. Eur J Immunol 2011; 41(7): 1913-1923

Langhans B, Ahrendt M, Nattermann J, Sauerbruch T, Spengler U. Comparative study of NK cell-mediated cytotoxicity using radioactive and flow cytometric cytotoxicity assays. J Immunol Methods 2005; 306(1-2): 161-168

Lanier LL, Corliss BC, Wu J, Leong C, Phillips JH. Immunoreceptor DAP12 bearing a tyrosine-based activation motif is involved in activating NK cells. Nature 1998; 391(6668): 703-707

Laport GG, Sheehan K, Baker J, Armstrong R, Wong RM, Lowsky R, Johnston LJ, Shizuru JA, Miklos D, Arai S, Benjamin JE, Weng WK, Negrin RS. Adoptive immunotherapy with cytokine-induced killer cells for patients with relapsed hematologic malignancies after allogeneic hematopoietic cell transplantation. Biol Blood Marrow Transplant 2011; 17(11): 1679-1687

Lecoeur H, Fevrier M, Garcia S, Riviere Y, Gougeon ML. A novel flow cytometric assay for quantitation and multiparametric characterization of cell-mediated cytotoxicity. J Immunol Methods 2001; 253(1-2): 177-187

Lee JC, Lee KM, Kim DW, Heo DS. Elevated TGF-beta1 secretion and down-modulation of NKG2D underlies impaired NK cytotoxicity in cancer patients. J Immunol 2004; 172(12): 7335-7340

Leuci V, Casucci GM, Grignani G, Rotolo R, Rossotti U, Vigna E, Gammaitoni L, Mesiano G, Fiorino E, Donini C, Pisacane A, Ambrosio LD, Pignochino Y, Aglietta M, Bondanza A, Sangiolo D. CD44v6 as innovative sarcoma target for CAR-redirected CIK cells. Oncoimmunology 2018; 7(5): e1423167

Leuci V, Donini C, Grignani G, Rotolo R, Mesiano G, Fiorino E, Gammaitoni L, D'Ambrosio L, Merlini A, Landoni E, Medico E, Capellero S, Giraudo L, Cattaneo G, Iaia I, Pignochino Y, Basirico M, Vigna E, Pisacane A, Fagioli F, Ferrone S, Aglietta M, Dotti G, Sangiolo D. CSPG4-Specific CAR.CIK Lymphocytes as a Novel Therapy for the Treatment of Multiple Soft-Tissue Sarcoma Histotypes. Clin Cancer Res 2020; 26(23): 6321-6334

Li G, Boucher JC, Kotani H, Park K, Zhang Y, Shrestha B, Wang X, Guan L, Beatty N, Abate-Daga D, Davila ML. 4-1BB enhancement of CAR T function requires NF-kappaB and TRAFs. JCI Insight 2018; 3(18): e121322

Li Y, Hermanson DL, Moriarity BS, Kaufman DS. Human iPSC-Derived Natural Killer Cells Engineered with Chimeric Antigen Receptors Enhance Anti-tumor Activity. Cell Stem Cell 2018; 23(2): 181-192.e15

Li Y, Mariuzza RA. Structural basis for recognition of cellular and viral ligands by NK cell receptors. Front Immunol 2014; 5: 123

Lichtenfels R, Biddison WE, Schulz H, Vogt AB, Martin R. CARE-LASS (calcein-release-assay), an improved fluorescence-based test system to measure cytotoxic T lymphocyte activity. J Immunol Methods 1994; 172(2): 227-239

Linn YC, Lau SK, Liu BH, Ng LH, Yong HX, Hui KM. Characterization of the recognition and functional heterogeneity exhibited by cytokine-induced killer cell subsets against acute myeloid leukaemia target cell. Immunology 2009; 126(3): 423-435

Linn YC, Niam M, Chu S, Choong A, Yong HX, Heng KK, Hwang W, Loh Y, Goh YT, Suck G, Chan M, Koh M. The anti-tumour activity of allogeneic cytokine-induced killer cells in patients who relapse after allogeneic transplant for haematological malignancies. Bone Marrow Transplant 2012; 47(7): 957-966

Lorenzo-Herrero S, Sordo-Bahamonde C, Gonzalez S, Lopez-Soto A. A Flow Cytometric NK Cell-Mediated Cytotoxicity Assay to Evaluate Anticancer Immune Responses In Vitro. Methods Mol Biol 2019; 1884: 131-139

Lu PH, Negrin RS. A novel population of expanded human CD3+CD56+ cells derived from T cells with potent in vivo antitumor activity in mice with severe combined immunodeficiency. J Immunol 1994; 153(4): 1687-1696

Lu X, Zhu A, Cai X, Jia Z, Han W, Ma L, Zhou M, Qian K, Cen L, Chen B. Role of NKG2D in cytokine-induced killer cells against multiple myeloma cells. Cancer Biol Ther 2012; 13(8): 623-629

Maccalli C, Giannarelli D, Chiarucci C, Cutaia O, Giacobini G, Hendrickx W, Amato G, Annesi D, Bedognetti D, Altomonte M, Danielli R, Calabro L, Di Giacomo AM, Marincola FM, Parmiani G, Maio M. Soluble NKG2D ligands are biomarkers associated with the clinical outcome to immune checkpoint blockade therapy of metastatic melanoma patients. Oncoimmunology 2017; 6(7): e1323618

Madjd Z, Spendlove I, Moss R, Bevin S, Pinder SE, Watson NF, Ellis I, Durrant LG. Upregulation of MICA on high-grade invasive operable breast carcinoma. Cancer Immun 2007; 7: 17

Magnani CF, Gaipa G, Lussana F, Belotti D, Gritti G, Napolitano S, Matera G, Cabiati B, Buracchi C, Borleri G, Fazio G, Zaninelli S, Tettamanti S, Cesana S, Colombo V, Quaroni M, Cazzaniga G, Rovelli A, Biagi E, Galimberti S, Calabria A, Benedicenti F, Montini E, Ferrari S, Introna M, Balduzzi A, Valsecchi MG, Dastoli G, Rambaldi A, Biondi A. Sleeping Beauty-engineered CAR T cells achieve antileukemic activity without severe toxicities. J Clin Invest 2020; 130(11): 6021-6033

Magnani CF, Mezzanotte C, Cappuzzello C, Bardini M, Tettamanti S, Fazio G, Cooper LJN, Dastoli G, Cazzaniga G, Biondi A, Biagi E. Preclinical Efficacy and Safety of CD19CAR Cytokine-Induced Killer Cells Transfected with Sleeping Beauty Transposon for the Treatment of Acute Lymphoblastic Leukemia. Hum Gene Ther 2018; 29(5): 602-613

Mamessier E, Sylvain A, Thibult ML, Houvenaeghel G, Jacquemier J, Castellano R, Goncalves A, Andre P, Romagne F, Thibault G, Viens P, Birnbaum D, Bertucci F, Moretta A, Olive D. Human breast cancer cells enhance self tolerance by promoting evasion from NK cell antitumor immunity. J Clin Invest 2011; 121(9): 3609-3622

Marten A, Renoth S, von Lilienfeld-Toal M, Buttgereit P, Schakowski F, Glasmacher A, Sauerbruch T, Schmidt-Wolf IG. Enhanced lytic activity of cytokine-induced killer cells

against multiple myeloma cells after co-culture with idiotype-pulsed dendritic cells. Haematologica 2001; 86(10): 1029-1037

Marten A, Ziske C, Schottker B, Renoth S, Weineck S, Buttgereit P, Schakowski F, von Rucker A, Sauerbruch T, Schmidt-Wolf IG. Interactions between dendritic cells and cytokine-induced killer cells lead to an activation of both populations. J Immunother 2001; 24(6): 502-510

Maude SL, Frey N, Shaw PA, Aplenc R, Barrett DM, Bunin NJ, Chew A, Gonzalez VE, Zheng Z, Lacey SF, Mahnke YD, Melenhorst JJ, Rheingold SR, Shen A, Teachey DT, Levine BL, June CH, Porter DL, Grupp SA. Chimeric antigen receptor T cells for sustained remissions in leukemia. N Engl J Med 2014; 371(16): 1507-1517

McGilvray RW, Eagle RA, Rolland P, Jafferji I, Trowsdale J, Durrant LG. ULBP2 and RAET1E NKG2D ligands are independent predictors of poor prognosis in ovarian cancer patients. Int J Cancer 2010; 127(6): 1412-1420

McGilvray RW, Eagle RA, Watson NF, Al-Attar A, Ball G, Jafferji I, Trowsdale J, Durrant LG. NKG2D ligand expression in human colorectal cancer reveals associations with prognosis and evidence for immunoediting. Clin Cancer Res 2009; 15(22): 6993-7002

McGinnes K, Chapman G, Marks R, Penny R. A fluorescence NK assay using flow cytometry. J Immunol Methods 1986; 86(1): 7-15

Mehta BA, Schmidt-Wolf IG, Weissman IL, Negrin RS. Two pathways of exocytosis of cytoplasmic granule contents and target cell killing by cytokine-induced CD3+ CD56+ killer cells. Blood 1995; 86(9): 3493-3499

Meng M, Li L, Li R, Wang W, Chen Y, Xie Y, Han R, Zhu K, Huang W, Yang L, Li S, Shi J, Tan W, Gao H, Zhao Y, Yang L, Tan J, Hou Z. A dynamic transcriptomic atlas of cytokine-induced killer cells. J Biol Chem 2018; 293(51): 19600-19612

Merker M, Pfirrmann V, Oelsner S, Fulda S, Klingebiel T, Wels WS, Bader P, Rettinger E. Generation and characterization of ErbB2-CAR-engineered cytokine-induced killer cells for the treatment of high-risk soft tissue sarcoma in children. Oncotarget 2017; 8(39): 66137-66153

Merker M, Salzmann-Manrique E, Katzki V, Huenecke S, Bremm M, Bakhtiar S, Willasch A, Jarisch A, Soerensen J, Schulz A, Meisel R, Bug G, Bonig H, Klingebiel T, Bader P, Rettinger E. Clearance of Hematologic Malignancies by Allogeneic Cytokine-Induced Killer Cell or Donor Lymphocyte Infusions. Biol Blood Marrow Transplant 2019; 25(7): 1281-1292

Mesiano G, Grignani G, Fiorino E, Leuci V, Rotolo R, D'Ambrosio L, Salfi C, Gammaitoni L, Giraudo L, Pisacane A, Butera S, Pignochino Y, Basirico M, Capozzi F, Sapino A, Aglietta M, Sangiolo D. Cytokine Induced Killer cells are effective against sarcoma cancer stem cells spared by chemotherapy and target therapy. Oncoimmunology 2018; 7(11): e1465161

Mullard A. FDA approves first CAR T therapy. Nat Rev Drug Discov 2017; 16(10): 669
Nagaraj S, Ziske C, Schmidt-Wolf IG. Human cytokine-induced killer cells have enhanced in vitro cytolytic activity via non-viral interleukin-2 gene transfer. Genet Vaccines Ther 2004; 2: 12

Nakajima H, Colonna M. 2B4: an NK cell activating receptor with unique specificity and signal transduction mechanism. Hum Immunol 2000; 61(1): 39-43

Narayan R, Benjamin JE, Shah O, Tian L, Tate K, Armstrong R, Xie BJ, Lowsky R, Laport G, Negrin RS, Meyer EH. Donor-Derived Cytokine-Induced Killer Cell Infusion as Consolidation after Nonmyeloablative Allogeneic Transplantation for Myeloid Neoplasms. Biol Blood Marrow Transplant 2019; 25(7): 1293-1303

Nishimura R, Baker J, Beilhack A, Zeiser R, Olson JA, Sega EI, Karimi M, Negrin RS. In vivo trafficking and survival of cytokine-induced killer cells resulting in minimal GVHD with retention of antitumor activity. Blood 2008; 112(6): 2563-2574

Nuckel H, Switala M, Sellmann L, Horn PA, Durig J, Duhrsen U, Kuppers R, Grosse-Wilde H, Rebmann V. The prognostic significance of soluble NKG2D ligands in B-cell chronic lymphocytic leukemia. Leukemia 2010; 24(6): 1152-1159

Oelsner S, Wagner J, Friede ME, Pfirrmann V, Genssler S, Rettinger E, Buchholz CJ, Pfeifer H, Schubert R, Ottmann OG, Ullrich E, Bader P, Wels WS. Chimeric antigen receptor-engineered cytokine-induced killer cells overcome treatment resistance of pre-B-cell acute lymphoblastic leukemia and enhance survival. Int J Cancer 2016; 139(8): 1799-1809

Ozdemir O. Flow cytometric cell-mediated cytotoxicity assay. J Immunol Methods 2007; 318(1-2): 158-159; author reply 160-151

Ozdemir O, Ravindranath Y, Savasan S. Cell-mediated cytotoxicity evaluation using monoclonal antibody staining for target or effector cells with annexinV/propidium iodide colabeling by fluorosphere-adjusted counts on three-color flow cytometry. Cytometry A 2003; 56(1): 53-60

Page M, Bejaoui N, Cinq-Mars B, Lemieux P. Optimization of the tetrazolium-based colorimetric assay for the measurement of cell number and cytotoxicity. Int J Immunopharmacol 1988; 10(7): 785-793

Papa S, Vitale M, Mariani AR, Roda P, Facchini A, Manzoli FA. Natural killer function in flow cytometry. I. Evaluation of NK lytic activity on K562 cell line. J Immunol Methods 1988; 107(1): 73-78

Park YP, Choi SC, Kiesler P, Gil-Krzewska A, Borrego F, Weck J, Krzewski K, Coligan JE. Complex regulation of human NKG2D-DAP10 cell surface expression: opposing roles of the gammac cytokines and TGF-beta1. Blood 2011; 118(11): 3019-3027

Paschen A, Sucker A, Hill B, Moll I, Zapatka M, Nguyen XD, Sim GC, Gutmann I, Hassel J, Becker JC, Steinle A, Schadendorf D, Ugurel S. Differential clinical significance of individual NKG2D ligands in melanoma: soluble ULBP2 as an indicator of poor prognosis superior to S100B. Clin Cancer Res 2009; 15(16): 5208-5215

Pievani A, Borleri G, Pende D, Moretta L, Rambaldi A, Golay J, Introna M. Dual-functional capability of CD3+CD56+ CIK cells, a T-cell subset that acquires NK function and retains TCR-mediated specific cytotoxicity. Blood 2011; 118(12): 3301-3310

Pizzitola I, Anjos-Afonso F, Rouault-Pierre K, Lassailly F, Tettamanti S, Spinelli O, Biondi A, Biagi E, Bonnet D. Chimeric antigen receptors against CD33/CD123 antigens efficiently target primary acute myeloid leukemia cells in vivo. Leukemia 2014; 28(8): 1596-1605

Poh SL, Linn YC. Immune checkpoint inhibitors enhance cytotoxicity of cytokine-induced killer cells against human myeloid leukaemic blasts. Cancer Immunol Immunother 2016; 65(5): 525-536

Quah BJ, Warren HS, Parish CR. Monitoring lymphocyte proliferation in vitro and in vivo with the intracellular fluorescent dye carboxyfluorescein diacetate succinimidyl ester. Nat Protoc 2007; 2(9): 2049-2056

Raulet DH. Roles of the NKG2D immunoreceptor and its ligands. Nat Rev Immunol 2003; 3(10): 781-790

Raulet DH, Gasser S, Gowen BG, Deng W, Jung H. Regulation of ligands for the NKG2D activating receptor. Annu Rev Immunol 2013; 31: 413-441

Ren J, Gwin WR, Zhou X, Wang X, Huang H, Jiang N, Zhou L, Agarwal P, Hobeika A, Crosby E, Hartman ZC, Morse MA, K HE, Lyerly HK. Adaptive T cell responses induced by oncolytic Herpes Simplex Virus-granulocyte macrophage-colony-stimulating factor therapy expanded by dendritic cell and cytokine-induced killer cell adoptive therapy. Oncoimmunology 2017; 6(4): e1264563

Rettinger E, Bonig H, Wehner S, Lucchini G, Willasch A, Jarisch A, Soerensen J, Esser R, Rossig C, Klingebiel T, Bader P. Feasibility of IL-15-activated cytokine-induced killer cell infusions after haploidentical stem cell transplantation. Bone Marrow Transplant 2013; 48(8): 1141-1143

Rettinger E, Huenecke S, Bonig H, Merker M, Jarisch A, Soerensen J, Willasch A, Bug G, Schulz A, Klingebiel T, Bader P. Interleukin-15-activated cytokine-induced killer cells may sustain remission in leukemia patients after allogeneic stem cell transplantation: feasibility, safety and first insights on efficacy. Haematologica 2016; 101(4): e153-156

Rettinger E, Kuci S, Naumann I, Becker P, Kreyenberg H, Anzaghe M, Willasch A, Koehl U, Bug G, Ruthardt M, Klingebiel T, Fulda S, Bader P. The cytotoxic potential of interleukin-15-stimulated cytokine-induced killer cells against leukemia cells. Cytotherapy 2012; 14(1): 91-103

Rettinger E, Meyer V, Kreyenberg H, Volk A, Kuci S, Willasch A, Koscielniak E, Fulda S, Wels WS, Boenig H, Klingebiel T, Bader P. Cytotoxic Capacity of IL-15-Stimulated Cytokine-Induced Killer Cells Against Human Acute Myeloid Leukemia and Rhabdomyosarcoma in Humanized Preclinical Mouse Models. Front Oncol 2012; 2: 32

Rico LG, Ward MD, Bradford JA, Petriz J. A Novel Flow Cytometric Method to Study Cytotoxic Activity in Whole Blood Samples. Cytometry A 2021; 99(5): 503-510

Rosenberg SA, Lotze MT, Muul LM, Leitman S, Chang AE, Ettinghausen SE, Matory YL, Skibber JM, Shiloni E, Vetto JT, et al. Observations on the systemic administration of

autologous lymphokine-activated killer cells and recombinant interleukin-2 to patients with metastatic cancer. N Engl J Med 1985; 313(23): 1485-1492

Rosenberg SA, Packard BS, Aebersold PM, Solomon D, Topalian SL, Toy ST, Simon P, Lotze MT, Yang JC, Seipp CA, et al. Use of tumor-infiltrating lymphocytes and interleukin-2 in the immunotherapy of patients with metastatic melanoma. A preliminary report. N Engl J Med 1988; 319(25): 1676-1680

Rosenberg SA, Yang JC, Sherry RM, Kammula US, Hughes MS, Phan GQ, Citrin DE, Restifo NP, Robbins PF, Wunderlich JR, Morton KE, Laurencot CM, Steinberg SM, White DE, Dudley ME. Durable complete responses in heavily pretreated patients with metastatic melanoma using T-cell transfer immunotherapy. Clin Cancer Res 2011; 17(13): 4550-4557

Saito H, Osaki T, Ikeguchi M. Decreased NKG2D expression on NK cells correlates with impaired NK cell function in patients with gastric cancer. Gastric Cancer 2012; 15(1): 27-33

Sampath P, Li J, Hou W, Chen H, Bartlett DL, Thorne SH. Crosstalk between immune cell and oncolytic vaccinia therapy enhances tumor trafficking and antitumor effects. Mol Ther 2013; 21(3): 620-628

Sangiolo D, Mesiano G, Gammaitoni L, Leuci V, Todorovic M, Giraudo L, Cammarata C, Dell'Aglio C, D'Ambrosio L, Pisacane A, Sarotto I, Miano S, Ferrero I, Carnevale-Schianca F, Pignochino Y, Sassi F, Bertotti A, Piacibello W, Fagioli F, Aglietta M, Grignani G. Cytokine-induced killer cells eradicate bone and soft-tissue sarcomas. Cancer Res 2014; 74(1): 119-129

Schlimper C, Hombach AA, Abken H, Schmidt-Wolf IG. Improved activation toward primary colorectal cancer cells by antigen-specific targeting autologous cytokine-induced killer cells. Clin Dev Immunol 2012; 2012: 238924

Schmeel FC, Schmeel LC, Gast SM, Schmidt-Wolf IG. Adoptive immunotherapy strategies with cytokine-induced killer (CIK) cells in the treatment of hematological malignancies. Int J Mol Sci 2014; 15(8): 14632-14648

Schmeel LC, Schmeel FC, Coch C, Schmidt-Wolf IG. Cytokine-induced killer (CIK) cells in cancer immunotherapy: report of the international registry on CIK cells (IRCC). J Cancer Res Clin Oncol 2015; 141(5): 839-849

Schmidt-Wolf IG, Finke S, Trojaneck B, Denkena A, Lefterova P, Schwella N, Heuft HG, Prange G, Korte M, Takeya M, Dorbic T, Neubauer A, Wittig B, Huhn D. Phase I clinical study applying autologous immunological effector cells transfected with the interleukin-2 gene in patients with metastatic renal cancer, colorectal cancer and lymphoma. Br J Cancer 1999; 81(6): 1009-1016

Schmidt-Wolf IG, Lefterova P, Johnston V, Huhn D, Blume KG, Negrin RS. Propagation of large numbers of T cells with natural killer cell markers. Br J Haematol 1994; 87(3): 453-458

Schmidt-Wolf IG, Lefterova P, Mehta BA, Fernandez LP, Huhn D, Blume KG, Weissman IL, Negrin RS. Phenotypic characterization and identification of effector cells involved in tumor cell recognition of cytokine-induced killer cells. Exp Hematol 1993; 21(13): 1673-1679

Schmidt-Wolf IG, Negrin RS, Kiem HP, Blume KG, Weissman IL. Use of a SCID mouse/human lymphoma model to evaluate cytokine-induced killer cells with potent antitumor cell activity. J Exp Med 1991; 174(1): 139-149

Southam CM, Brunschwig A, Levin AG, Dizon QS. Effect of leukocytes on transplantability of human cancer. Cancer 1966; 19(11): 1743-1753

Springer TA, Dustin ML. Integrin inside-out signaling and the immunological synapse. Curr Opin Cell Biol 2012; 24(1): 107-115

Stern-Ginossar N, Gur C, Biton M, Horwitz E, Elboim M, Stanietsky N, Mandelboim M, Mandelboim O. Human microRNAs regulate stress-induced immune responses mediated by the receptor NKG2D. Nat Immunol 2008; 9(9): 1065-1073

Sun WW, Dou JX, Zhang L, Qiao LK, Shen N, Zhao Q, Gao WY. Killing effects of Huaier Granule combined with DC-CIK on nude mice transplanted with colon carcinoma cell line. Oncotarget 2017; 8(28): 46081-46089

Takada A, Yoshida S, Kajikawa M, Miyatake Y, Tomaru U, Sakai M, Chiba H, Maenaka K, Kohda D, Fugo K, Kasahara M. Two novel NKG2D ligands of the mouse H60 family with differential expression patterns and binding affinities to NKG2D. J Immunol 2008; 180(3): 1678-1685

Teichmann JV, Ludwig WD, Seibt-Jung H, Thiel E. Induction of lymphokine-activated killer cell against human leukemia cells in vitro. Blut 1989; 59(1): 21-24

Thorne SH, Negrin RS, Contag CH. Synergistic antitumor effects of immune cell-viral biotherapy. Science 2006; 311(5768): 1780-1784

Toth G, Szollosi J, Vereb G. Quantitating ADCC against adherent cells: Impedance-based detection is superior to release, membrane permeability, or caspase activation assays in resolving antibody dose response. Cytometry A 2017; 91(10): 1021-1029

Upshaw JL, Arneson LN, Schoon RA, Dick CJ, Billadeau DD, Leibson PJ. NKG2D-mediated signaling requires a DAP10-bound Grb2-Vav1 intermediate and phosphatidylinositol-3-kinase in human natural killer cells. Nat Immunol 2006; 7(5): 524-532

Urlaub D, Hofer K, Muller ML, Watzl C. LFA-1 Activation in NK Cells and Their Subsets: Influence of Receptors, Maturation, and Cytokine Stimulation. J Immunol 2017; 198(5): 1944-1951

Valiante NM, Trinchieri G. Identification of a novel signal transduction surface molecule on human cytotoxic lymphocytes. J Exp Med 1993; 178(4): 1397-1406

Venkataraman GM, Suciu D, Groh V, Boss JM, Spies T. Promoter region architecture and transcriptional regulation of the genes for the MHC class I-related chain A and B ligands of NKG2D. J Immunol 2007; 178(2): 961-969

Verneris MR, Baker J, Edinger M, Negrin RS. Studies of ex vivo activated and expanded CD8+ NK-T cells in humans and mice. J Clin Immunol 2002; 22(3): 131-136

Verneris MR, Ito M, Baker J, Arshi A, Negrin RS, Shizuru JA. Engineering hematopoietic grafts: purified allogeneic hematopoietic stem cells plus expanded CD8+ NK-T cells in the treatment of lymphoma. Biol Blood Marrow Transplant 2001; 7(10): 532-542

Verneris MR, Karimi M, Baker J, Jayaswal A, Negrin RS. Role of NKG2D signaling in the cytotoxicity of activated and expanded CD8+ T cells. Blood 2004; 103(8): 3065-3072

Voskoboinik I, Whisstock JC, Trapani JA. Perforin and granzymes: function, dysfunction and human pathology. Nat Rev Immunol 2015; 15(6): 388-400

Waldhauer I, Goehlsdorf D, Gieseke F, Weinschenk T, Wittenbrink M, Ludwig A, Stevanovic S, Rammensee HG, Steinle A. Tumor-associated MICA is shed by ADAM proteases. Cancer Res 2008; 68(15): 6368-6376

Weiden PL, Flournoy N, Thomas ED, Prentice R, Fefer A, Buckner CD, Storb R. Antileukemic effect of graft-versus-host disease in human recipients of allogeneic-marrow grafts. N Engl J Med 1979; 300(19): 1068-1073

Weiss T, Schneider H, Silginer M, Steinle A, Pruschy M, Polic B, Weller M, Roth P. NKG2D-Dependent Antitumor Effects of Chemotherapy and Radiotherapy against Glioblastoma. Clin Cancer Res 2018; 24(4): 882-895

Wongkajornsilp A, Somchitprasert T, Butraporn R, Wamanuttajinda V, Kasetsinsombat K, Huabprasert S, Maneechotesuwan K, Hongeng S. Human cytokine-induced killer cells specifically infiltrated and retarded the growth of the inoculated human cholangiocarcinoma cells in SCID mice. Cancer Invest 2009; 27(2): 140-148

Wu J, Song Y, Bakker AB, Bauer S, Spies T, Lanier LL, Phillips JH. An activating immunoreceptor complex formed by NKG2D and DAP10. Science 1999; 285(5428): 730-732

Wu JD, Higgins LM, Steinle A, Cosman D, Haugk K, Plymate SR. Prevalent expression of the immunostimulatory MHC class I chain-related molecule is counteracted by shedding in prostate cancer. J Clin Invest 2004; 114(4): 560-568

Yamaguchi K, Chikumi H, Shimizu A, Takata M, Kinoshita N, Hashimoto K, Nakamoto M, Matsunaga S, Kurai J, Miyake N, Matsumoto S, Watanabe M, Yamasaki A, Igishi T, Burioka N, Shimizu E. Diagnostic and prognostic impact of serum-soluble UL16-binding protein 2 in lung cancer patients. Cancer Sci 2012; 103(8): 1405-1413

Yin X, Lu X, Xiuwen Z, Min Z, Xiao R, Mao Z, Zhang Q. Role of NKG2D in cytokine-induced killer cells against lung cancer. Oncol Lett 2017; 13(5): 3139-3143

Zaritskaya L, Shurin MR, Sayers TJ, Malyguine AM. New flow cytometric assays for monitoring cell-mediated cytotoxicity. Expert Rev Vaccines 2010; 9(6): 601-616

Zhang J, Larrocha PS, Zhang B, Wainwright D, Dhar P, Wu JD. Antibody targeting tumor-derived soluble NKG2D ligand sMIC provides dual co-stimulation of CD8 T cells and enables sMIC(+) tumors respond to PD1/PD-L1 blockade therapy. J Immunother Cancer 2019; 7(1): 223

Zhang J, Liu D, Li G, Staveley-O'Carroll KF, Graff JN, Li Z, Wu JD. Antibody-mediated neutralization of soluble MIC significantly enhances CTLA4 blockade therapy. Sci Adv 2017; 3(5): e1602133

Zhang L, Wang J, Wei F, Wang K, Sun Q, Yang F, Jin H, Zheng Y, Zhao H, Wang L, Yu W, Zhang X, An Y, Yang L, Zhang X, Ren X. Profiling the dynamic expression of checkpoint molecules on cytokine-induced killer cells from non-small-cell lung cancer patients. Oncotarget 2016; 7(28): 43604-43615

Zhang Y, Schmidt-Wolf IGH. Ten-year update of the international registry on cytokine-induced killer cells in cancer immunotherapy. J Cell Physiol 2020; 235(12): 9291-9303

Zhao YK, Jia CM, Yuan GJ, Liu W, Qiu Y, Zhu QG. Expression and clinical value of the soluble major histocompatibility complex class I-related chain A molecule in the serum of patients with renal tumors. Genet Mol Res 2015; 14(2): 7233-7240

Ziske C, Marten A, Schottker B, Buttgereit P, Schakowski F, Gorschluter M, von Rucker A, Scheffold C, Chao N, Sauerbruch T, Schmidt-Wolf IG. Resistance of pancreatic carcinoma cells is reversed by coculturing NK-like T cells with dendritic cells pulsed with tumor-derived RNA and CA 19-9. Mol Ther 2001; 3(1): 54-60

Zoll B, Lefterova P, Csipai M, Finke S, Trojaneck B, Ebert O, Micka B, Roigk K, Fehlinger M, Schmidt-Wolf GD, Huhn D, Schmidt-Wolf IG. Generation of cytokine-induced killer cells using exogenous interleukin-2, -7 or -12. Cancer Immunol Immunother 1998; 47(4): 221-226

Zou Y, Li F, Hou W, Sampath P, Zhang Y, Thorne SH. Manipulating the expression of chemokine receptors enhances delivery and activity of cytokine-induced killer cells. Br J Cancer 2014; 110(8): 1992-1999

9. Achknowledgements

The last 4 years in Bonn were an important experience in my life, for which I am very grateful. I have learned a lot, both scientifically and personally. I would like to take this opportunity to thank all people that made this thesis possible.

Particularly, I would like to thank my supervisor Prof. Dr. Ingo Schmidt-Wolf for taking me as one of his PhD students and teaching me how to be a scientist. I am grateful for his enormous supports with valuable discussions and suggestions. Thank him for taking time when it was needed and being always open to listen to me and giving me helpful ideas for my questions and any problems that arose. I would also like to thank my second supervisor Prof. Dr. Hans Weiher for his helpful discussions and suggestions in the annual committee report and for his support and review of this thesis. I want to thank Prof. Dr. Michael Muders and Prof. Dr. Dirk Skowasch for being part of my dissertation committee. Furthermore, I would like to thank my colleagues, Julia Schmatz for her kindly help in my start of PhD, Maria Fitria Setiawan and Oliver Rudan for the great organizing and coordinating work they have always been doing for the lab, Amit Sharma for his constructive suggestions and help in my English writing, other Chinese colleagues (Ying Zhang, Yutao Li, Yulu Wang, FangFang Ge) for their friendly help and support both in my work and daily life, David Stephan for inviting me to enjoy my first experience of carnival, my neighbor Alvaro Peralta for all the fun we had together in the house and in your party. Lastly, but importantly, I am grateful for my parents and my wife for always believing in me, your love and support brought me so far.